In presenting the dissertation as a partial fulfillment of the requirements for an advanced degree from the Georgia Institute of Technology, I agree that the Library of the Institute shall make it available for inspection and circulation in accordance with its regulations governing materials of this type. I agree that permission to copy from, or to publish from, this dissertation may be granted by the professor under whose direction it was written, or, in his absence, by the Dean of the Graduate Division when such copying or publication is solely for scholarly purposes and does not involve potential financial gain. It is understood that any copying from, or publication of, this dissertation which involves potential financial gain will not be allowed without written permission.

3/17/65
b

LAMINAR FREE CONVECTION ABOUT INCLINED ISOTHERMAL SURFACES FOR FLUIDS WITH TEMPERATURE DEPENDENT PROPERTIES

A THESIS

Presented to

The Faculty of the Graduate Division

by

Will T. McKie, Jr.

In Partial Fulfillment

of the Requirements for the Degree

Doctor of Philosophy in the

School of Mechanical Engineering

Georgia Institute of Technology

June, 1968

LAMINAR FREE CONVECTION ABOUT INCLINED ISOTHERMAL SURFACES FOR FLUIDS WITH TEMPERATURE DEPENDENT PROPERTIES

Approved:

Chairman

Date approved by Chairman: 5/23/68

ACKNOWLEDGMENTS

The author is indebted to many individuals who have contributed to the success of this work. In particular, he would like to express his sincere appreciation to Dr. C. W. Gorton, who continued to serve as Thesis Adviser throughout the extended period of time required to complete the work. Without his interest and guidance this work could not have been finished. The assistance of the members of the reading committee, Dr. G. T. Colwell and Dr. W. F. Black, during preparation of the thesis is greatly appreciated.

The author would like to express appreciation to the National Science Foundation for a Science Faculty Fellowship and to the Georgia Institute of Technology for both a Schlumberger Fellowship and a Ford Foundation loan.

Finally, the author wishes to acknowledge the long standing friendship of Professor A. G. Holmes. Through the years his advice and encouragement has contributed greatly to the success of this endeavor. The author's deepest appreciation must go to his wife and children for their infinite patience and their unending source of strength.

TABLE OF CONTENTS

(Continued)

TABLE OF CONTENTS (Concluded)

LIST OF ILLUSTRATIONS

(Continued)

LIST OF ILLUSTRATIONS (Concluded)

LIST OF TABLES

SUMMARY

The two-dimensional, natural convection flow in the neighborhood of a heated flat plate inclined at various angles from the vertical position was studied both analytically and experimentally. Air and oil were used for both studies to provide widely different Prandtl numbers.

The analytical work involved representing the partial differential equations of change by finite difference equations. For the numerical work with oil these equations retained the effects of variable properties, but the air studies were done with the constant property version of the equations of change. The property variation of the oil was accounted for by using appropriate functions of temperature. The validity of this approach was tested by comparison with results reported by Ostrach for the vertical plate and constant fluid properties. Velocity and temperature profiles calculated by the finite difference method compared favorably with those given by Ostrach.

This method was used to solve the equations of change, including momentum equations parallel and normal to the surface, the energy equation, and the continuity equation. For the oil studies, variation of property values were included by using appropriate functions of temperature for each of

the fluid properties. The results included the average Nusselt number and the velocity, temperature, and pressure profiles for 25 cases in oil and 25 cases in air. The angle of inclination was changed from zero to 45 degrees.

The velocity and temperature profiles showed little change due to the change in the angle of inclination. The heat transfer from the plate surface and the shear stress at the wall both decreased as the plate was inclined. The pressure profiles for the inclined plates indicated that the pressure was not constant along horizontal lines. The pressure near the wall was greater than the local hydrostatic pressure and the pressure difference increased as the angle of inclination increased.

The numerical results were compared with available experimental results for a wide range of Prandtl and Grashof numbers and for the same angles of inclination previously mentioned.

The equation

$$Nu_{\infty} = 0.65\left[\frac{Pr_{\infty}^{2.25}\, GR_{\infty}(\cos\theta)^{0.7}}{1.1 + Pr_{\infty}}\right]^{1/4}$$

is based on a correlation of the numerical and experimental results. All property values in this equation should be evaluated at the ambient temperature. Correlations of the numerical results were also obtained with properties evaluated at the ambient temperature and at the film temperature.

LIST OF SYMBOLS

A,B,C,D	coefficients used in the various difference equations
C_p	specific heat
F'	function defined by Ostrach, see equation 51, page 50
g	local acceleration of gravity
Gr	Grashof number
h	local heat transfer coefficient
$\bar{h}$	average heat transfer coefficient
H	function defined by Ostrach, see equation 51, page 50
k	thermal conductivity
L	length of plate
Nu	Nusselt number
p	pressure
p_s	hydrostatic pressure, $p_s = \rho_\infty \frac{g}{g_c}(y \sin\theta - x\cos\theta)$
$\bar{P}$	$p - p_s$
Pr	Prandtl number
T	temperature
u	velocity component parallel to the plate
v	velocity component normal to the plate
x	coordinate direction parallel to the plate
y	coordinate direction normal to the plate
α	thermal diffusivity
η	function defined by Ostrach, see equation 51, page 50

θ	angle of inclination, measured from vertical
μ	dynamic viscosity
υ	kinematic viscosity
ρ	density

Subscripts

f	refers to film temperature
i, j	refers to grid point
w	refers to wall temperature
∞	refers to ambient temperature

CHAPTER I

INTRODUCTION

Interest in this topic was generated by a study of the experimental work done by Garrison (1) on free convection heat transfer from isothermal cones and the theoretical study by Merk and Prins (2). During the present study a similarity solution for the cone was developed which provided a means for studying the velocity profiles parallel and normal to the surface and the temperature profile. Analysis of the velocity profiles indicated that the usual boundary layer assumption that the velocity normal to the surface was smaller than the velocity parallel to the surface was no longer valid. This meant that the momentum equation normal to the surface should have been included in the analysis. An investigation of the other terms in this momentum equation disclosed another feature of the boundary layer flow about inclined surfaces which had not been accounted for in the solutions mentioned above. In a normal gravitational field, the gravitational force acts vertically. For inclined surfaces this produces force components acting parallel and normal to the surface, and the normal component may act towards or away from the surface depending on the surface orientation.

Previous Work Related to Present Problem

By eliminating the momentum equation normal to the surface, Merk and Prins were able to develop the general relations for similar solutions for isothermal axisymmetric surfaces and to show that the cone has such a solution. However, approximate techniques were utilized to arrive at an expression for the Nusselt number. Hering and Grosh (3) subsequently showed that similar solutions for the cone could be obtained if the wall temperature distribution was a power function of the distance along a cone ray. They discuss the cases of isothermal surface, linear surface temperature variation, and constant heat flux. Numerical integration of the differential equations for the first two cases for a Prandtl number of 0.7 were presented. The results of the isothermal cone agree with the approximate solution of Merk and Prins. Hering and Grosh also found agreement with previously published experimental results for vertical surfaces (cylinders and planes), horizontal wires, spheres, and blocks in air, water, alcohol, and oil when the gravitational acceleration was interpreted as the component parallel to the body surface. The gravitational acceleration component parallel to the surface was used by Kreith (4) in a modification of an accepted relationship for the vertical plate which was derived by Eckert and presented very completely by Holman (5).

The results of experiments by Rich (6) using a Mach-Zehnder interferometer for plates inclined from zero to 40 degrees also led to a conclusion that the modified vertical plate equation referred to above would predict the Nusselt number within 10 percent. Rich also states that the transition from laminar to turbulent flow occurs at lower Grashof numbers as the inclination of the plate is increased. A discussion of this paper by Ostrach indicates that the treatment of the pressure gradient terms was the same as that used in solutions for the vertical plate. The increased effect of the component of the body force term normal to the surface should require the inclusion of the momentum equation normal to the surface. Ostrach states that the pressure normal to the surface has the same magnitude as the body force component in that direction. Also in the discussion of this paper, Rutkowski and Tribus commented that the effect of inclining the surface apparently was small and that accurate apparatus should be used in any further study.

The numerous papers on free convection from vertical surfaces provided further insight into the general nature of the problem. An analysis given in Bird, Stewart, and Lightfoot (7) indicates that a correlation of the form

$$Nu = C\,(Pr\ Gr)^{1/4}$$

with C a weak function of the Prandtl number only, is correct for laminar flow in the boundary layer. The similar solution presented by Ostrach (8) verifies this. The results of this analysis were shown to correspond closely with results of the approximate analysis by Eckert which was mentioned earlier. This study was made for flow about a vertical plate and the momentum equation normal to the surface was not used.

McAdams (9) presents a semi-empirical analysis of several experimental efforts and evaluates the coefficient C as a single constant. As is pointed out by Ostrach, this correlation holds in a limited range of Prandtl numbers (for air and water). The results of experiments with oil performed by Lorenz (10) do not show good agreement with the results of Ostrach's and Eckert's analyses and are more compatible with the correlation derived by McAdams. The experimental work of Touloukian, Hawkins, and Jacob (11) for vertical cylinders in water and ethylene glycol produced a correlation similar to that of McAdams. They also obtained data for turbulent free convection and present an interesting discussion of the method of correlating data in the turbulent range. Further discussion of this is given by Brown and Marco (12).

A method of obtaining similarity solutions for free convection from vertical plates and cylinders has also been

used by Yang (13). The momentum equation normal to the surface was omitted in this analysis also.

A study of the asymptotic behavior of heat transfer in laminar boundary layers for large Prandtl numbers was presented by Morgan and Warner (14). This analysis was based on the fact that, for large Prandtl numbers, the conduction term in the energy equation is important only in a region that is thin compared with the velocity boundary layer and that in this region both conduction and convection are equally important. A transformation (based on the Prandtl number) of the coordinate normal to the body surface produces a form of the energy equation in which the conduction and convection terms are balanced with respect to their asymptotic dependence on the Prandtl number. The behavior of the local heat transfer coefficient can be deduced immediately. For the case of the vertical plate the authors succeed once again in showing that the Nusselt number is dependent on the one-fourth power of the Prandtl number-Grashof number product. They also indicate a correlation of the form derived by McAdams (9) but with slightly higher coefficients.

In a paper by Stewartson (15) on free convection from a horizontal plate both momentum equations were included in the original differential equations. However, before a similar solution was obtained one of the body force terms was reduced to zero (the horizontal plate solution). An

interesting method of including the pressure term was also presented. Because several terms were omitted, this solution is not applicable to the present problem directly but study of the various aspects of the solution led to the conclusion that similarity approaches would not provide an adequate description for inclined surfaces.

Two papers by Tritton (16,17) present valuable information on experimental techniques used in studies of turbulent free convection on inclined plates. Transition to turbulent flow was also studied. The description of the plate heating arrangement shows the need for varying the heat flux along the plate and indicates that the difference in flow patterns above and below the plate would require a different heat flux distribution for each side to maintain isothermal conditions simultaneously. Tritton found that the component of the body force normal to the plate causes a stratification of the flow. The Richardson number is an indication of the importance of the normal body force compared with that of the shear forces. The stratification has a stabilizing effect on the convection below a heated inclined plate where hotter fluid is above colder fluid. Above a heated plate the situation is reversed and the stratification is destabilizing. Further discussion of stratification is given by Prandtl (18).

Recently, Michiyoshi (19) has presented a solution

for natural convection from an inclined plate under conditions that the Prandtl number is near one. The solution is based on the flat ellipse approximate method in which the integral boundary layer relations are solved by assuming velocity and temperature profiles. The results of these numerical calculations show the effect of the angle of inclination and predict a difference for the flow above and the flow below the plate. For the flow below the plate inclined at angles up to 60 degrees from the vertical the results can be correlated directly with the cosine of the angle raised to the one fourth power.

Free convection analyses that included variable property effects were presented by Sparrow and Gregg (20) and by Fritsch and Grosh (21). Both presented a similarity transformation for reducing the compressible flow equations to ordinary differential equations. Sparrow and Gregg introduced the variable properties by specifying various functions of temperature. They also present a justification for the choice of reference temperature to make the variable property solution compatible with the constant property solutions. Fritsch and Grosh used tabulated density-temperature data for water near the critical state and a numerical differentiation procedure to introduce the variable property effects.

Experimental results for free convection from an

inclined flat plate in air have been obtained by Douglass (24) and Patel (25). Experimental results for free convection from an inclined flat plate in oil have been obtained by Farmer (26), Morris (27), Barnes (28), Moorehead (29), and Young (30). The experimental work of Farmer was reported in a paper by Farmer and McKie (31).

Research Objective

The objective of the proposed study will be to investigate the effects of variable properties and the angle of surface inclination on the natural convection from an isothermal flat plate by using a finite difference scheme. The numerical procedure will be flexible enough to allow the introduction of property relations applicable for different fluids. Experimental results are available for both air and oil as the heat transfer medium and the property relations applicable to these fluids will be used in the analytical calculations.

In the study of the effect of the angle of inclination the influence of terms ordinarily omitted from the momentum equations for boundary layer flow will be investigated. These additional terms are expected to contribute more to the solution as the angle of inclination is increased. For angles of inclination approaching 45 degrees, the momentum equation normal to the surface may be needed for a complete mathematical model of the flow. This

equation will be retained in the analytical solution and its contribution will be noted. The results of both the experimental and the analytical investigations will be combined to give a single correlation for the heat transfer coefficient.

CHAPTER II

FORMULATION OF THE MATHEMATICAL MODEL

The general considerations involved in the formulation of a mathematical model of the two dimensional, natural convection flow caused by a heated flat plate inclined at various angles from the vertical position is discussed in this chapter. To conform to previously performed experimental tests, the angle of inclination, measured from the vertical, is to be varied from 0 to 45 degrees. The model should reflect the variation of physical properties with temperature when such variation is a significant effect.

The governing equations were considered to be the equations of change for the steady plane-flow of a non-isothermal Newtonian fluid. The results of the derivation given in Appendix D, page 109, are as follows:

$$\rho\left[u\frac{\partial u}{\partial x} + v\frac{\partial u}{\partial y}\right] = \frac{\partial}{\partial x}\left[2\mu\frac{\partial u}{\partial x}\right] + \frac{\partial}{\partial y}\left[\mu\left(\frac{\partial u}{\partial y} + \frac{\partial v}{\partial x}\right)\right]$$

$$-g_c\frac{\partial \bar{P}}{\partial x} + \rho_\infty g\cos\theta\left[1 - \frac{\rho}{\rho_\infty}\right] \qquad (1)$$

$$\rho\left(u\frac{\partial v}{\partial x} + v\frac{\partial v}{\partial y}\right) = \frac{\partial}{\partial x}\left[\mu\left(\frac{\partial u}{\partial y} + \frac{\partial v}{\partial x}\right)\right] + \frac{\partial}{\partial y}\left(2\mu\ \frac{\partial v}{\partial y}\right)$$

$$-g_c\ \frac{\partial \bar{P}}{\partial y} - \rho_\infty\, g\, \sin\theta\left(1 - \frac{\rho}{\rho_\infty}\right) \qquad (2)$$

$$\rho\, c_p\left(u\frac{\partial T}{\partial x} + v\frac{\partial T}{\partial y}\right) = \frac{\partial}{\partial x}\left(k\frac{\partial T}{\partial x}\right) + \frac{\partial}{\partial y}\left(k\frac{\partial T}{\partial y}\right) \qquad (3)$$

$$\frac{\partial u}{\partial x} + \frac{\partial v}{\partial y} = 0 \qquad (4)$$

For two-dimensional flow in the neighborhood of an inclined surface the pertinent boundary conditions are:

$$y = 0 \quad u = v = 0 \quad T = T_w$$

$$y \to \infty \quad u = 0 \quad T = T_\infty \quad \bar{P} = 0 \qquad (5)$$

In equations (1) and (2), the symbol, $\bar{P}$, is the difference in pressure measured from the hydrostatic condition. The effect of compressibility on the continuity equation was neglected.

The four equations describing the motion contain four dependent variables, u, v, T, and $\bar{P}$, in terms of the two independent variables, x and y, and with the associated boundary conditions the basis for a model is established. If the resulting mathematical model is used to describe cases which include the variation of property values, the physical properties would normally be considered functions of temperature only. In all cases, the density, ρ, in the

term $(1-\rho/\rho_\infty)$ in equations (1) and (2) would be considered as a function of temperature. These partial differential equations are coupled and must be solved simultaneously. They are non-linear and, for variable property studies, will contain functions of temperature specifying the property values according to each fluid considered.

The complex nature of the problem as described eliminates the possibility of obtaining a solution in closed form. Retention of non-linear terms and variable properties indicates the need for a numerical method using a finite difference technique as the proper procedure for this solution. Generally, finite difference schemes must be structured with a definite grid pattern and definite boundary values. The type of finite difference scheme, the geometry of the finite difference grid, and the physical extent of the grid pattern all would affect the behavior of the solution and these characteristics of the model will have to be chosen judiciously to provide an acceptable solution.

A reduced version of equations (1), (2), (3), and (4) may be formulated to retain the essential physical character of the natural convection flow and provide a reasonable evaluation, using the criterion stated above, of any proposed finite difference scheme. These equations are:

$$u\frac{\partial u}{\partial x} + v\frac{\partial u}{\partial y} = \upsilon_\infty \frac{\partial^2 u}{\partial y^2} + g\left[1 - \frac{\rho}{\rho_\infty}\right] \qquad (6)$$

$$u\frac{\partial T}{\partial x} + v\frac{\partial T}{\partial y} = \alpha_\infty \frac{\partial^2 T}{\partial y^2} \tag{7}$$

$$\frac{\partial u}{\partial x} + \frac{\partial v}{\partial y} = 0 \tag{8}$$

The boundary conditions for these equations are:

$$y = 0 \quad u = v = 0 \quad T = T_w$$

$$y \to \infty \quad u = 0 \quad T = T_\infty \tag{9}$$

These equations are essentially the same as the equations used by Ostrach (8) for the similarity solution for natural convection from a vertical plate. Only the body force term has been changed so that any function, $\rho(T)$, may be employed. The use of these equations would permit an evaluation of the validity of the results by direct comparison with the results obtained by Ostrach.

A detailed discussion of the derivation of the finite difference equations will be presented in the following chapter. The grid pattern which satisfied all the criteria previously stated is shown in Figure 1, page 13. All boundaries of the grid except the plate area were considered to have values of $u = v = 0$ and $T = T_\infty$. The portion of the grid boundary which is considered to be the plate was assigned the boundary conditions of $u = v = 0$ and $T = T_w$. This imposed conditions along the upper and lower boundaries of the grid and restricted the value of v along the grid

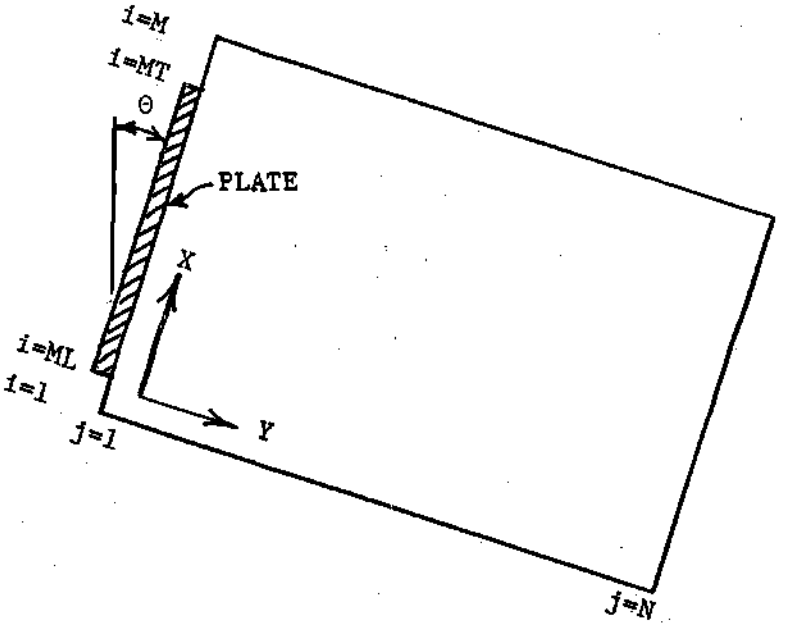

Figure 1. Finite Difference Grid Pattern.

line, j = N. The finite difference scheme which was used to calculate the values of u, v, and T at the internal points in the grid was developed so that the effects of the artificial boundary conditions stated above were effectively masked and the velocity and temperature profiles retained their desired characteristics.

This complete specification of values for all boundary points of the grid was required because the computer programs were generalized to allow for any combination of signs for the velocity components. After the numerical solutions were obtained, it was observed that only one combination, namely $u \geq 0$ and $v \leqq 0$, had occurred. Thus, only one version of the difference equations was actually utilized during computation. The boundary values along the upper grid line were never included in the calculations. The restriction of v = 0 was also removed from all grid boundaries except the plate itself.

Along the grid line, j = 1, below the plate, $1 \leqq i \leqq ML$, and above the plate $MT \leqq i \leqq M$, several modifications of the boundary values were investigated. Each of these modifications involved assuming a temperature distribution along these lines which provided a continuous change from $T = T_\infty$ to $T = T_W$. The final choice of the step-wise change in T occurring at the plate was based on the comparison of the results of this investigation and the results reported

by Ostrach (8).

In all cases investigated, the solution near the leading edge of the plate was not valid. The local velocity and temperature profiles did not exhibit the proper shape, and the local values of the convection coefficient, h(x), remained finite. To improve the numerical integration of the local values of h(x) in calculating the average heat transfer coefficient, $\bar{h}$, for the plate, the assumption that h(x) was proportional to $x^{-1/4}$ was used in the first intervals of the grid patterns. The implementation of this procedure and an analysis of the results will be described in detail in the following chapters. This method provided a finite difference scheme and a grid pattern which allowed numerical computation of velocity and temperature profiles and the average Nusselt number with sufficient accuracy.

Thus, the mathematical model is formulated in such a manner that several versions of the partial differential equations describing the motion may be converted to finite difference equations and used to calculate values of the dependent variables within a particular grid pattern. This grid pattern was chosen so that the results were applicable to convective flow past a heated flat plate in a semi-infinite region. The effect of inclination of the plate will be studied by inclining the entire grid pattern.

CHAPTER III

METHOD OF SOLUTION OF THE MATHEMATICAL PROBLEM

Basically, the method of solution involves the approximation of the differential equations by using finite differences. The resulting difference equations were then used to solve for the values of the dependent variables at each point in the finite difference grid pattern. The method of solving for the dependent variables must insure that the difference equations are satisfied at each grid point. If this is accomplished, the accuracy of the solution depends on the mesh size.

Of the several methods of solving difference equations, only conventional iteration of the explicit steady state equations proved successful. The unsteady state method proposed by Hellums (22) exhibited unstable characteristics which appeared to be independent of the size of the time increment. Hellums also accounted for the density variation by introducing the coefficient of thermal expansion. The iteration was unsuccessful until the equations were written so that all the coefficients were positive. This produced what Richtmyer (23) calls positive type difference equations and in general requires four different

sets of equations at each grid point. The particular set of equations which should be used depends on the sign of the local velocity components. The use of these conditions in the unsteady state method to determine stability criteria is well documented but no reference could be found of their application in conventional iteration techniques. This particular innovation of the use of conventional iteration techniques was responsible for the solution converging to the desired results for a plate suspended in a semi-infinite body of fluid. Other attempts at iteration produced solutions with reversed flow characteristics far from the plate.

The derivation of the positive type difference equations for the check solution using the equations similar to those of Ostrach will be presented next. After that the difference equations for the present study will be developed and the method of iteration explained.

The Difference Equations for the Check Solution

The derivation of the difference equation approximation for the differential equation (7) must in general consider the four possible cases in which the u and v velocities may be either positive or negative. The flat plate, however, provides a special condition in which the u velocity is always positive or zero and the v velocity is always negative or zero. Under these circumstances, only

one of the four cases need be considered. The difference equations for the other three cases are presented along with the computer programs in Appendices B and C. As written, the programs will admit any sign combination for the velocity components. Inspection of the numerical results indicated that the conjecture given above is correct. The grid notation for a general point within the grid pattern is given in Figure 2, page 20.

For the case of $u_{i,j} \geq 0$ and $v_{i,j} \leq 0$, a backward difference approximation must be used for $\partial T/\partial x$, and a forward difference approximation must be used for $\partial T/\partial y$. This will insure that all the coefficients will be positive when the difference equation is rearranged to solve for $T_{i,j}$. The standard central difference approximation for $\partial^2 T/\partial y^2$ may be used. This results in the following difference equation:

$$u_{i,j}\left(\frac{T_{i,j}-T_{i-1,j}}{\Delta x}\right) + v_{i,j}\left(\frac{T_{i,j+1}-T_{i,j}}{\Delta y}\right) = \alpha_{\infty}\left(\frac{T_{i,j+1}-2T_{i,j}+T_{i,j-1}}{(\Delta y)^2}\right) \qquad (10)$$

Because this equation will be valid for only $u_{i,j} \geq 0$ and $v_{i,j} \leq 0$ it may be changed to

$$|u_{i,j}|\left(\frac{T_{i,j}-T_{i-1,j}}{\Delta x}\right) - |v_{i,j}|\left(\frac{T_{i,j+1}-T_{i,j}}{\Delta y}\right) = \alpha_{\infty}\left[\frac{T_{i,j+1}-2T_{i,j}+T_{i,j-1}}{(\Delta y)^2}\right] \qquad (11)$$

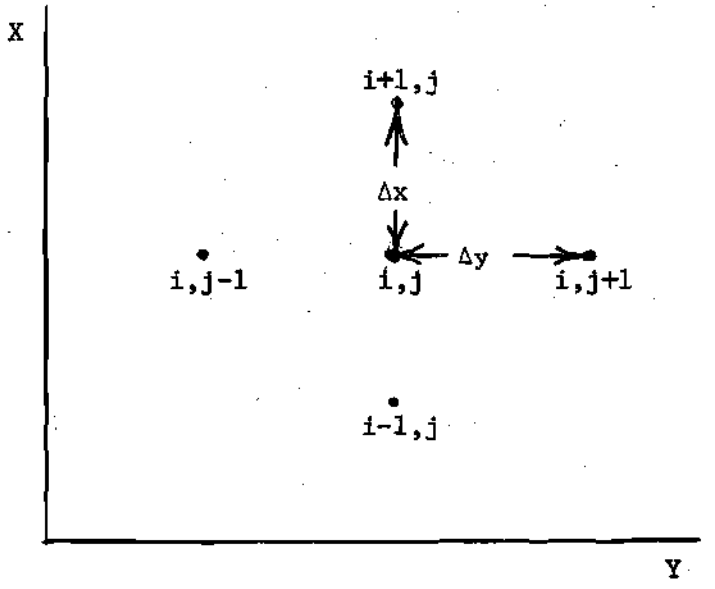

Figure 2. Notation for General Grid Point.

The coefficients in this equation may be conveniently written

$$A_y = \frac{\alpha_\infty}{(\Delta y)^2}$$

$$B = \frac{|u_{i,j}|}{\Delta x} \qquad (12)$$

$$C = \frac{|v_{i,j}|}{\Delta y}$$

Substituting equations (12) into equation (11) results in reduced form

$$B(T_{i,j}-T_{i-1,j})-C(T_{i,j+1}-T_{i,j})=A_y(T_{i,j+1}-2T_{i,j}+T_{i,j-1})$$

This may be solved for $T_{i,j}$, as follows

$$T_{i,j} = \frac{A_y(T_{i,j+1}+T_{i,j-1}) + B\,T_{i-1,j} + C\,T_{i,j+1}}{2A_y + B + C} \qquad (13)$$

The sum of the four coefficients on the right side of equation (13) is

$$\frac{2A_y}{2A_y+B+C} + \frac{B}{2A_y+B+C} + \frac{C}{2A_y+B+C} = 1 \qquad (14)$$

Thus, by defining the coefficients as in equations (12) so that they are always positive, and using the appropriate finite difference approximations as shown in equation (10), the sum of the coefficients in equation (13) is unity. These two conditions are sufficient to guarantee that $T_{i,j}$

is bounded by the four values of temperature at the adjacent grid points. Equation (13) is used at every point in the grid and provides the guarantee that each temperature so calculated is bounded by the values of the temperature at the adjacent points. Since the entire grid is bounded by $T = T_W$ and $T = T_\infty$ then no interior point can have a value outside these limits. This insures the stability of the solution and contributes to the ability of this method to correct for the artificially imposed restrictions at the finite grid boundaries. There is no tendency for down flow along the $j = N$ grid line with this method.

The momentum equation, (6), may be transformed in a similar manner except for the non-linear condition involving the u velocity and for the additional term which accounts for the variation of density. As an example, for the case of $u_{i,j} \geq 0$ and $v_{i,j} \leq 0$. A backward difference should be used for both $\partial u/\partial x$ and a forward difference is required for $\partial u/\partial y$, resulting in the following equation

$$u_{i,j}\left(\frac{U_{i,j}-U_{i-1,j}}{\Delta x}\right) + v_{i,j}\left(\frac{U_{i,j+1}-U_{i,j}}{\Delta y}\right) =$$

$$\upsilon_\infty \left[\frac{u_{i,j+1}-2u_{i,j}+u_{i,j-1}}{(\Delta y)^2}\right] + g\left(1-\frac{\rho_{i,j}}{\rho_\infty}\right) \qquad (15)$$

The value of $\rho_{i,j}$ is calculated as a function of the value of $T_{i,j}$. To resolve the non-linearity existing in the first term, the first $u_{i,j}$ is considered known and taken as the

old value at the grid point, the remaining $u_{i,j}$ terms are grouped together in a manner similar to that of the $T_{i,j}$ terms in the energy equation previously discussed. The coefficients B and C remain as previously defined and a new coefficient, A_y, must be defined as

$$A_y = \frac{\mu_\infty}{(\Delta y)^2} \tag{16}$$

Introducing these coefficients into equation (15) gives

$$B(u_{i,j}-u_{i-1,j}) - C(u_{i,j+1}-u_{i,j}) =$$

$$A_y(u_{i,j+1}-2u_{i,j}+u_{i,j-1}) + g\left(1-\frac{\rho_{i,j}}{\rho_\infty}\right) \tag{17}$$

Equation (17) may be solved for $u_{i,j}$ to yield

$$u_{i,j} = \frac{A_y(u_{i,j+1}+u_{i,j-1}) + B\,u_{i-1,j} + C\,u_{i,j+1}+g\left(1-\frac{\rho_{i,j}}{\rho_\infty}\right)}{2A_y + B + C} \tag{18}$$

The additional term in equation (18) insures that the u velocity can not be negative because $\rho_{i,j} \leq \rho_\infty$. The magnitude of the first portion of the equation (18) is bounded by the values of u at the adjacent points. Without the contribution of the last term, the value of u would remain zero.

The continuity equation (8) may be written in finite difference form as

$$\frac{u_{i+1,j}-u_{i-1,j}}{2\Delta x} + \frac{v_{i,j}-v_{i,j-1}}{\Delta y} = 0$$

This equation may be solved for $v_{i,j}$ to give

$$v_{i,j} = v_{i,j-1} - \frac{\Delta y}{2\Delta x}(u_{i-1,j} - u_{i-1,j}) \qquad (19)$$

This form is utilized so that new values of $v_{i,j}$ depend only on $v_{i,j-1}$ and the solution may be started along the line $j = 1$ which contains the plate and continued to the outer edge of the grid pattern.

The numerical solution of equations (13), (18), and (19) may be started with any assumed set of values of u, v, and T throughout the grid pattern. Equations (13) and (18) may be iterated over the grid and equation (19) is used to update the values of v. The iteration is continued until the three equations are essentially satisfied at each point in the grid. A practical criterion to judge the degree of convergence to a solution may be developed by summing the absolute change of both u and T at each point in the grid from one iteration to the next. The change in the average value of the Nusselt number from one iteration to the next also should be reduced to at least one order of magnitude below the desired accuracy level for the Nusselt number. The calculation for the average Nusselt number is described below. When the sum of the changes in the u and T values and the change in the average Nusselt number had been reduced sufficiently, the iteration was terminated.

The local value of the heat transfer coefficient may

be calculated by equating the heat transfer per unit area to the heat transfer per unit area by conduction in the layer of fluid adjacent to the wall. This gives the equation

$$h(x)\ (T_w-T_\infty) = -k\left(\frac{\partial T}{\partial y}\right)_{y=0} \tag{20}$$

The partial derivative may be approximated by

$$\left(\frac{\partial T}{\partial y}\right)_{y=0} \simeq \frac{T_w-T_{i,2}}{T_w-T_\infty} \tag{21}$$

An equation for h_i at each grid point along the plate may be derived by substituting equation (21) into equation (20). Thus,

$$h_i = \frac{k}{\Delta y}\,\frac{T_w-T_{i,2}}{T_w-T_\infty} \tag{22}$$

The average value of the heat transfer coefficient is defined as

$$\bar{h}\int_0^L dx = \int_0^L h(x)\ dx$$

or

$$\bar{h} = \frac{1}{L}\int_0^L h(x)\ dx \tag{23}$$

Because the numerical solution did not accurately reflect

the trend of h(x) as x approached zero, the integration indicated in equation (23) must be done in two parts. Over the interval from x = 0 to x = x_3, the heat transfer coefficient is assumed to be given by

$$h_1(x) = \frac{C_1}{x^{1/4}} \tag{24}$$

The constant, C_1, is determined so that $h_1(x_3)$ will have the same magnitude as h_3 calculated by equation (22). In the interval from x = x_3 to x = L the integration will be performed numerically using h_i from equation (22). At the point, x = x_3, the values of h calculated by equations (22) and (24) must be equal so the following expression may be obtained.

$$\frac{k}{\Delta y}\frac{T_w-T_{3,2}}{T_w-T_\infty} = \frac{C_1}{x_3^{1/4}}$$

From this, the value of C_1 may be determined as

$$C_1 = \frac{x_3^{1/4}k(T_w-T_{3,2})}{\Delta y(T_w-T_\infty)} \tag{25}$$

Equation (33) may now be rewritten as

$$\bar{h}L = \int_o^{x_3} h_1(x)\,dx + \int_{x_3}^{L} h_i dx$$

$$= C_1\int_o^{x_3} x^{-1/4}dx + \int_{x_3}^{L} h_i dx$$

$$= \frac{x_3^{1/4} k(T_w - T_{3,2})}{\Delta y (T_w - T_\infty)} \left(\frac{4}{3} x_3^{3/4}\right) + \frac{k}{\Delta y (T - T_\infty)} \int_{x_3}^{L} (T_w - T_{i,2}) dx$$

$$= \frac{4}{3} \frac{x_3 k (T_w - T_{3,2})}{\Delta y (T_w - T_\infty)} + \frac{k}{\Delta y (T_w - T_\infty)} \int_{x_3}^{L} (T_w - T_{i,2}) \, dx$$

This last expression may be converted to an equation for the average Nusselt number. After trying several grid points for x_3 and comparing the results with those of Ostrach, the most favorable value was found to be $x_3 = 2\Delta x$. This gives

$$Nu_\infty = \frac{\bar{h} L}{k_\infty} = \frac{8}{3} \left(\frac{\Delta x}{\Delta y}\right) \frac{(T_w - T_{3,2})}{(T_w - T_\infty)} + \frac{1}{\Delta y (T_w - T_\infty)} \int_{x_3}^{L} (T_w - T_{i,2}) dx \quad (26)$$

The integration indicated in the last term must be done by a numerical method such as Simpson's Rule.

The results of the calculations will be presented in detail in Chapter IV. The velocity and temperature profiles and the average Nusselt number determined by these calculations will compare with the results reported by Ostrach.

The Difference Equations for the Variable Property Solution

The basic differential equations (1), (2), (3), and (4) were converted to difference equations in the following manner. Consider first the energy equation

$$\rho C_p\left(u\frac{\partial T}{\partial x} + v\frac{\partial T}{\partial y}\right) = \frac{\partial}{\partial x}\left(k\frac{\partial T}{\partial x}\right) + \frac{\partial}{\partial y}\left(k\frac{\partial T}{\partial y}\right) \tag{3}$$

The variation of the thermal conductivity may be accounted for by expanding the two terms on the right to give the following equation

$$\rho C_p\left(u\frac{\partial T}{\partial x} + v\frac{\partial T}{\partial y}\right) = k\left(\frac{\partial^2 T}{\partial x^2} + \frac{\partial^2 T}{\partial y^2}\right)$$

$$+ \left(\frac{\partial T}{\partial x}\right)\left(\frac{\partial k}{\partial x}\right) + \left(\frac{\partial T}{\partial y}\right)\left(\frac{\partial k}{\partial y}\right) \tag{27}$$

A positive difference equation for $T_{i,j}$ is desired and the sign of the coefficients, $\partial k/\partial x$ and $\partial k/\partial y$, must be determined. For liquids, k decreases as the temperature increases and $\partial k/\partial y$ will be positive while $\partial k/\partial x$ will be negative. The opposite is true for gases. Since oil is the fluid of primary interest in this study of variable properties, the last two terms on the right side of equation (27) will be approximated using a backwards difference for $\partial T/\partial x$ and a forward difference for $\partial T/\partial y$.

For the case when $u_{i,j} \geq 0$ and $v_{i,j} \leq 0$, the derivative $\partial T/\partial x$ on the left side of equation (27) must be approximated with a backwards difference and $\partial T/\partial y$ must be approximated with a forward difference. This will give an equation of the form

$$(\rho C_p)_{i,j}\left[u_{i,j}\left(\frac{T_{i,j}-T_{i-1,j}}{\Delta x}\right)+v_{i,j}\left(\frac{T_{i,j+1}-T_{i,j}}{\Delta y}\right)\right]= \tag{28}$$

$$K_{i,j}\left[\frac{T_{i+1,j}-2T_{i,j}+T_{i-1,j}}{(\Delta x)^2}+\frac{T_{i,j+1}-2T_{i,j}+T_{i,j-1}}{(\Delta y)^2}\right]+$$

$$\left(\frac{k_{i+1,j}-k_{i-1,j}}{2\Delta x}\right)\left(\frac{T_{i,j}-T_{i-1,j}}{\Delta x}\right)+\left(\frac{k_{i,j+1}-k_{i,j-1}}{2\Delta y}\right)\left(\frac{T_{i,j+1}-T_{i,j}}{\Delta y}\right)$$

A more convenient form for equation (28) may be obtained by dividing by $k_{i,j}$ and grouping terms as shown in the next equation

$$\left(\frac{\rho C_p}{k}\right)_{i,j}\left[\left(\frac{u_{i,j}}{\Delta x}\right)(T_{i,j}-T_{i-1,j})+\left(\frac{v_{i,j}}{\Delta y}\right)(T_{i,j+1}-T_{i,j})\right]=$$

$$\frac{1}{(\Delta x)^2}(T_{i+1,j}-2T_{i,j}+T_{i-1,j})+\frac{1}{(\Delta y)^2}(T_{i,j+1}-2T_{i,j}+T_{i,j-1})+ \tag{29}$$

$$\left[\frac{k_{i+1,j}-k_{i-1,j}}{2(\Delta x)^2 k_{i,j}}\right](T_{i,j}-T_{i-1,j})+\left[\frac{k_{i,j+1}-k_{i,j-1}}{2(\Delta y)^2 k_{i,j}}\right](T_{i,j+1}-T_{i,j})$$

The following terms are defined.

$$A_1=\frac{1}{(\Delta x)^2} \qquad B_1=\frac{1}{(\Delta y)^2}$$

$$A_2=\frac{\left|k_{i+1,j}-k_{i-1,j}\right|}{2(\Delta x)^2 k_{i,j}} \qquad B_2=\frac{\left|k_{i,j+1}-k_{i,j-1}\right|}{2(\Delta y)^2 k_{i,j}}$$

$$C=\left(\frac{\rho C_p}{k}\right)_{i,j}\frac{\left|u_{i,j}\right|}{\Delta x} \qquad D=\left(\frac{\rho C_p}{k}\right)_{i,j}\frac{\left|v_{i,j}\right|}{\Delta y} \tag{30}$$

These terms may be substituted into equation (29) and

particular signs changed to account for $\partial k/\partial x < 0$ and $\partial k/\partial y$ being positive. The resulting equation is

$$C(T_{i,j}-T_{i-1,j}) - D(T_{i,j+1}-T_{i,j}) =$$

$$A_1(T_{i+1,j}-2T_{i,j}+T_{i-1,j})+B_1(T_{i,j+1}-2T_{i,j}+T_{i,j-1})$$

$$-A_2(T_{i,j}-T_{i-1,j}) + B2(T_{i,j+1}-T_{i,j}) \qquad (31)$$

Equation (31) can be solved for $T_{i,j}$ to give

$$T_{i,j} =$$

$$\frac{A_1T_{i+1,j}+(A_1+A_2+C)T_{i-1,j} + (B_1+B_2+D)T_{i,j+1}+B_1T_{i,j-1}}{2A_1 + A_2 + 2B_1 + B_2 + C + D} \qquad (32)$$

Every coefficient in equation (32) is positive and the sum of all the coefficients is unity. This is sufficient to guarantee that $T_{i,j}$ will be bounded by temperature values at the adjacent grid points. It should be pointed out that the coefficients A_2, B_2, C, and D depend on the grid location, while only A_1 and B_1 are independent of the grid location.

The momentum equation in the x direction may be written as

$$\rho\left(u\frac{\partial u}{\partial x} + v\frac{\partial u}{\partial y}\right) =$$

$$\frac{\partial}{\partial x}(2\mu\frac{\partial u}{\partial x})+ \frac{\partial}{\partial y}[\mu(\frac{\partial u}{\partial y}+\frac{\partial v}{\partial x})] - g_c\frac{\partial \bar{P}}{\partial x}+\rho_\infty g\cos\theta(1-\frac{\rho}{\rho_\infty}) \qquad (1)$$

The variation of μ may be accounted for by expanding this equation in the following manner.

$$\rho\left(u\frac{\partial u}{\partial x} + v\frac{\partial u}{\partial y}\right) = 2\mu\frac{\partial^2 u}{\partial x^2} + 2\left(\frac{\partial \mu}{\partial x}\right)\left(\frac{\partial u}{\partial x}\right) + \mu\frac{\partial^2 u}{\partial y^2} + \mu\frac{\partial^2 v}{\partial x \partial y} +$$

$$\left(\frac{\partial \mu}{\partial y}\right)\left(\frac{\partial u}{\partial y} + \frac{\partial v}{\partial x}\right) - g_c\frac{\partial \bar{P}}{\partial x} + \rho_\infty g \cos\theta \left(1 - \frac{\rho}{\rho_\infty}\right)$$

The terms involving μ may be regrouped to give

$$\rho\left(u\frac{\partial u}{\partial x} + v\frac{\partial u}{\partial y}\right) = \mu\left(\frac{\partial^2 u}{\partial x^2} + \frac{\partial^2 u}{\partial y^2}\right) + 2\left(\frac{\partial \mu}{\partial x}\right)\left(\frac{\partial u}{\partial x}\right) +$$

$$\left(\frac{\partial \mu}{\partial y}\right)\left(\frac{\partial u}{\partial y} + \frac{\partial v}{\partial x}\right) + \mu\frac{\partial}{\partial x}\left(\frac{\partial u}{\partial x} + \frac{\partial v}{\partial y}\right)^{0} -$$

$$g_c\frac{\partial \bar{P}}{\partial x} + \rho_\infty g \cos\theta \left(1 - \frac{\rho}{\rho_\infty}\right) \qquad (33)$$

The term that is cancelled from this equation has been eliminated because of the continuity equation which will be used. The continuity equation is equation (4).

The derivatives of viscosity will be coefficients in the difference equation and their sign is important in choosing whether forward or backwards differences will be used. For liquids, the viscosity decreases as the temperature increases, and $\partial\mu/\partial y$ will be positive while $\partial\mu/\partial x$ will be negative. For gases the opposite is true. This indicates that, for oil, the derivative $\partial u/\partial x$ must be approximated with a backward difference and $\partial u/\partial y$ must be

approximated with a forward difference.

The difference equation for the case of $u_{i,j} \geq 0$ and $v_{i,j} \leq 0$ may be written as

$$\rho_{i,j}\left[u_{i,j}\left(\frac{u_{i,j}-u_{i-1,j}}{\Delta x}\right)+v_{i,j}\left(\frac{u_{i,j+1}-u_{i,j}}{\Delta y}\right)\right] =$$

$$\mu_{i,j}\left[\frac{u_{i+1,j}-2u_{i,j}+u_{i-1,j}}{(\Delta x)^2} + \frac{u_{i,j+1}-2u_{i,j}+u_{i,j-1}}{(\Delta y)^2}\right]$$

$$+ 2\left(\frac{\mu_{i+1,j}-\mu_{i-1,j}}{2\Delta x}\right)\left(\frac{u_{i,j}-u_{i-1,j}}{\Delta x}\right)$$

$$+\left(\frac{\mu_{i,j+1}-\mu_{i,j-1}}{2\Delta y}\right)\left(\frac{u_{i,j+1}-u_{i,j}}{\Delta y} + \frac{v_{i+1,j}-v_{i-1,j}}{2\Delta x}\right)$$

$$- g_c\left(\frac{\bar{P}_{i+1,j}-\bar{P}_{i-1,j}}{2\Delta x}\right) + \rho_\infty g \cos\theta \left(1 - \frac{\rho_{i,j}}{\rho_\infty}\right) \qquad (34)$$

The following coefficients are defined

$$A_1 = \frac{\mu_{i,j}}{(\Delta x)^2} \qquad B_1 = \frac{\mu_{i,j}}{(\Delta y)^2}$$

$$A_2 = \frac{|\mu_{i\Delta 1,j}-\mu_{i-1,j}|}{(\Delta x)^2} \qquad B_2 = \frac{|\mu_{i,j\Delta 1}-\mu_{i,j-1}|}{2(\Delta y)^2}$$

$$C = \rho_{i,j}\frac{|u_{i,j}|}{\Delta x} \qquad D = \rho_{i,j}\frac{|v_{i,j}|}{\Delta y} \qquad (35)$$

These coefficients, when substituted into equation (47) give the following equation.

$$C(u_{i,j}-u_{i-1,j}) - D(u_{i,j+1}-u_{i,j}) =$$

$$A_1(u_{i+1,j}-2u_{i,j}+u_{i-1,j}) + B_1(u_{i,j+1}-2u_{i,j}+u_{i,j-1})$$

$$-A_2(u_{i,j}-u_{i-1,j})$$

$$+B_2\left[u_{i,j+1}-u_{i,j} + \frac{\Delta y}{2\Delta x}(v_{i+1,j}-v_{i-1,j})\right]$$

$$- \frac{g_c}{2\Delta x}(\bar{P}_{i+1,j}-\bar{P}_{i-1,j}) + \rho_\infty g \cos\theta \left(1 - \frac{\rho_{i,j}}{\rho_\infty}\right) \qquad (36)$$

Equation (49) can be solved to give the following expression for $u_{i,j}$.

$$u_{i,j} =$$

$$\left[A_1u_{i+1,j}+(A_1+A_2+C)u_{i-1,j} + (B_1+B_2+D)u_{i,j+1} + D\,u_{i,j-1}\right.$$

$$+B_2\left(\frac{\Delta y}{2\Delta x}\right)(v_{i+1,j}-v_{i-1,j}) + \rho_\infty\ g \cos\theta \left(1 - \frac{\rho_{i,j}}{\rho_\infty}\right)$$

$$\left. - \frac{g_c}{2\Delta x}(\bar{P}_{i+1,j}-\bar{P}_{i-1,j})\right] / (2A_1+A_2+2B_1+B_2+C+D) \qquad (37)$$

The momentum equation in the y direction can be written as

$$\rho\left(u\frac{\partial v}{\partial x} + v\frac{\partial v}{\partial y}\right) = \frac{\partial}{\partial x}\left[\mu\left(\frac{\partial u}{\partial y} + \frac{\partial v}{\partial x}\right)\right]$$

$$\frac{\partial}{\partial y}\left(2\mu\frac{\partial v}{\partial y}\right) - g_c\frac{\partial \bar{P}}{\partial y} - \rho_\infty g \sin\theta \left(1 - \frac{\rho}{\rho_\infty}\right) \qquad (2)$$

The derivatives which involve μ can be expanded in the following manner

$$\rho\left(u\frac{\partial v}{\partial x} + v\frac{\partial v}{\partial y}\right) = \mu\frac{\partial^2 u}{\partial x \partial y} + \mu\frac{\partial^2 v}{\partial x^2} + \left(\frac{\partial \mu}{\partial x}\right)\left(\frac{\partial u}{\partial y} + \frac{\partial v}{\partial x}\right)$$

$$+2\mu\frac{\partial^2 v}{\partial y^2} + 2\left(\frac{\partial \mu}{\partial y}\right)\left(\frac{\partial v}{\partial y}\right) - g_c\frac{\partial \bar{P}}{\partial y} - \rho_\infty g \sin\theta\left(1 - \frac{\rho}{\rho_\infty}\right)$$

This equation can be rewritten as follows

$$\rho\left(u\frac{\partial v}{\partial x} + v\frac{\partial v}{\partial y}\right) = \mu\left(\frac{\partial^2 v}{\partial x^2} + \frac{\partial^2 v}{\partial y^2}\right) + 2\left(\frac{\partial \mu}{\partial y}\right)\left(\frac{\partial v}{\partial y}\right)$$

$$+\left(\frac{\partial \mu}{\partial x}\right)\left(\frac{\partial u}{\partial y} + \frac{\partial v}{\partial x}\right) + \mu\frac{\partial}{\partial y}\left(\frac{\partial u}{\partial x} + \frac{\partial v}{\partial y}\right) \to 0$$

$$-g_c\frac{\partial \bar{P}}{\partial y} - \rho_\infty g \sin\theta\left(1 - \frac{\rho}{\rho_\infty}\right) \qquad (38)$$

The term that is cancelled from this equation has been eliminated because of the continuity equation which will be used. The continuity equation is equation (4).

This equation will be used to calculate the pressure at each grid point based on the values of u, v, and T which have already been calculated. There is no stability problem associated with this determination, and central differences may be used in all terms except the pressure term. It will be desirable to use a forward difference approximation for the pressure term so that it may be used sequentially, starting at the outer edge of the boundary layer and

proceeding toward the plate. Because of this, only a single difference equation will be required.

Equation (38) can be transformed into a difference equation as follows.

$$\rho_{i,j}\left[u_{i,j}\left(\frac{v_{i+1,j}-v_{i-1,j}}{2\Delta x}\right) + v_{i,j}\left(\frac{v_{i,j+1}-v_{i,j-1}}{2\Delta y}\right)\right]$$

$$= -\rho_{\infty}\, g \sin\theta \left(1 - \frac{\rho_{i,j}}{\rho_{\infty}}\right)$$

$$+\mu_{i,j}\left[\frac{v_{i+1,j}-2v_{i,j}+v_{i-1,j}}{(\Delta x)^2} + \frac{v_{i,j+1}-2v_{i,j}+v_{i,j-1}}{(\Delta y)^2}\right]$$

$$+2\left(\frac{\mu_{i,j+1}-\mu_{i,j-1}}{2\Delta y}\right)\left(\frac{v_{i,j+1}-v_{i,j-1}}{2\Delta y}\right) - g_c\left(\frac{\bar{P}_{i,j+1}-\bar{P}_{i,j}}{\Delta y}\right)$$

$$+\left(\frac{\mu_{i+1,j}-\mu_{i-1,j}}{2\Delta x}\right)\left[\left(\frac{u_{i,j+1}-u_{i,j-1}}{2\Delta y}\right) + \left(\frac{v_{i+1,j}-v_{i-1,j}}{2\Delta x}\right)\right]$$

This equation can be solved for $\bar{P}_{i,j}$ to obtain

$$\bar{P}_{i,j} = \bar{P}_{i,j+1} - \frac{\Delta y}{g_c}\left\{\frac{\mu_{i,j}}{(\Delta x)^2}\left(v_{i+1,j}-2v_{i,j}+v_{i-1,j}\right)\right.$$

$$+ \frac{\mu_{i,j}}{(\Delta y)^2}\left(v_{i,j+1}-2v_{i,j}+v_{i,j-1}\right)$$

$$\left. + \left[\frac{\mu_{i,j+1}-\mu_{i,j-1}}{2(\Delta y)^2}\right]\left(v_{i,j+1}-v_{i,j-1}\right)\right.$$

$$+\left[\frac{\mu_{i+1,j}-\mu_{i-1,j}}{4(\Delta x)^2}\right]\left[\left(\frac{\Delta x}{\Delta y}\right)(u_{i,j+1}-u_{i,j-1}) + (v_{i+1,j}-v_{i-1,j})\right]$$

$$- \rho_\infty g \sin\theta \left(1 - \frac{\rho_{i,j}}{\rho_\infty}\right)$$

$$- \rho_{i,j}\left[\frac{u_{i,j}}{2\Delta x}(v_{i+1,j}-v_{i-1,j}) + \frac{v_{i,j}}{2\Delta y}(v_{i,j+1}-v_{i,j-1})\right]\Big\} \quad (39)$$

The continuity equation for the variable property solution is the same as the continuity equation for the check solution previously described. The finite difference form was derived as

$$v_{i,j} = v_{i,j-1} - \frac{\Delta y}{2\Delta x}(u_{i+1,j}-u_{i-1,j}) \qquad (19)$$

Equations (19), (32), (37), and (39) must be satisfied at each point in the grid. Starting with any set of assumed values for u, v, T, and $\bar{P}$, equations (32) and (37) may be iterated over the grid and equations (19) and (39) are used to update the values of v and $\bar{P}$, respectively. The iteration is continued until the convergence criterion is satisfied. The calculation for the average Nusselt number is performed in the same manner as outlined previously in the discussion of the check solution. To account for the variation in thermal conductivity, however, equation (26) is altered to the following form which includes the local thermal conductivity evaluated by averaging the values at the wall and at the first grid point. The form which is

applicable for the variable property case is

$$Nu_{\infty} = \frac{\bar{h}L}{k_{\infty}} = \frac{4}{3}\left(\frac{\Delta x}{\Delta y}\right)\left(\frac{k_{3,1}+k_{3,2}}{k_{\infty}}\right)\frac{(T_w-T_{3,2})}{(T_w-T_{\infty})}$$

$$+ \frac{1}{2k_{\infty}\Delta y(T-T_{\infty})}\int_{x_3}^{L}(k_{i,1}+k_{i,2})(T_w-T_{\infty})\,dx \qquad (40)$$

The integration indicated in the last term must be done by a numerical method such as Simpson's Rule.

The Difference Equations for the Constant Property Solution

In some cases, the variation of physical properties is not too severe over the range of temperature which will be encountered. When this is true, a simpler version of the equations of change (1), (2), (3), and (4), will produce satisfactory results with much less numerical computation. The reduced set of equations is

$$\frac{\partial u}{\partial x} + \frac{\partial v}{\partial y} = 0 \qquad (41)$$

$$u\frac{\partial u}{\partial x}+v\frac{\partial u}{\partial y} = \upsilon_{\infty}\left(\frac{\partial^2 u}{\partial x^2} + \frac{\partial^2 u}{\partial y^2}\right) - \frac{g_c}{\rho_{\infty}}\frac{\partial \bar{P}}{\partial x} + g\cos\theta\left(1-\frac{\rho}{\rho_{\infty}}\right) \qquad (42)$$

$$u\frac{\partial v}{\partial x} + v\frac{\partial v}{\partial y} = \upsilon_{\infty}\left(\frac{\partial^2 v}{\partial x^2} + \frac{\partial^2 v}{\partial y^2}\right) - \frac{g_c}{\rho_{\infty}}\frac{\partial \bar{P}}{\partial y} - g\sin\theta\left(1-\frac{\rho}{\rho_{\infty}}\right) \qquad (43)$$

$$u\frac{\partial T}{\partial x} + v\frac{\partial T}{\partial y} = \alpha_{\infty}\left(\frac{\partial^2 T}{\partial x^2} + \frac{\partial^2 T}{\partial y^2}\right) \qquad (44)$$

The finite difference approximations for these equations may be derived in the same manner as those in the preceeding examples. Only the final form of each equation will be presented here.

Equation (44) includes one additional term that was not considered in the transformation of equation (7) to a difference equation. This additional term is approximated as

$$\alpha_\infty \frac{\partial^2 T}{\partial x^2} \simeq \alpha_\infty \frac{T_{i+1,j}-2T_{i,j}+T_{i-1,j}}{(\Delta x)^2}$$

The coefficient A_x is defined as

$$A_x = \frac{\alpha_\infty}{(\Delta x)^2} \tag{45}$$

Three other coefficients have been defined previously. They are

$$A_y = \frac{\alpha_\infty}{(\Delta y)^2}$$

$$B = \frac{|u_{i,j}|}{\Delta x}$$

$$C = \frac{|v_{i,j}|}{\Delta y} \tag{12}$$

The equation for $T_{i,j}$ is written as

$$T_{i,j} = \frac{(A_y+C)T_{i,j+1}+A_yT_{i,j-1}+A_xT_{i+1,j}+(A_x+B)T_{i-1,j}}{2\,A_x + 2\,A_y + B + C} \qquad (46)$$

The momentum equation in the x direction, (42), contains two additional terms which were not considered in equation (6). These two terms are approximated as

$$\upsilon_\infty \frac{\partial^2 u}{\partial x^2} \simeq \upsilon_\infty \left[\frac{u_{i+1,j}-2u_{i,j}+u_{i-1,j}}{(\Delta x)^2}\right]$$

$$\frac{g_c}{\rho_\infty}\frac{\partial P}{\partial x} \simeq \frac{g_c}{\rho_\infty}\left[\frac{\bar{P}_{i+1,j}-\bar{P}_{i-1,j}}{2\Delta x}\right]$$

The coefficients that are applicable to this equation are

$$A_x = \frac{\upsilon_\infty}{(\Delta x)^2} \qquad A_y = \frac{\upsilon_\infty}{(\Delta y)^2}$$

$$B = \frac{|u_{i,j}|}{\Delta x} \qquad C = \frac{|v_{i,j}|}{\Delta y} \qquad (47)$$

The final equation for $u_{i,j}$ is

$$u_{i,j} = \left[(A_y+C)u_{i,j+1} + A_yu_{i,j-1}+A_xu_{i+1,j}\right.$$

$$+ (A_x+B)u_{i-1,j}+g\cos\theta\left(1-\frac{\rho_{i,j}}{\rho_\infty}\right)$$

$$\left. - \frac{g_c}{\rho_\infty}\left(\frac{\bar{P}_{i+1,j}-\bar{P}_{i-1,j}}{2\Delta x}\right)\right] /(2A_x+2_y+B+C) \qquad (48)$$

The momentum equation in the y direction was not included in the check solution but may be approximated in

the same manner as equation (2) of the variable property solution. This equation will be used to solve for the pressure and no provision for sign changes in the velocity components is required. The difference equation form of equation (43) is written as

$$u_{i,j}\left(\frac{v_{i+1,j}-v_{i-1,j}}{2\Delta x}\right)+ v_{i,j}\left(\frac{v_{i,j+1}-v_{i,j-1}}{2\Delta y}\right)$$

$$= \upsilon_{\infty}\left[\frac{v_{i+1,j}-2v_{i,j}+v_{i,j-1}}{(\Delta x)^2}\right.$$

$$\left. + \frac{v_{i,j+1}-2v_{i,j}+v_{i,j-1}}{(\Delta y)^2}\right]- \frac{g_c}{\rho_{\infty}}\left(\frac{\bar{P}_{i,j+1}-\bar{P}_{i,j}}{\Delta y}\right)-g \sin\theta \left(1- \frac{\rho_{i,j}}{\rho_{\infty}}\right)$$

This equation is solved for $P_{i,j}$ to obtain

$$\bar{P}_{i,j} = \bar{P}_{i,j+1} -\left(\frac{\rho_{\infty}\Delta y}{g_c}\right)\left\{\upsilon_{\infty}\left[\frac{v_{i+1,j}-2v_{i,j}+v_{i-1,j}}{(\Delta x)^2}\right.\right.$$

$$\left. + \frac{v_{i,j+1}-2v_{i,j}+v_{i,j-1}}{(\Delta y)^2}\right] - g \sin\theta \left(1 - \frac{\rho_{i,j}}{\rho_{\infty}}\right)$$

$$\left. - u_{i,j}\left(\frac{v_{i+1,j}-v_{i-1,j}}{2\Delta x}\right) - v_{i,j}\left(\frac{v_{i,j+1}-v_{i,j-1}}{2\Delta y}\right)\right\} \qquad (49)$$

The continuity equation, (41), is the same as the one for the check solution. The finite difference equation has previously been given as

$$v_{i,j} = v_{i,j-1} - \frac{\Delta y}{2\Delta x}(u_{i+1,j} - u_{i-1,j}) \qquad (19)$$

The solution to the constant property version of the original equations is complete when equations (19), (46), (48), and (49), have been satisfied at each grid point. The same criterion for judging convergence of the iteration should be employed here. The average Nusselt number may be calculated by using equation (26) which was derived for the check solution but is applicable here because the thermal conductivity is considered constant.

CHAPTER IV

EXPERIMENTAL PROGRAM

An experimental program was undertaken at Mississippi State University to provide data on average heat transfer rates from inclined isothermal flat plates. This program was directed and closely supervised by the author. It was carried out by seven graduate students and the individual phases were the subject of their (Master's) theses in Mechanical Engineering, (24), (25), (26), (27), (28), (29), and (30).

The first two theses, (24) and (25), describe the experimental studies with air as the heat transfer medium. The last five theses describe the experiments performed with oil as the heat transfer medium. Each thesis is a separate work, complete within itself, describing the experimental apparatus and procedure, correlating the individual results, and presenting an error analysis for that portion of the total program. Each student was advised about the work which had been done and the scope of the total program. His work was closely supervised and the need for accuracy and correct experimental techniques was emphasized. Within the framework of correct and valid observation each student was allowed to analyze his data as he desired.

The results of these seven experiments were gratifying. Each student accepted his role in the overall program and performed his individual portion adequately. The primary contribution of Douglass (24) was the construction of the apparatus used in the air experiment. He demonstrated that the heating arrangement could maintain an isothermal plate surface. The data that he took were inconsistent which was attributed to errors in measurement at low power input settings. Patel (25) revised the instrumentation and was able to achieve reproducible results. The data still exhibited considerable scatter which was considered normal for free convection experiments in gases.

The experiments in oil were initiated by Farmer (26). He was responsible for the construction of the apparatus and the initial checkout of the instrumentation. His data were taken for the vertical plate only and was reported in a paper by Farmer and McKie (31). The other four experiments were performed for angles of inclination of 20, 30, 40, and 45 degrees. Although individual differences in experimental technique can be recognized when the entire set of data is analyzed, the experimental results of the individuals were correlated with a correlation coefficient greater than 0.97 for four sets and greater than 0.92 for the remaining set of data.

The details of the individual experiments and the

reported results may be obtained from the theses. The data will be presented on several of the figures given in the next chapter to complete the results of both the theoretical and experimental parts of the total problem.

CHAPTER V

ANALYSIS AND RESULTS

The general results of the analytical work may be divided into two categories: the average Nusselt number and velocity, temperature, and pressure profiles for each different set of boundary conditions. The experimental results consist of only the average Nusselt number. The analytical work was divided into three sections. The first was a check solution designed primarily to verify the analytical method. The other two sections include the variable property solution for oil and the constant property solution for air. Experimental results for both air and oil are presented.

Analytical Results

Check Solution

The check solution was used to determine the grid pattern and geometry and to verify the numerical calculation for the average Nusselt number. The finite difference calculations described in Chapter III were carried out for six different plate temperatures with air as the fluid medium. The iteration of each case was terminated when the change in the u velocity component was reduced to less than 0.001 feet per second at each point in the grid and the

change in the temperature was less than 0.0005 degrees Fahrenheit at each point. The calculation of the average Nusselt number was made after each iteration and at termination of the iteration procedure that Nusselt number was changing about 0.02 from one iteration to the next. The numerical integration for the average Nusselt number was performed using the approximation, $h \simeq x^{-1/4}$, over the first two grid points and Simpson's Rule over the remainder of the plate. The results are given in Table 1, page 47. For comparison, the Nusselt number was calculated using the equation:

$$Nu_{Ostrach} = 0.66 \left(\frac{Gr_\infty}{4}\right)^{1/4} \qquad (50)$$

which was recommended by Ostrach for a Prandtl number of 0.7. Figures 3 and 4, pages 48 and 49, show the comparison between the present theoretical results and that of Ostrach. The deviation at the higher Grashof numbers may be explained by the difficulty in determining the degree of convergence of the iterative procedure. For these solutions the change in the average Nusselt number was not utilized as part of the convergence test because, at this point, the final method of calculating the Nusselt number had not been determined. The choice of $x_3 = 2\ \Delta x$ was based on these results and the change in the Nusselt number was incorporated in the convergence tests for subsequent solutions.

Table 1. Analytical Results for Check Solution

T_w	T_∞	Pr_∞	Gr_∞	Nu_∞	$Nu_{Ostrach}$
120	70	0.7	3.1×10^9	108.7	109.7
140	70	0.7	4.3×10^9	117.6	119.3
180	70	0.7	6.7×10^9	130.5	133.7
200	70	0.7	7.9×10^9	135.4	139.3
240	70	0.7	1.0×10^{10}	143.6	148.9
280	70	0.7	1.3×10^{10}	150.2	157.3

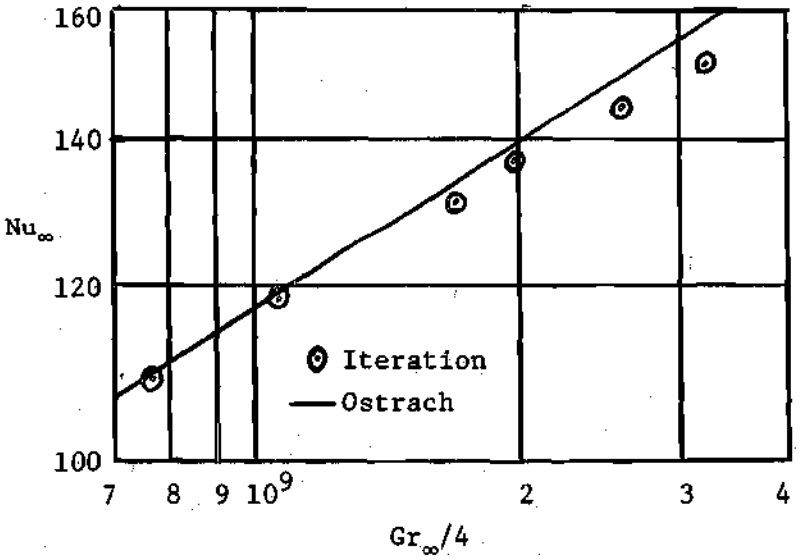

Figure 3. Comparison of Iteration Solution with Ostrach.

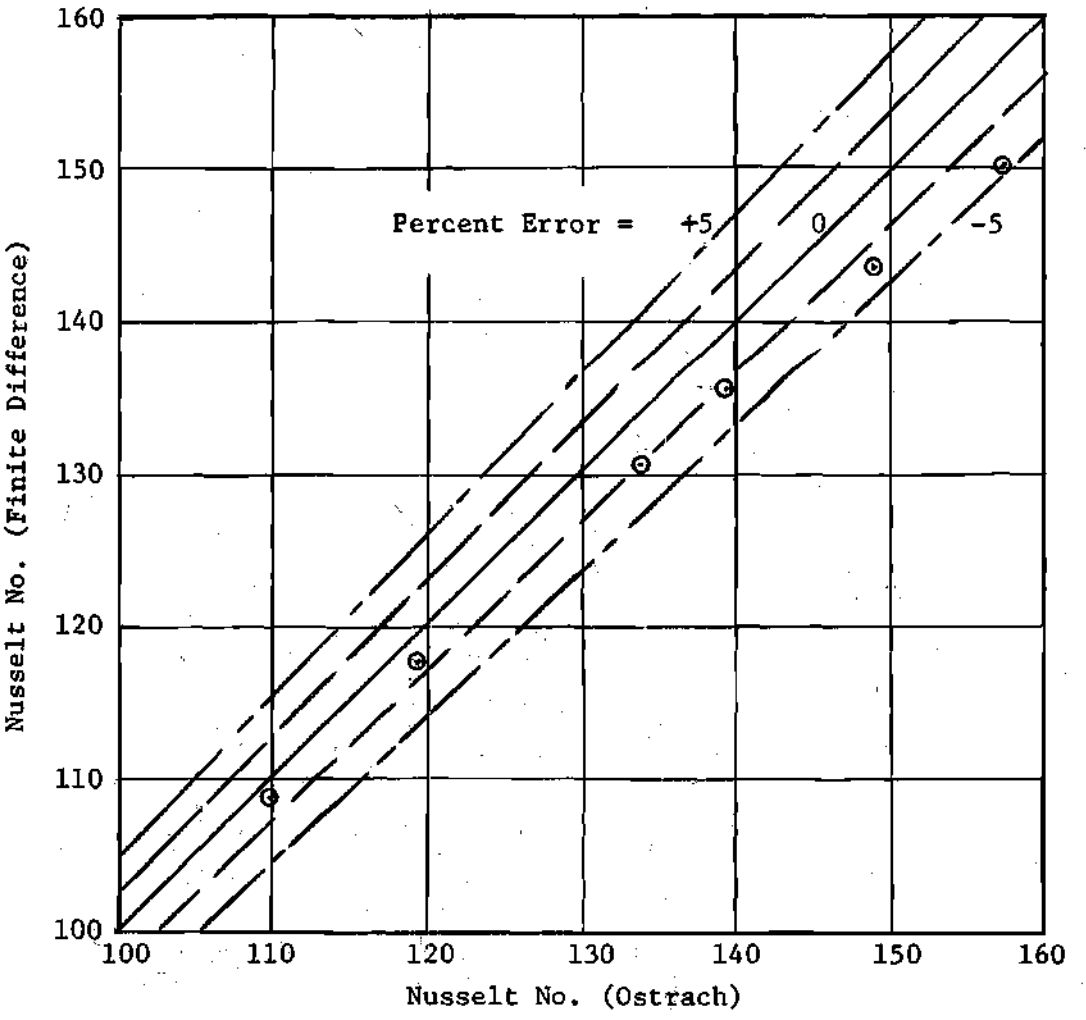

Figure 4. Comparison of Nusselt Numbers.

A further comparison with the work of Ostrach is obtained by calculating the dimensionless parameters η, F', and H defined by Ostrach as

$$\eta = \left(\frac{Gr_x}{4}\right)^{1/4} \frac{y}{x}$$

$$F'(\eta) = \frac{ux/\upsilon_\infty}{2\sqrt{Gr_x}}$$

$$H(\eta) = \frac{T-T_\infty}{T_w-T_\infty} \qquad (51)$$

Figures 5 and 6, pages 51 and 52, show how the iterative procedure of this investigation compares with the similarity solution of Ostrach. Profiles at three positions along the plate are presented.

It is noted that the temperature profiles show excellent agreement, but the velocity profiles tend to diverge at the outer edge of the boundary layer. The body force term used in this part of the present investigation was the only departure from the equations used by Ostrach. However, in the vicinity of the plate the results are almost identical and there is good overall agreement between the results of this investigation and those of Ostrach.

Variable Property Solution for Oil

The physical properties of the Necton-45 oil used in the experimental investigation were expressed as functions

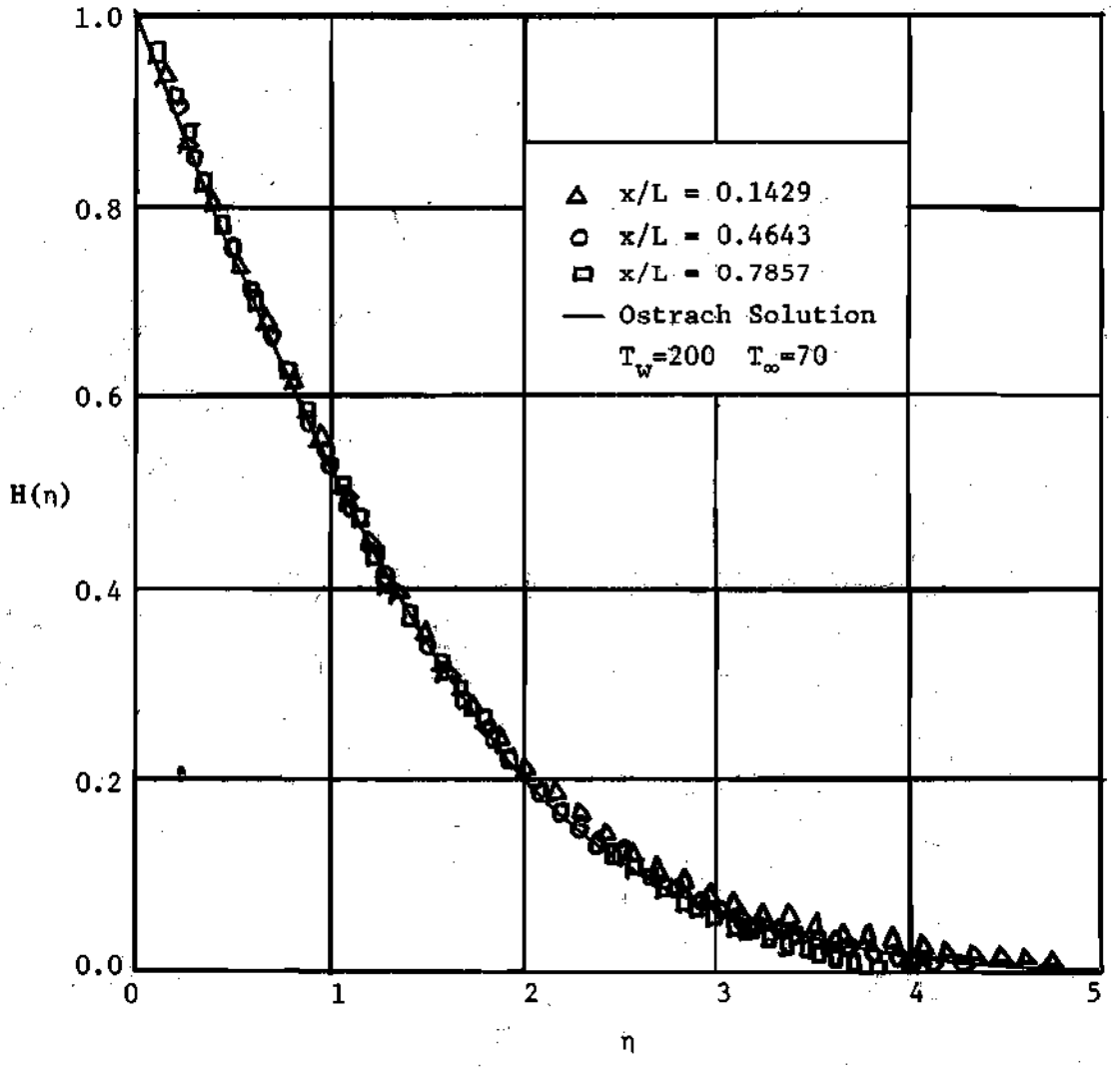

Figure 5. Comparison of Temperature Profiles.

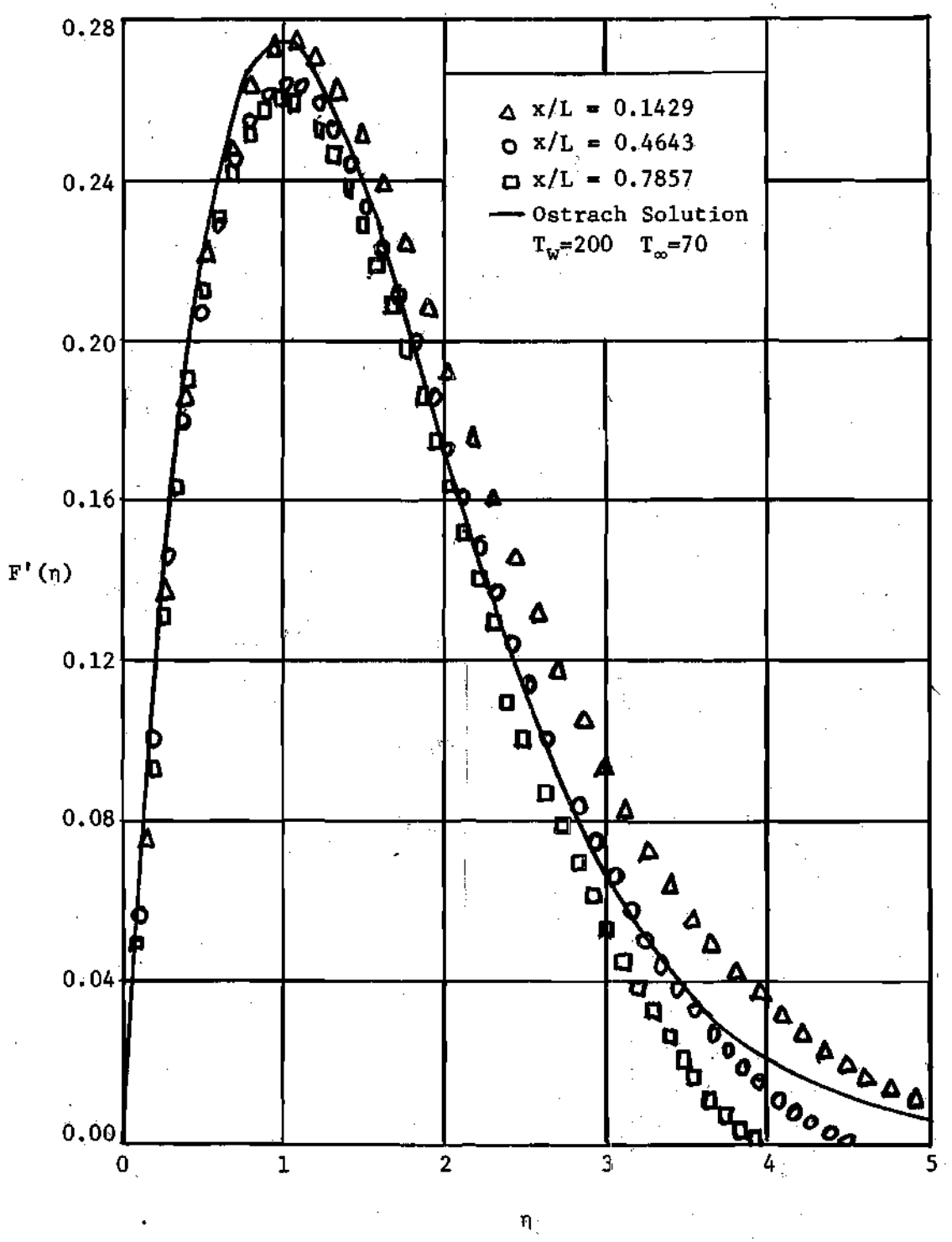

Figure 6. Comparison of Velocity Profiles.

of temperature and used in this solution. These functions are given in Appendix A. The finite difference equations discussed in Chapter III which retained the variable property terms were used, and an iteration procedure similar to that of the check solution was employed. The same convergence criterion based on reducing the relative change in velocity and temperature values between iterations to an acceptable level, while observing also the relative change in the Nusselt number, was used in this case. Twenty five separate sets of boundary conditions were considered. There were five different conditions of the temperatures T_w and T_∞, with five angles of inclination for each. The boundary conditions for temperature were chosen to provide a wide range in the Prandtl number (by varying T_∞) and in the Grashof number (by varying $T_w - T_\infty$). Angles of inclination from the vertical were 0, 20, 30, 40, and 45 degrees.

The numerical integration procedure for calculating the Nusselt number was the same as before. The Nusselt numbers for these 25 calculations are summarized in Table 2, page 54.

The plate was one foot in length and the grid pattern extended 0.1429 feet below the lower edge and above the upper edge. Twenty nine grid points were included along the plate with four additional points above and four additional points below the plate. Sixty grid points were evenly

Table 2. Analytical Results for Variable Property Solution

T_w	T_∞	Pr_∞	Gr_∞	Angle of Inclination				
				0°	20°	30°	40°	45°
				Nu_∞				
120	40	3792	9.3×10^4	132	131	129	127	125
180	50	2563	3.4×10^5	182	181	178	174	172
220	60	1794	8.7×10^5	216	215	212	207	204
240	70	1295	1.8×10^6	236	234	231	226	223
260	100	565	9.5×10^6	263	260	257	251	246

spaced in the direction normal to the plate. The physical dimension in this direction was chosen so that about ten grid points would fall within the boundary layer before the velocity component parallel to the plate attained its maximum value. The physical dimension of the flow field in the direction normal to the plate thus varied from a minimum of 0.037 feet to a maximum 0.1 feet.

Figures 7, 8, 9, 10, and 11, pages 56, 57, 58, 59, and 60, show u velocity, temperature, and pressure profiles at three positions up the plate. These locations are 0.1071, 0.5, and 0.8929 feet from the leading edge (grid lines i=8, 19, and 30). The temperature boundary conditions are the same for each of these. The angle of inclination is the parameter that has various values. The u velocity and the temperature profiles exhibit expected results for the fluid flowing upward past a heated plate. The pressure profile shows that in all cases the pressure near the surface is greater than the hydrostatic pressure existing at the plate surface. The y direction is horizontal for the vertical plate only. In the other four cases, the inclination of the plate would cause a local increase in the hydrostatic pressure at points outward along a line normal to the plate. The pressure increase from the local hydrostatic condition may be visualized from these figures by simply superimposing the local variation of the hydrostatic pressure shown in

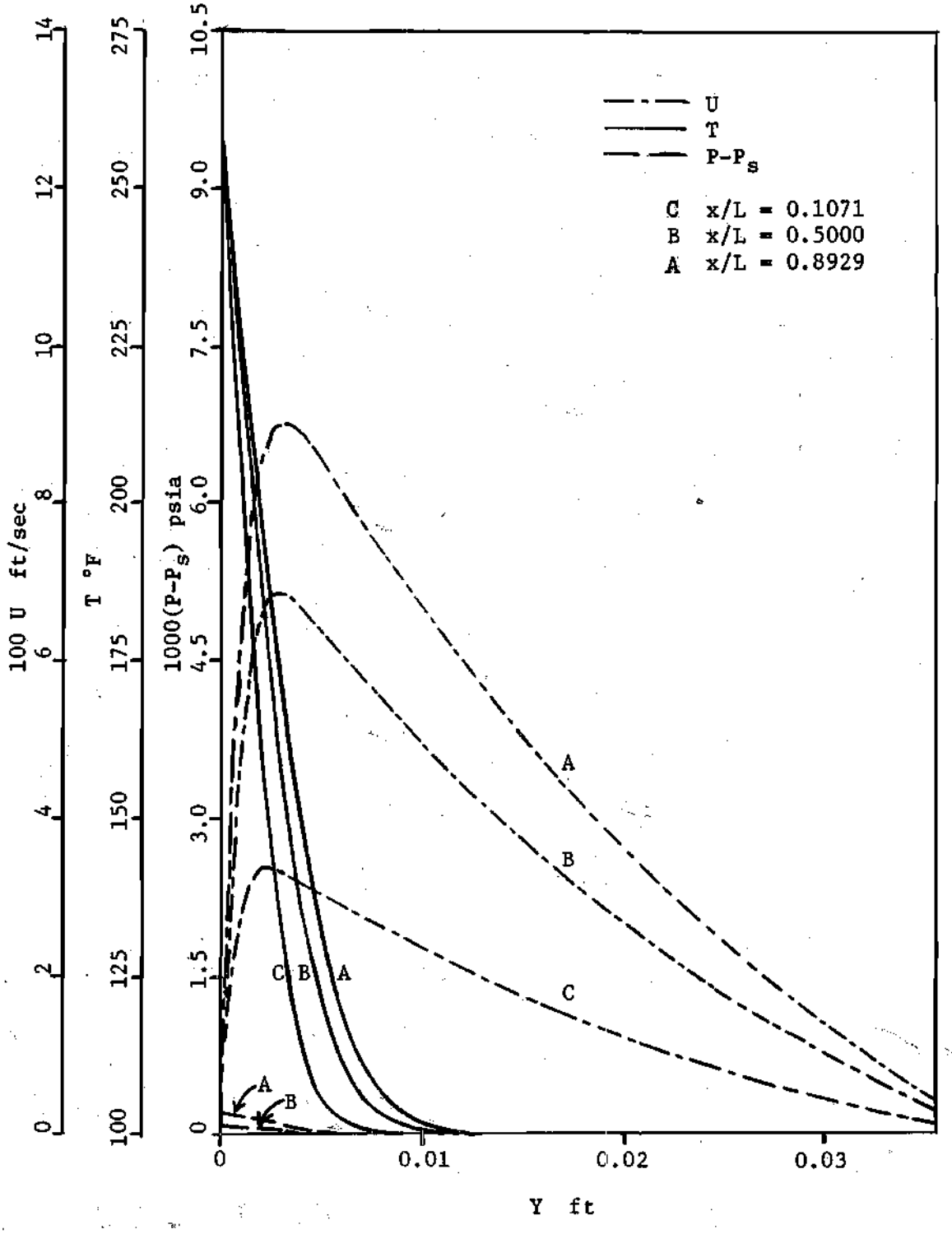

Figure 7. Profiles for Oil Experiment at θ=0°.

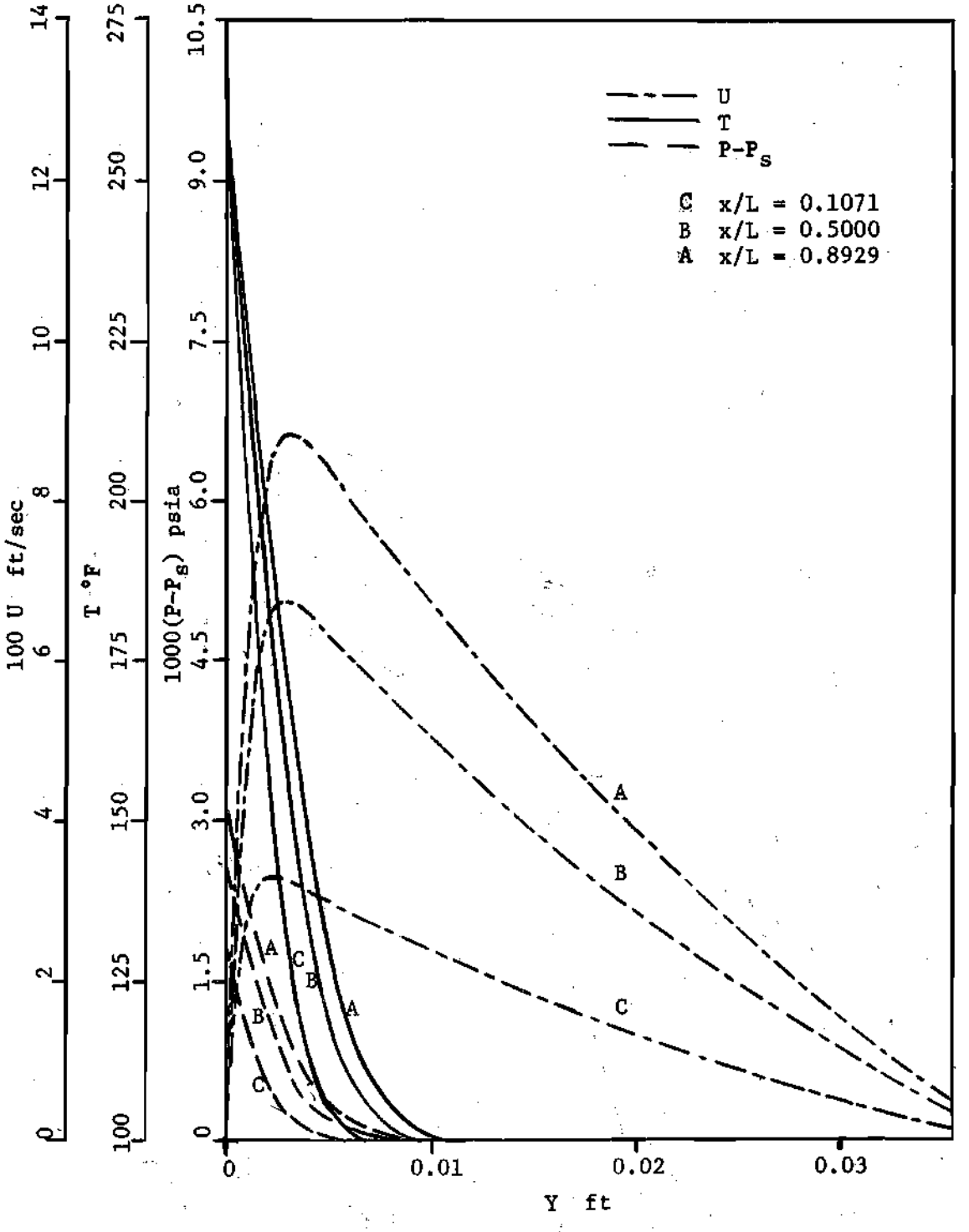

Figure 8. Profiles for Oil Experiment at θ=20°.

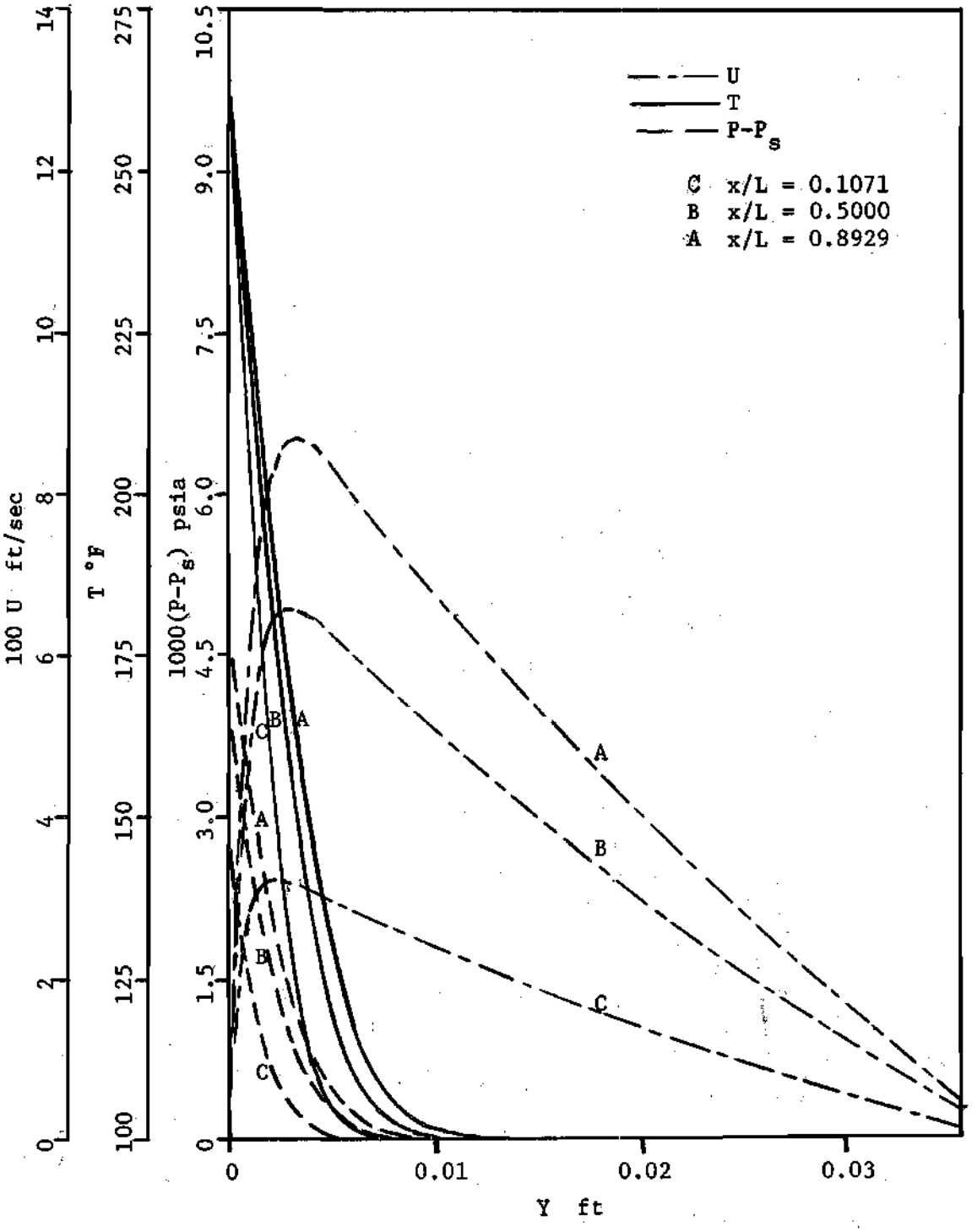

Figure 9. Profiles for Oil Experiment at Θ=30°.

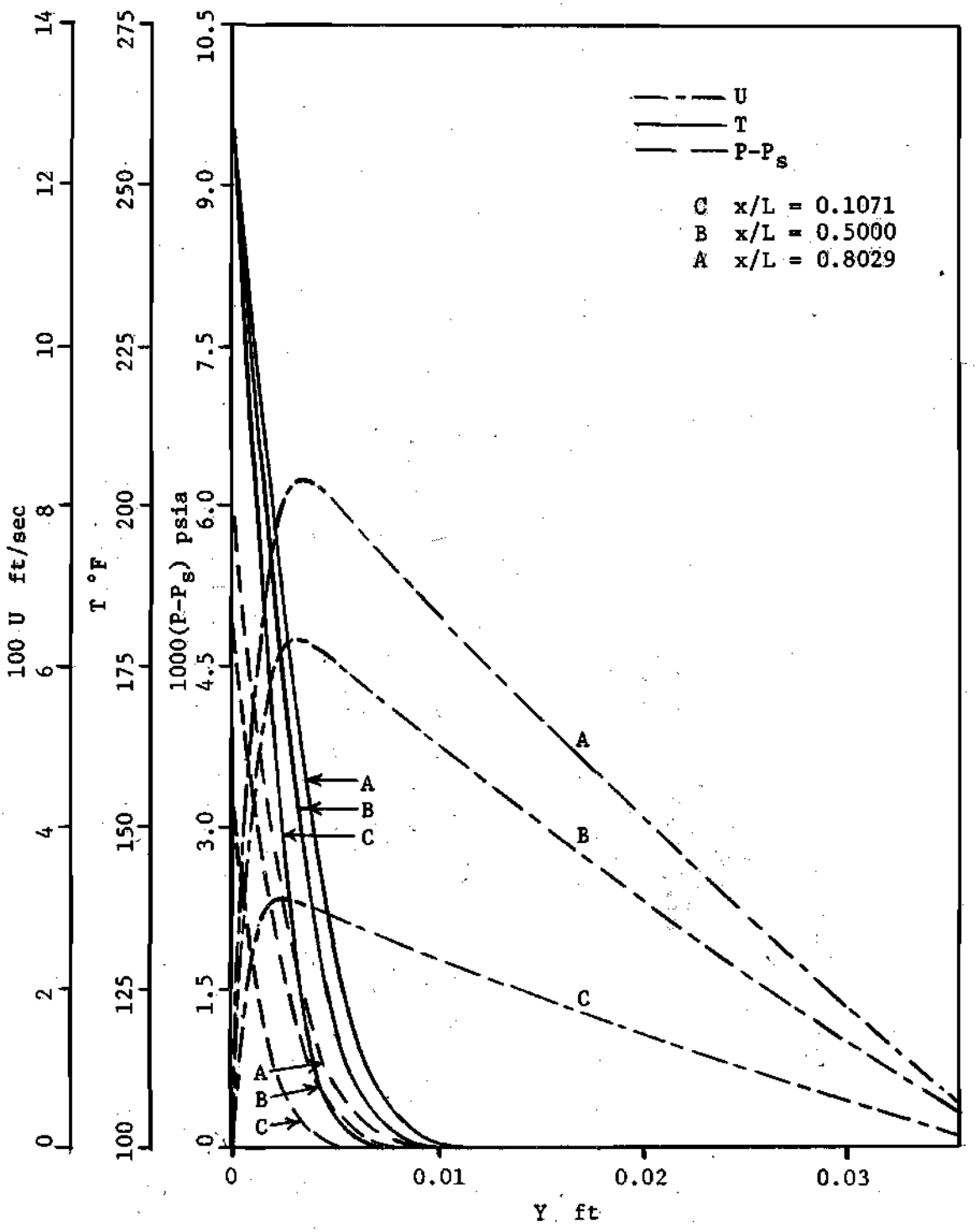

Figure 10. Profiles for Oil Experiment at Θ=40°.

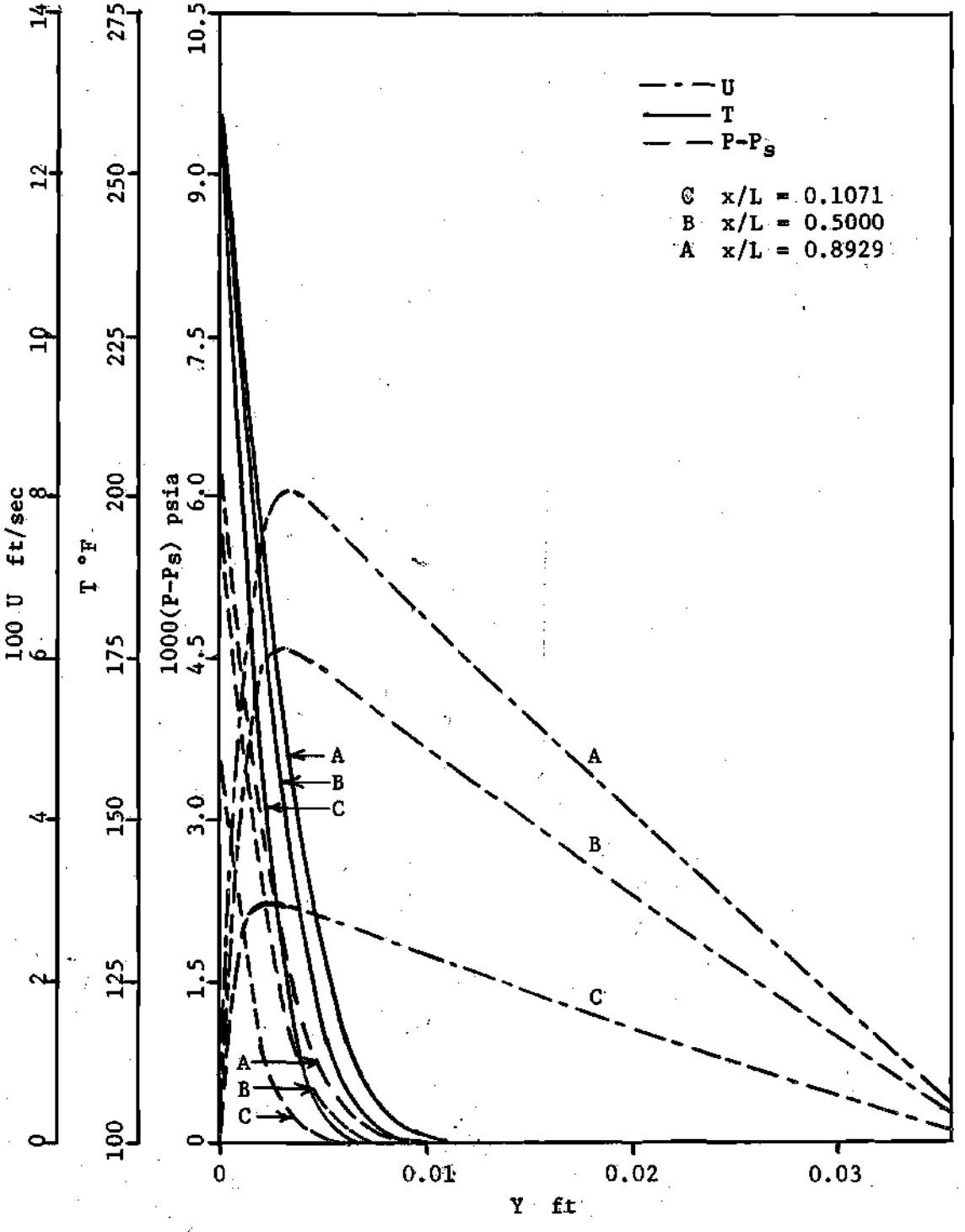

Figure 11. Profiles for Oil Experiment at θ=45°.

Figure 12, page 62. This results in curves showing a pressure increase from the local hydrostatic pressure that will be similar to Figure 13, page 62. These curves show that the difference in surface pressure and local hydrostatic pressure increases up the plate.

Figure 14, page 63, shows the pressure profiles for the line normal to the midpoint of the plate for the five angles of inclination. The hydrostatic reference pressure for these curves is the same. If curves such as Figure 13, page 62, were drawn, the local hydrostatic pressure would vary with the angle of inclination. It is apparent from these curves that the pressure is not 'impressed across the boundary layer' in the normal direction nor is the pressure constant along the horizontal lines.

Figure 15, page 64, depicts the u velocity profile at the midpoint of the plate for the five angles of inclination. As the plate is inclined the maximum value of the u velocity decreases, but the u velocity at the outer edge of the boundary layer becomes larger. There is very little effect in the vicinity of the wall and the shear stress at the wall would be approximately independent of the angle of inclination. Also the curves in the region near the wall do not cross and the shear stress will decrease for increasing angles of inclination.

The temperature profiles at the midpoint of the plate

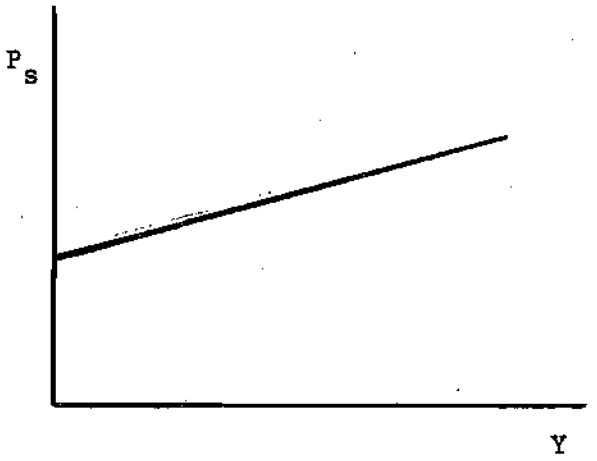

Figure 12. Hydrostatic Pressure.

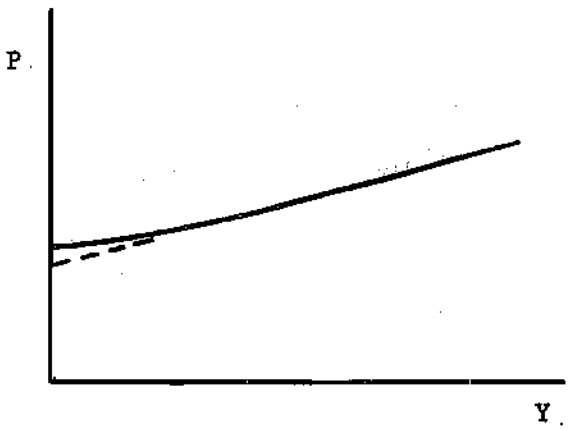

Figure 13. Pressure Profile Relative to Local Hydrostatic Pressure.

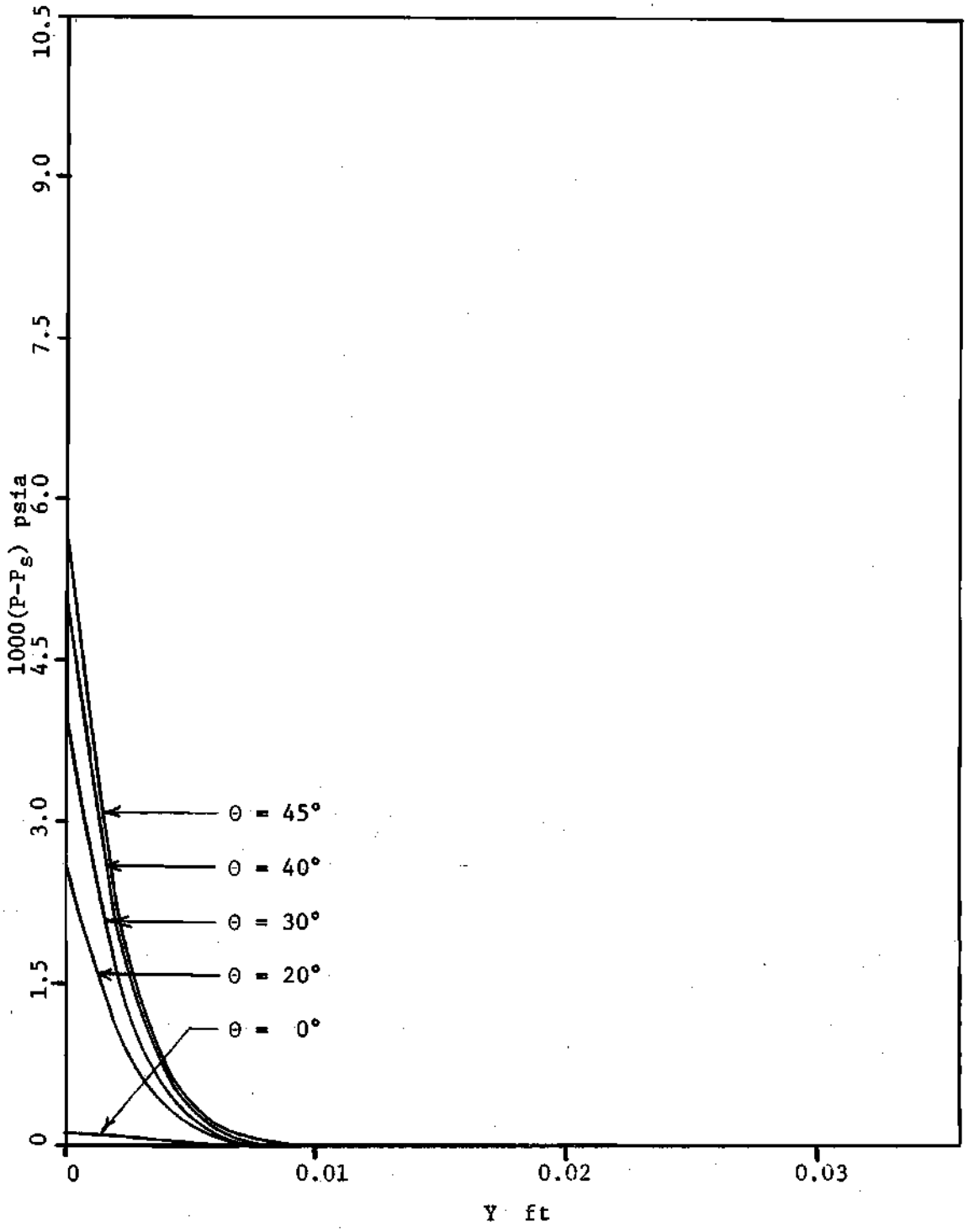

Figure 14. Pressure Profiles at Midpoint of Plate.

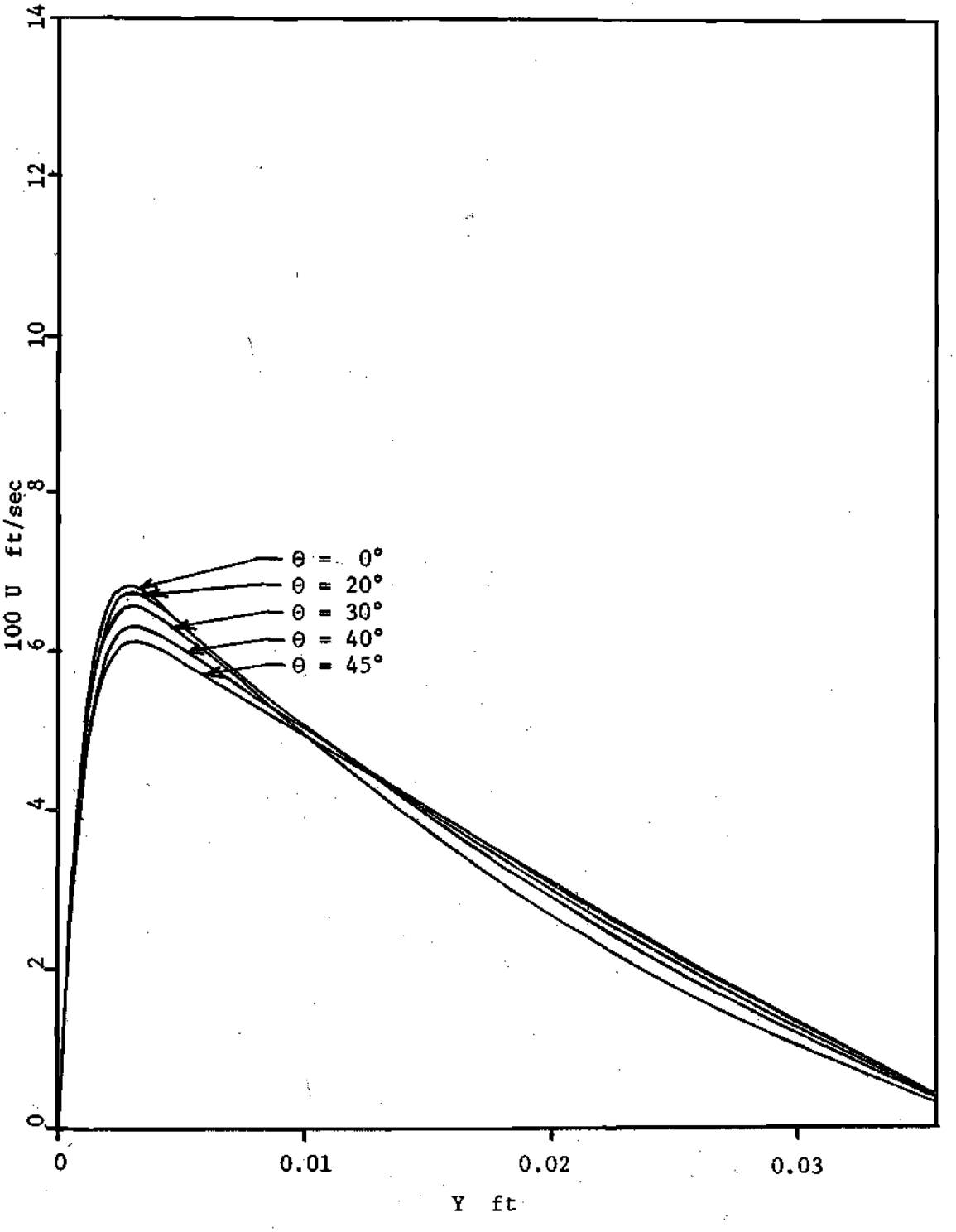

Figure 15. Velocity Profiles at Midpoint of Plate.

for the five angles of inclination are shown in Figures 16 and 17, pages 66 and 67. Figure 16 is included only to show the relative thicknesses of the thermal and the hydrodynamic boundary layers. Figure 17 indicates the slightly higher values of temperature that result (along the midpoint profile) when the plate is inclined. This figure includes only the first nine intervals in the grid pattern.

The other twenty solutions for the remaining four boundary conditions for temperature are similar to the ones just discussed. A correlation of the Nusselt number as a function of the Prandtl number and the Grashof number and the angle of inclination will be discussed later.

Constant Property Solution for Air

The finite difference equations developed in Chapter III for the case of constant physical properties were used in the theoretical solutions for air. Twenty five separate sets of boundary conditions were used. As before, five different conditions of the temperatures, T_w and T_∞, were chosen, and the same five angles of inclination were studied for each. The numerical results for the Nusselt number are summarized in Table 3, page 68.

The physical height for the plate considered in this study was three feet because experiments were carried out with a plate of this size. The flow field extended 0.4286 feet above the upper edge. Twenty nine grid points were

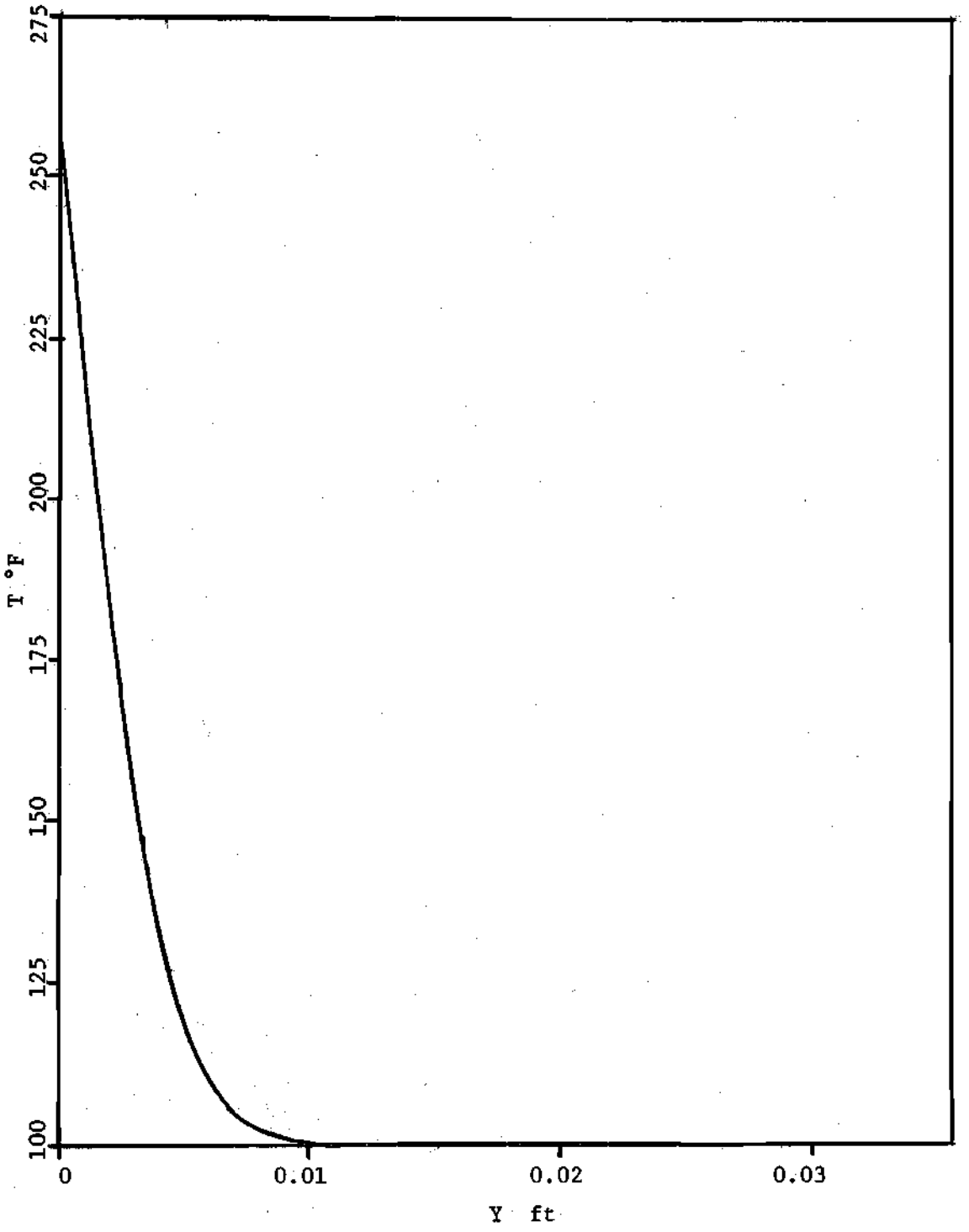

Figure 16. Complete Temperature Profile at Midpoint of Plate.

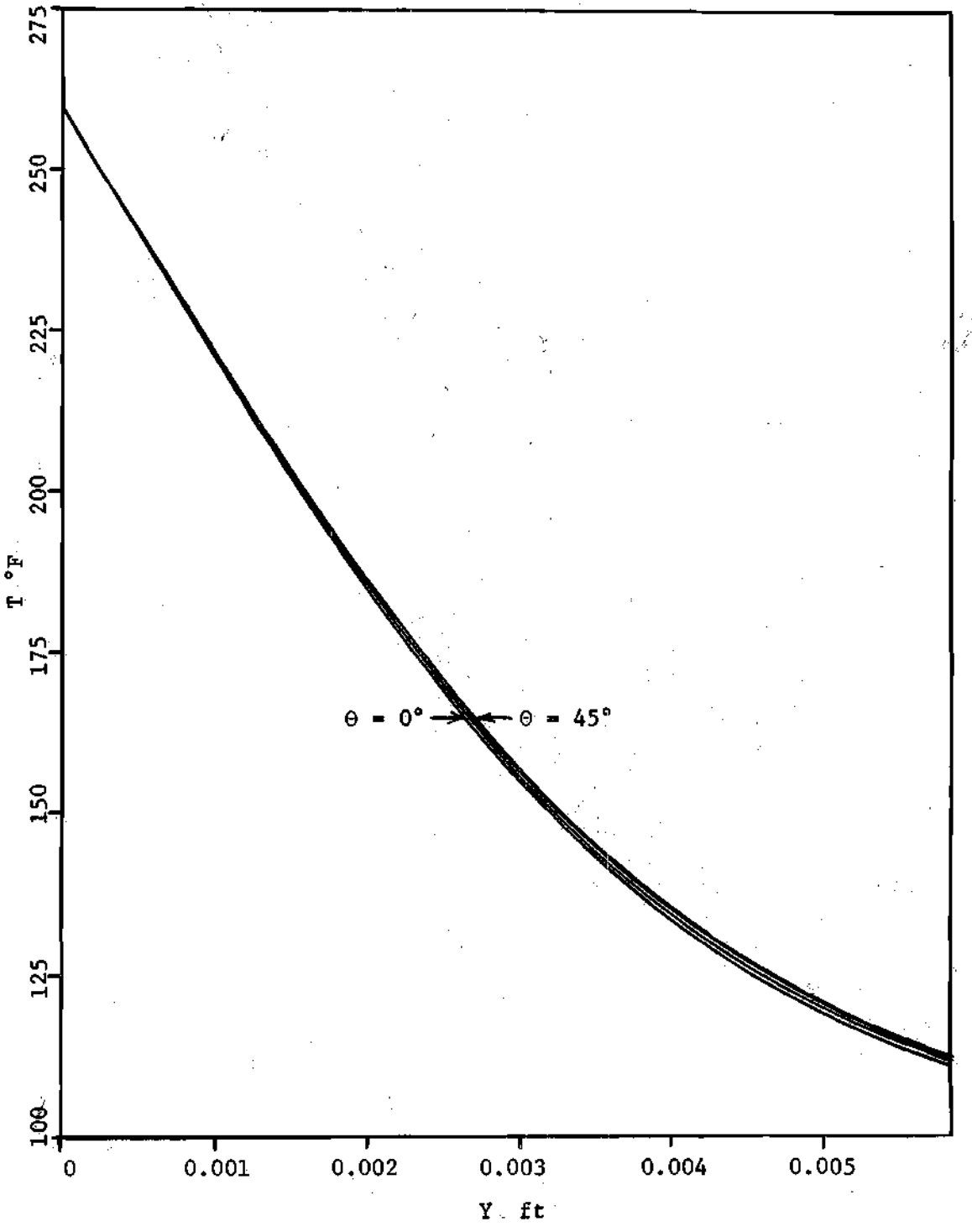

Figure 17. Partial Temperature Profile at Midpoint of Plate.

Table 3. Analytical Results for Constant Property Solution

T_w	T	Pr_∞	Gr_∞	Angle of Inclination				
				0°	20°	30°	40°	45°
				Nu_∞				
120	70	0.7	3.1×10^9	109	108	106	103	101
160	70	0.7	5.5×10^9	126	124	121	118	116
200	70	0.7	8.0×10^9	137	135	132	128	125
240	70	0.7	1.0×10^{10}	145	143	140	136	133
280	70	0.7	1.3×10^{10}	152	149	146	142	139

included along the plate with four grid points both above and below the plate. Sixty grid points were used in the direction normal to the plate in this investigation, with the physical size being determined in a similar fashion to the previous investigation. The maximum value of y varied from 0.05 to 0.065 feet during these calculations.

Figures 18, 19, 20, 21, and 22, pages 70, 71, 72, 73, and 74, show representative u velocity, temperature, and pressure profiles at three positions along the plate. These locations were 0.3214, 1.5, and 2.6786 feet from the leading edge (grid lines i=8, 19, and 30). Figures 23, 24, and 25, pages 75, 76, and 77, present a comparison of the profiles for a single grid line, at the midpoint of the plate, as the angle of inclination is varied. These figures display results similar to those previously discussed and the same comments apply in this case.

Comparison of Solutions With and Without the Normal Momentum Equation

As part of the overall numerical investigation of this problem, three other solutions were generated. A solution for oil using the same four equations as in the solutions previously described was done with the property values considered constant and evaluated at T_{∞}. Solutions for both air and oil, with constant properties, were done with only the continuity equation, momentum equation, parallel to

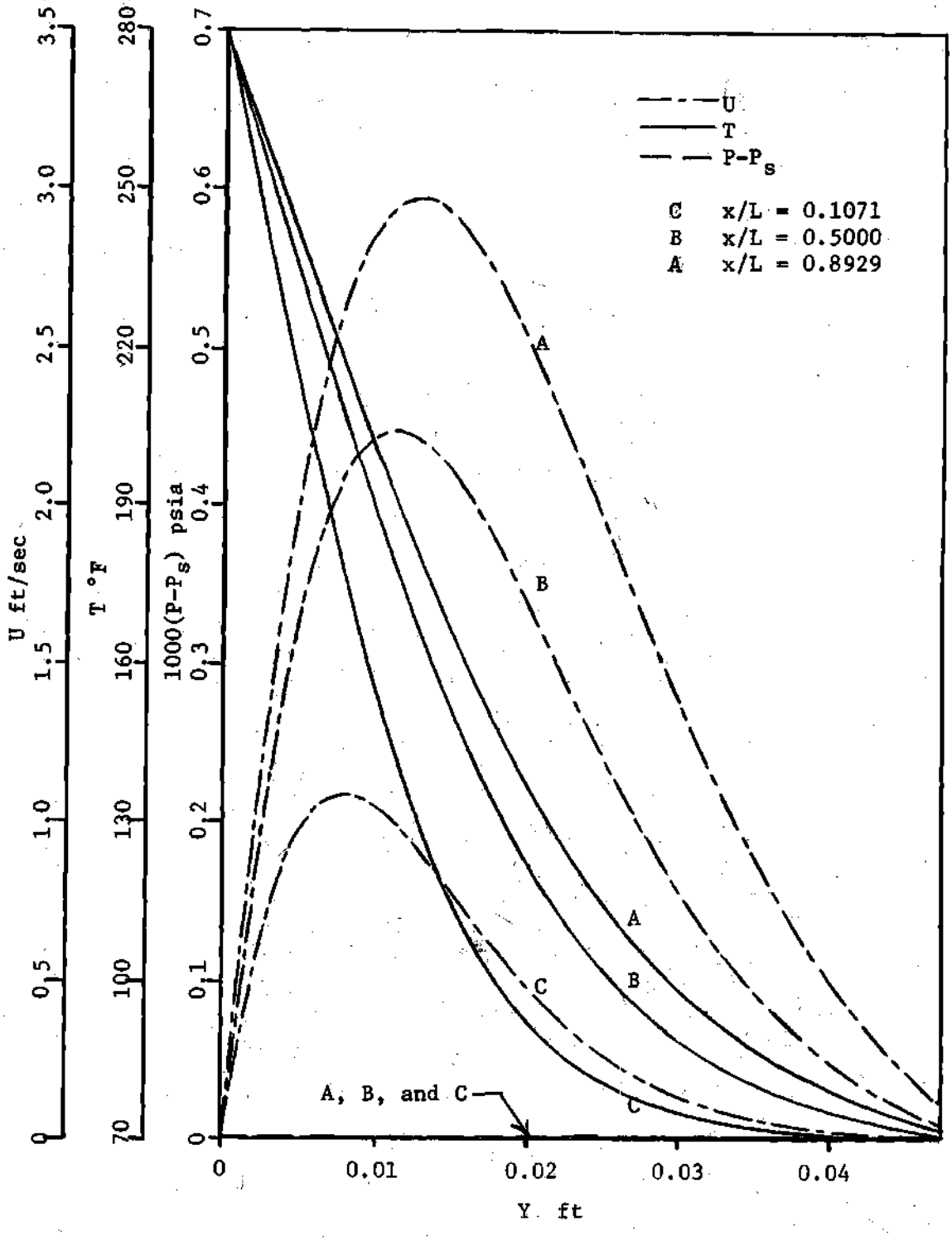

Figure 18. Profiles for Air Experiment at $\theta=0°$.

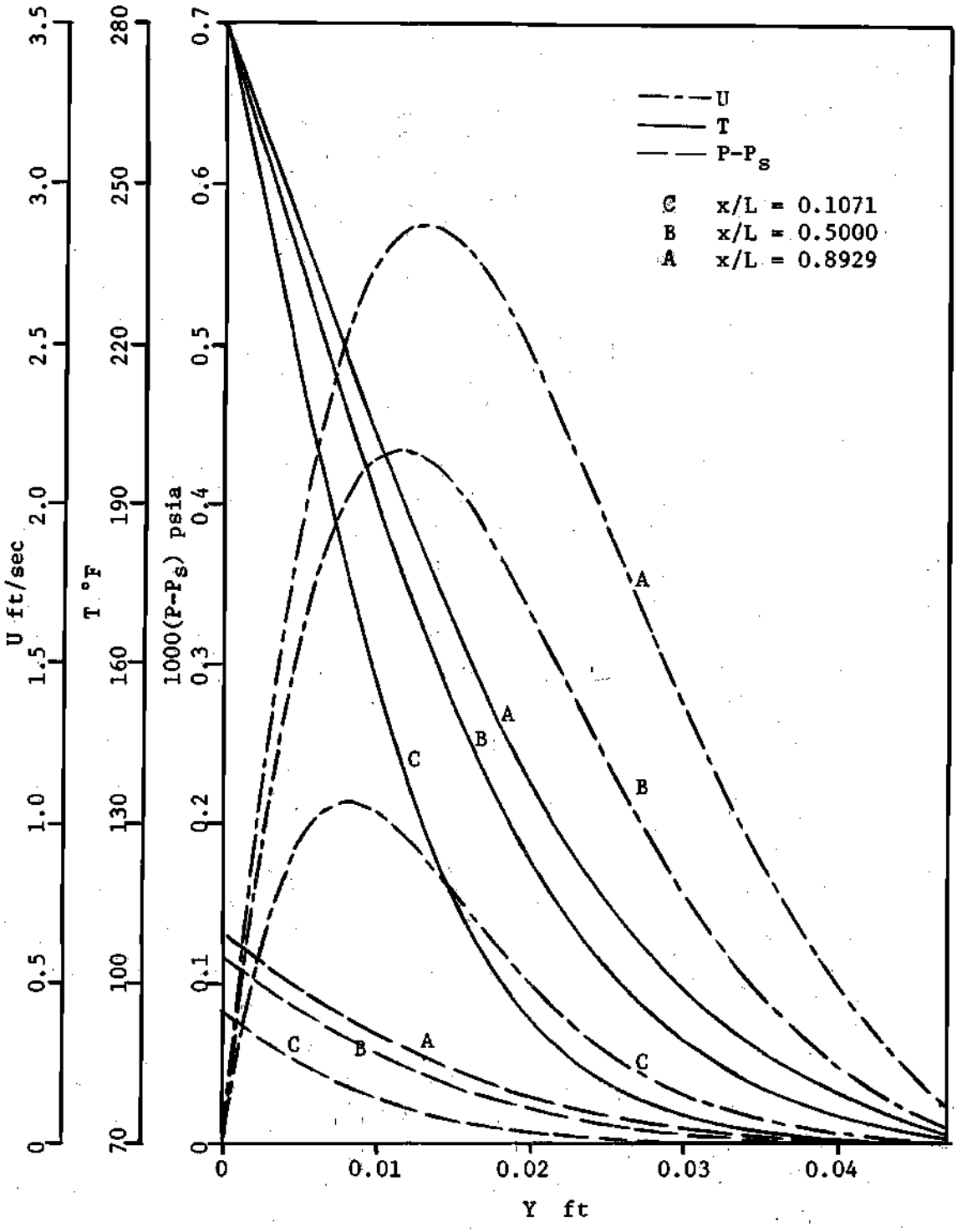

Figure 19. Profiles for Air Experiment at Θ=20°.

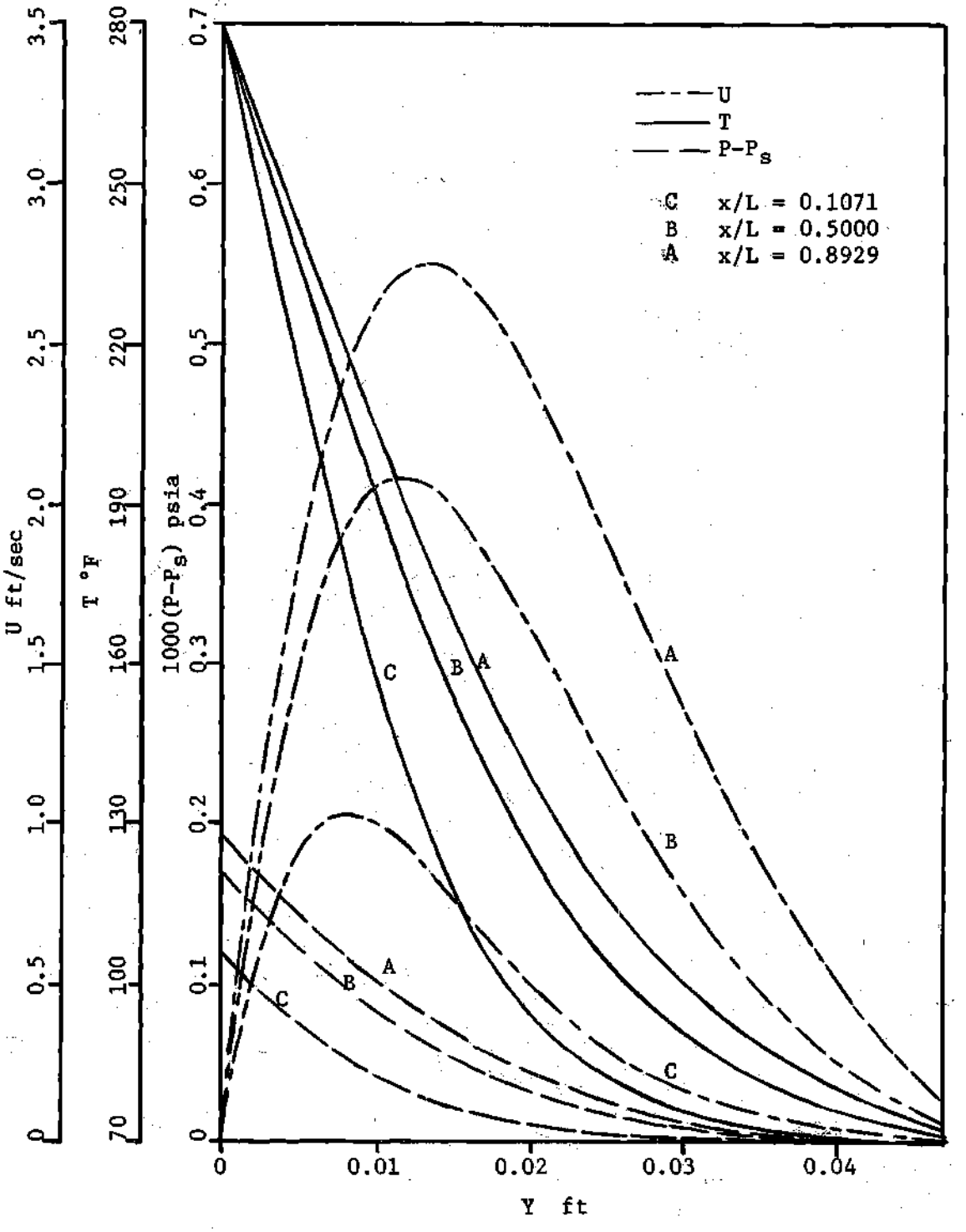

Figure 20. Profiles for Air Experiment at θ=30°.

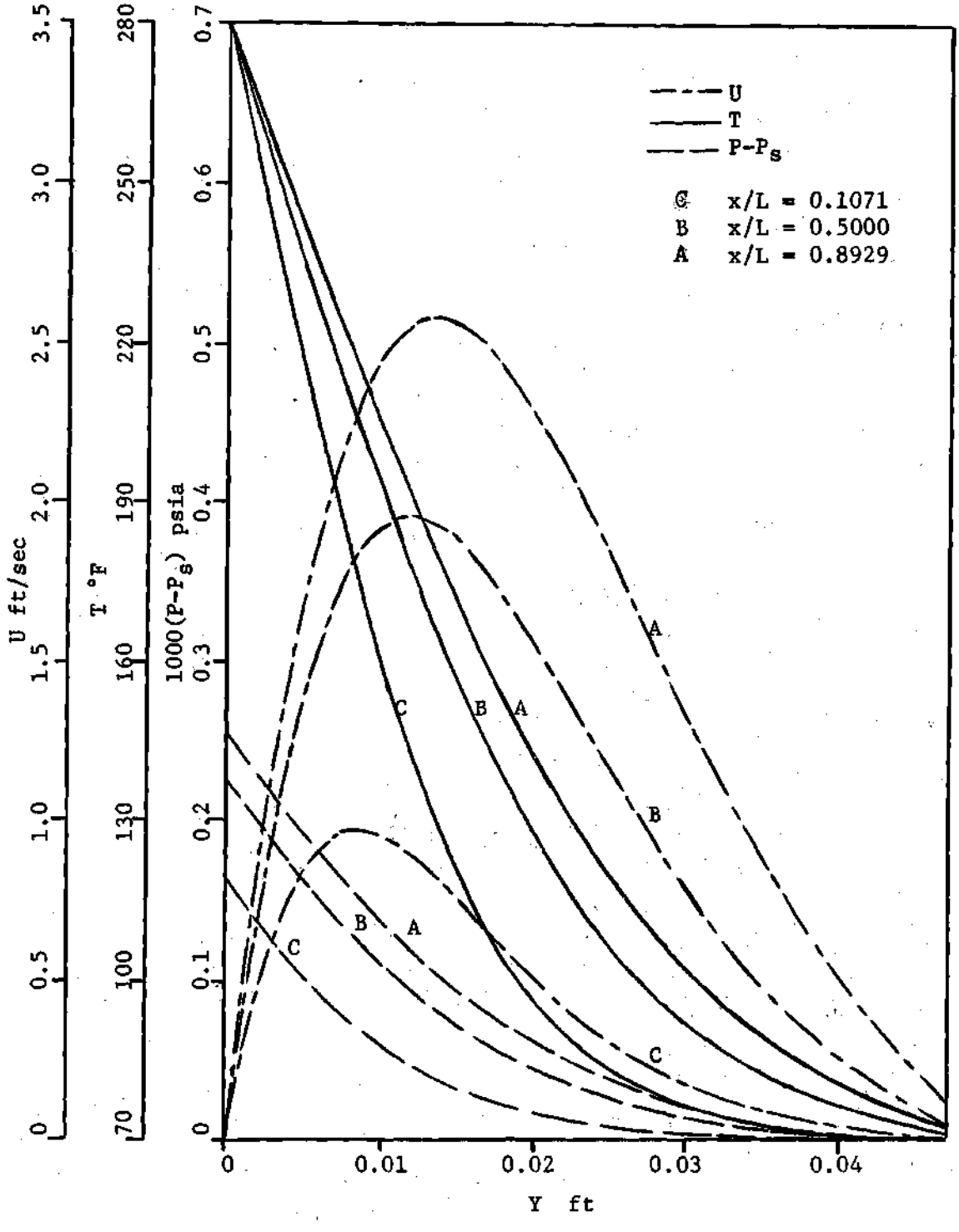

Figure 21. Profiles for Air Experiment at θ=40°.

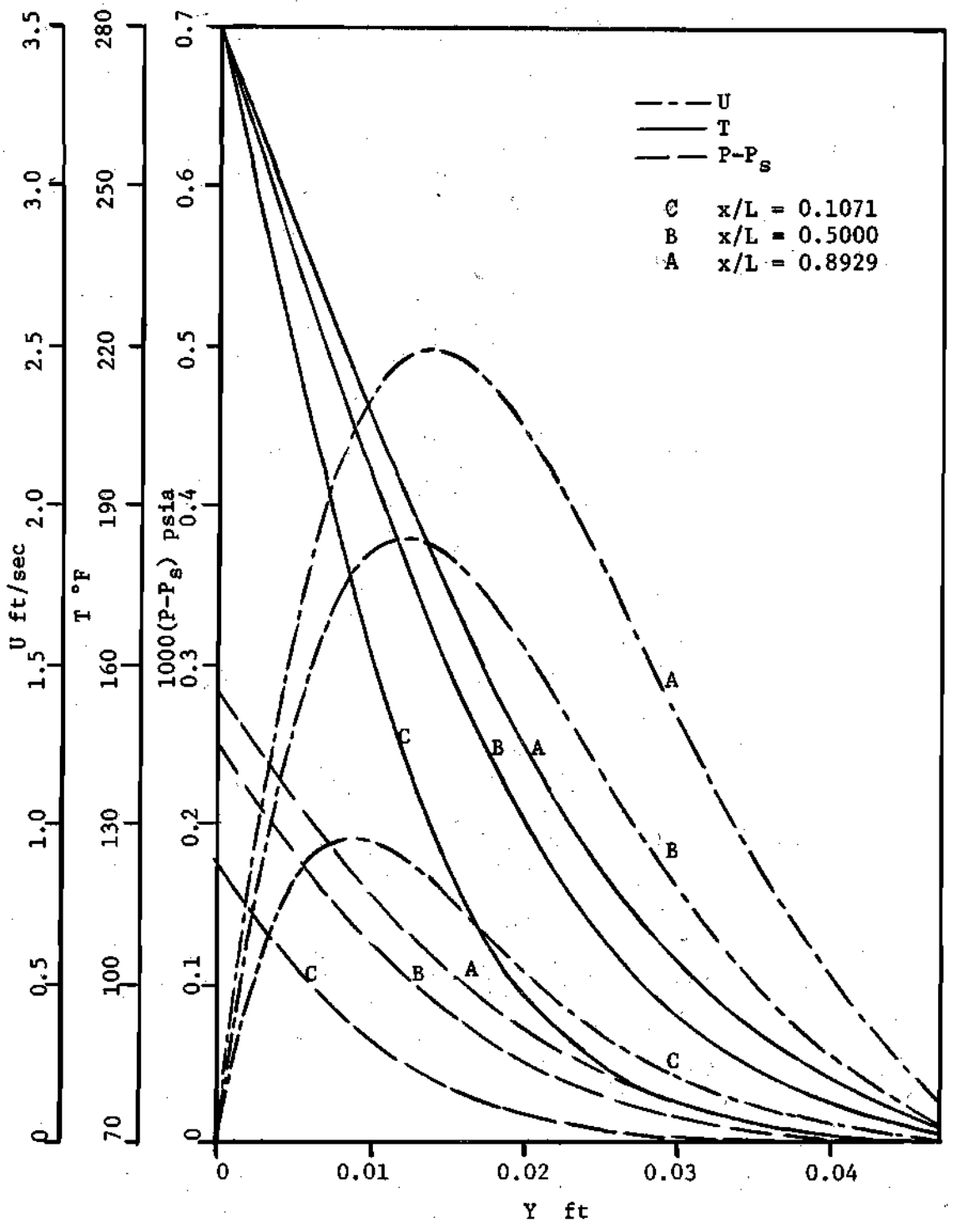

Figure 22. Profiles for Air Experiment at θ=45°.

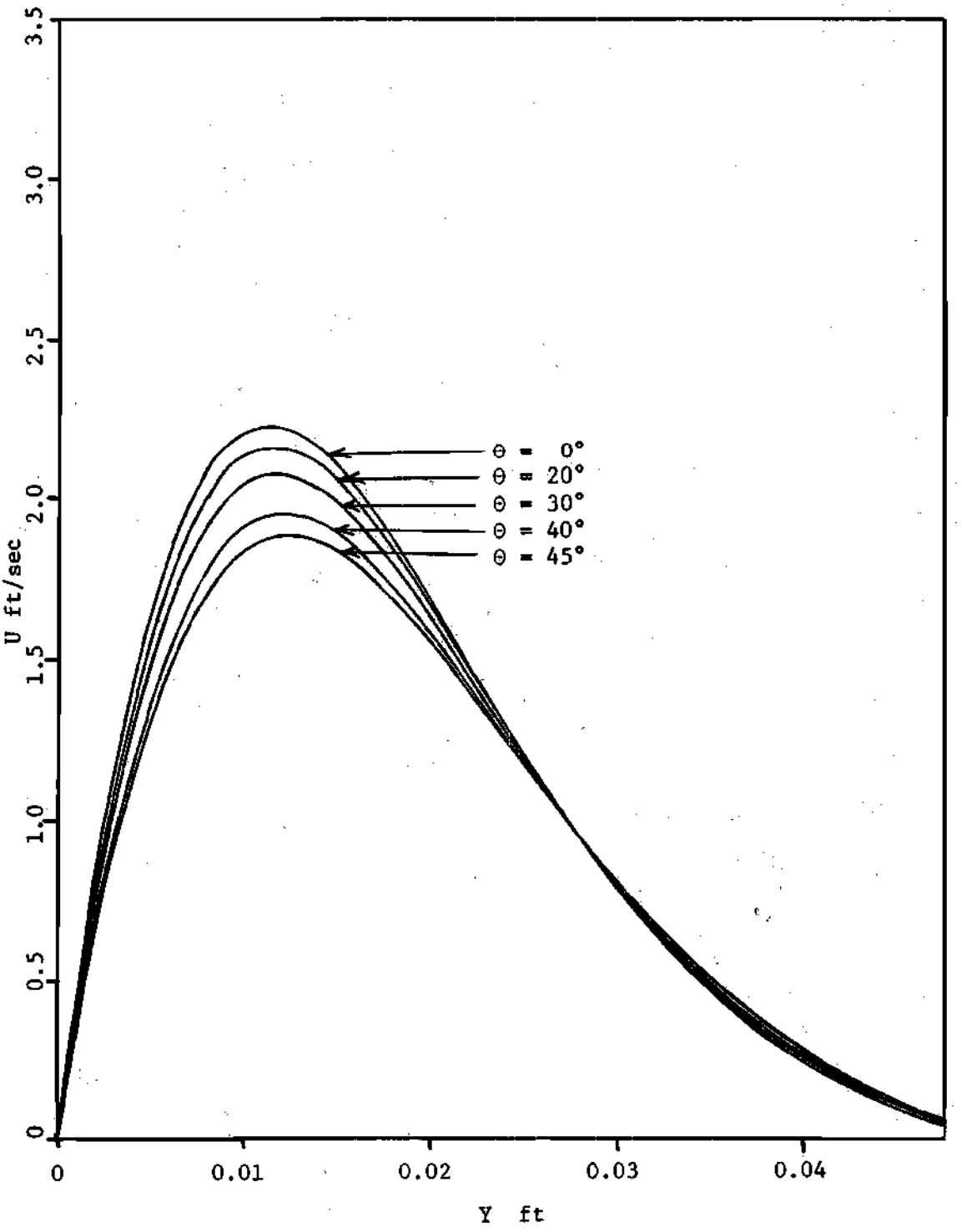

Figure 23. Velocity Profiles at Midpoint of Plate.

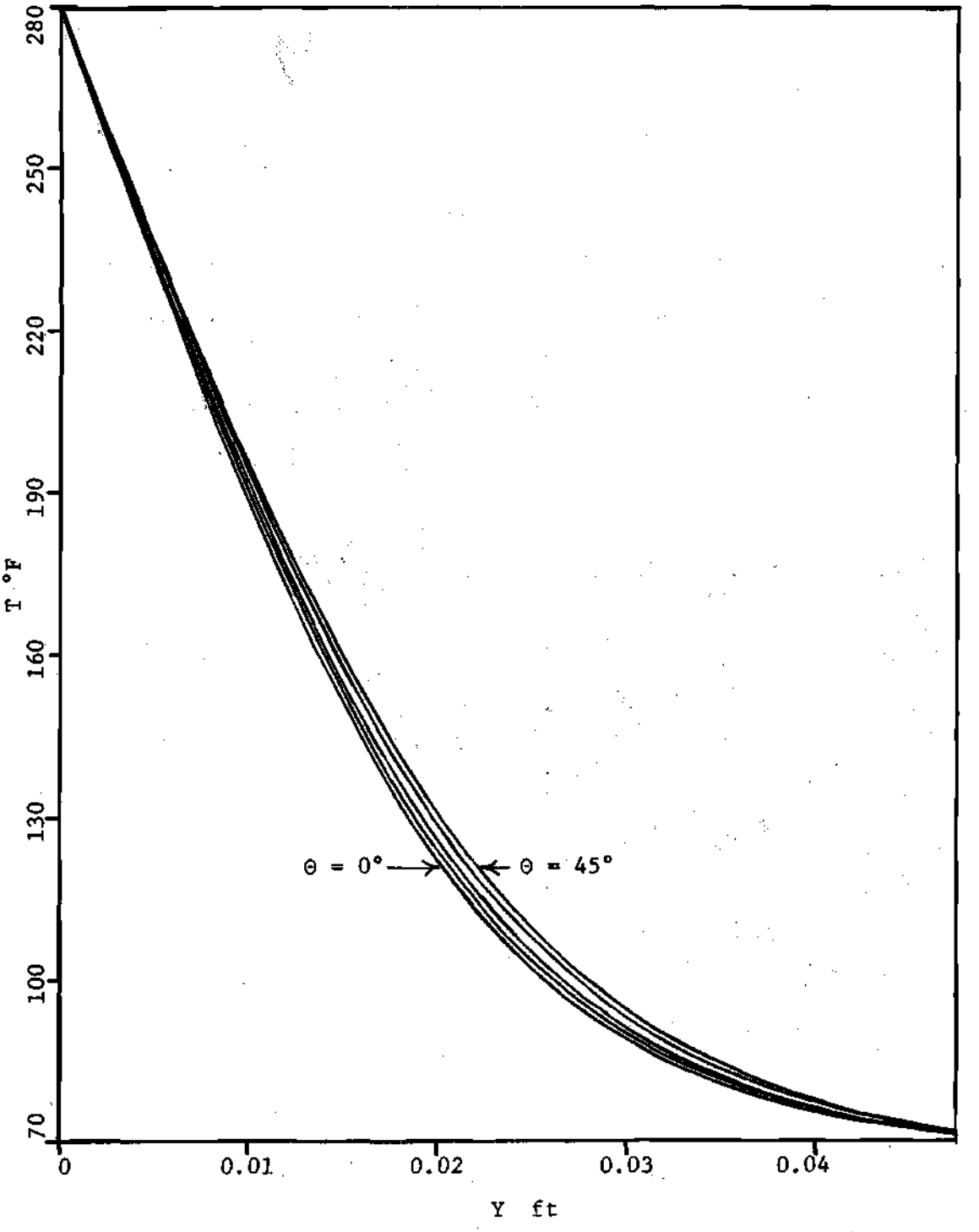

Figure 24. Temperature Profiles at Midpoint of Plate.

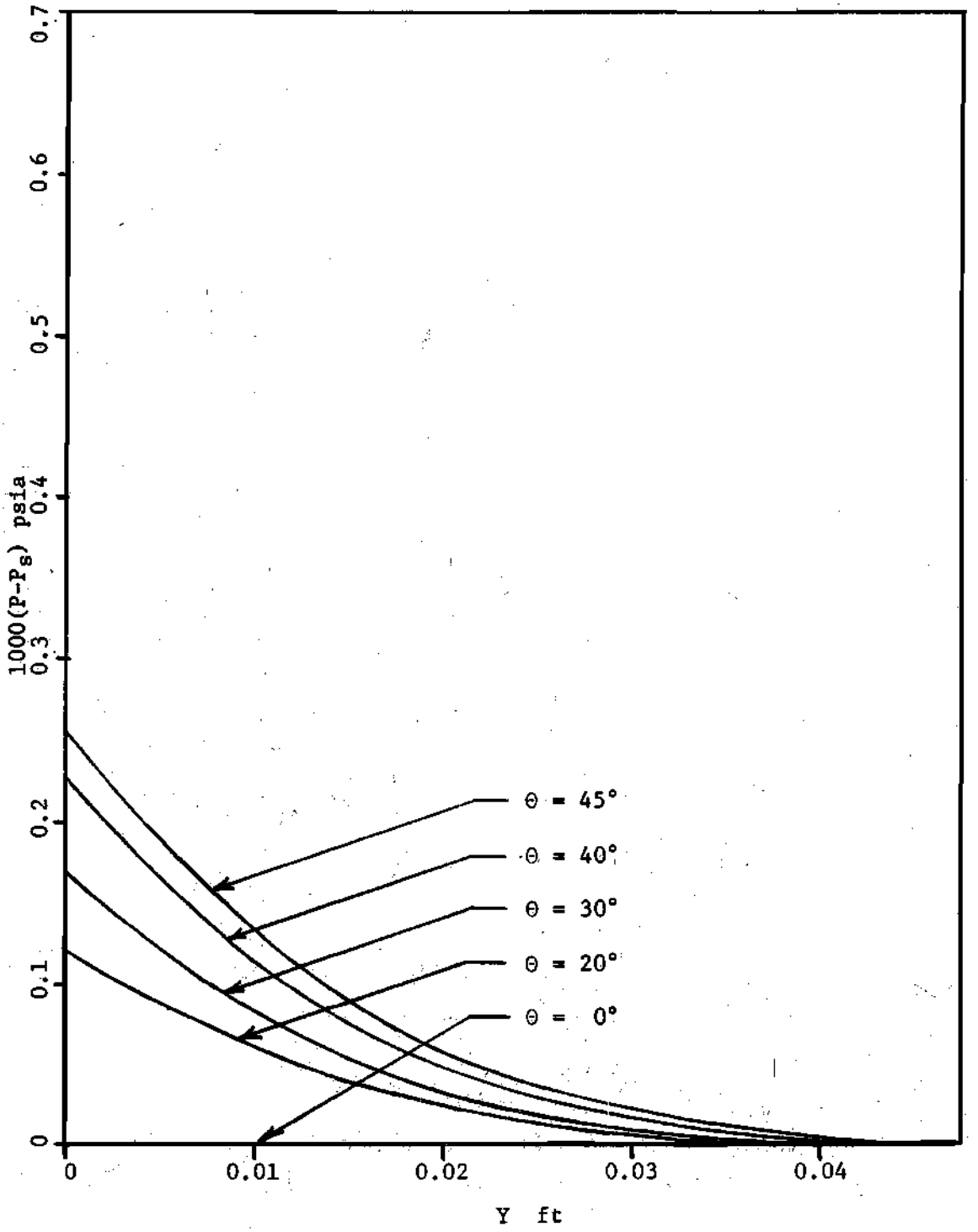

Figure 25. Pressure Profiles at Midpoint of Plate.

the plate, and the energy equation. In addition to the omission of the momentum equation normal to the plate, the pressure gradient term in the momentum equation parallel to the plate was eliminated. No other changes in the equations were made and the method of solution was the same.

The differences in the solutions for air when the normal momentum equation was added are very minor. Figures 26 and 27, pages 79 and 80, show characteristic profiles for the oil solutions for angles of inclination of zero and 45 degrees, respectively. The effect of including the normal momentum equation was much more pronounced for the zero angle of inclination and was almost negligible at 45 degrees.

The magnitude of the v velocity increased more rapidly when the normal momentum equation was included for the vertical plate. At an inclination of 45° an opposite trend was noticed with a slightly lower v velocity magnitude for the solution including the normal momentum equation.

The magnitude of the u velocity was greater for the solutions including the momentum equation normal to the plate and only slight differences were noted in the temperature profiles.

Comparison of Constant and Variable Property Solutions for Oil

The effect of holding the viscosity constant at its maximum value, at T_∞, produced significant differences in

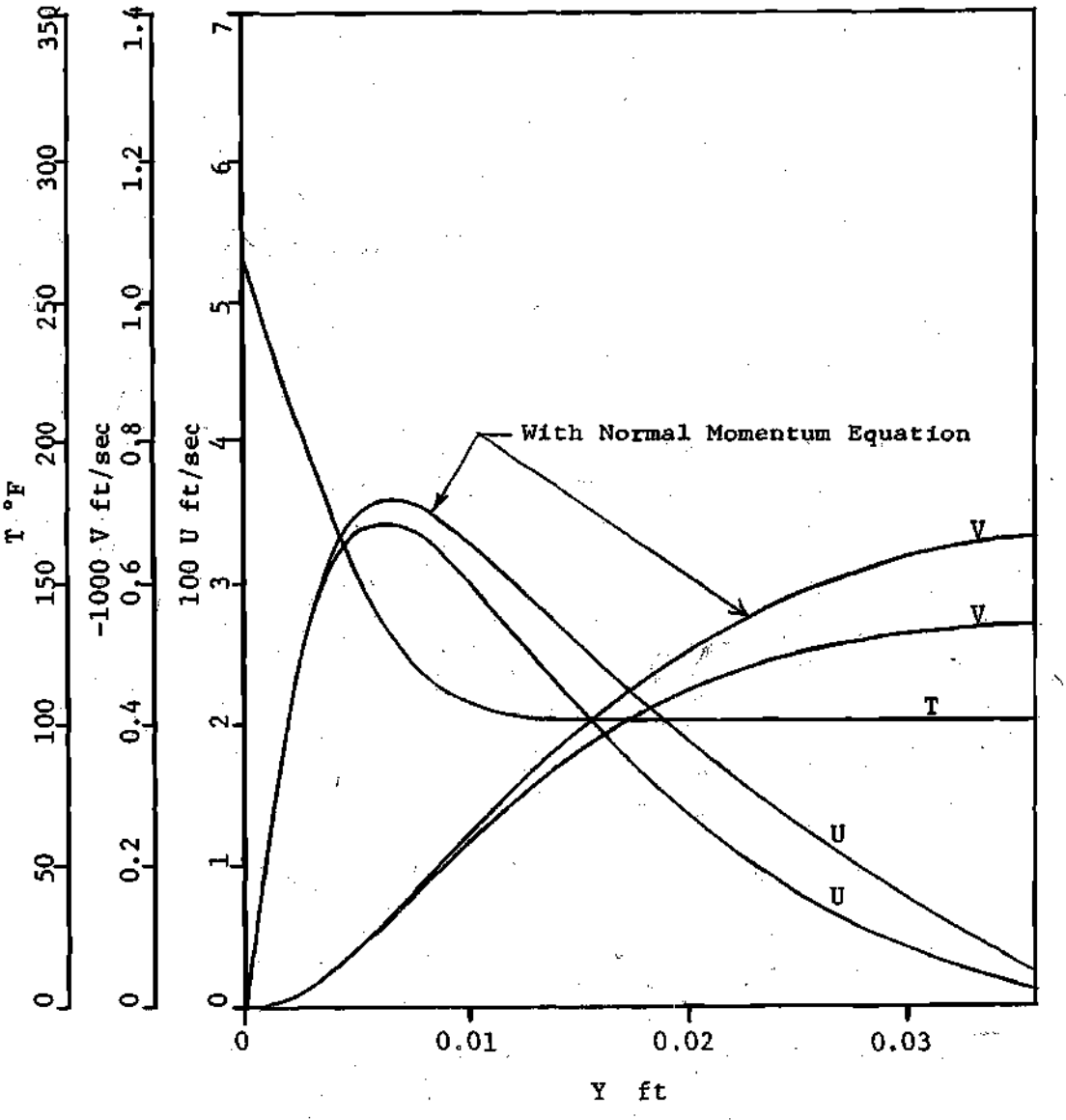

Figure 26. Comparison of Profiles With and Without the Normal Momentum Equation for $\theta=0°$.

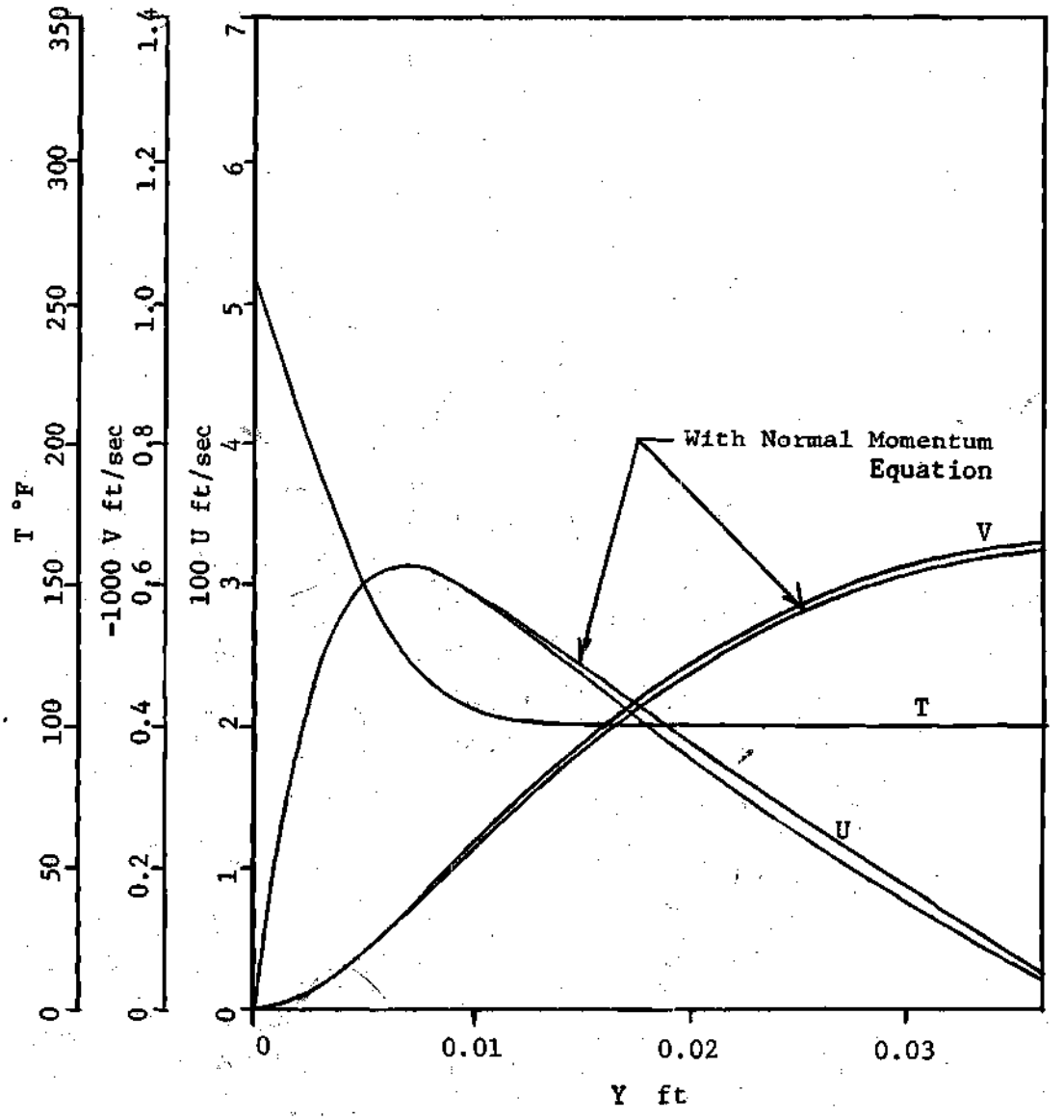

Figure 27. Comparison of Profiles With and Without the Normal Momentum Equation for $\theta=45°$.

these two solutions. Figures 28 and 29, pages 82 and 83, show profiles for the vertical plate and for the plate inclined at 45 degrees, respectively. The differences are slightly more pronounced at 45 degrees than for the vertical.

Because the temperature increases near the surface, the viscosity decreases, and the magnitude of the u velocity component almost doubles for the variable property solution. This increase in motion reduces the temperature from that of the constant property solution. To satisfy the continuity equation, the magnitude of the v velocity must be greater in the variable property solution.

For the 45 degree case, the pressure profile has a greater magnitude in the constant property solution. The pressure effect also extends further out into the flow field for the constant property solution.

Experimental Results

The experiments reported in the seven theses, (24), (25), (26), (27), (28), (29), and (30), were carried out in air and oil with the plates inclined at various angles of inclination from zero to forty five degrees. In the oil experiments provision was made in the design of the apparatus to reduce the ambient conditions to a low of 28.3 degrees Fahrenheit. This provided an extremely high Prandtl number of 5526. For the oil, the smallest Prandtl number

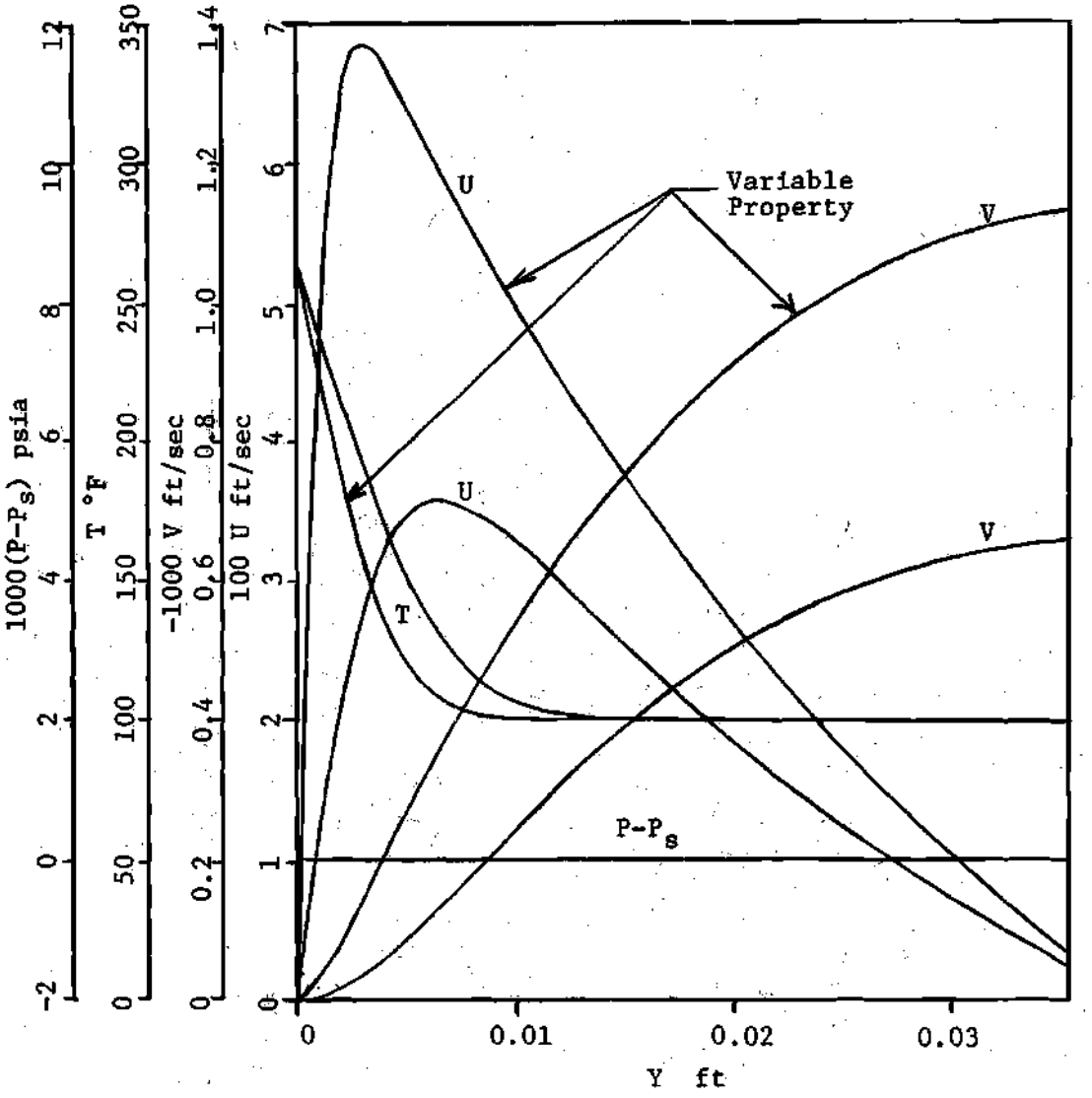

Figure 28. Comparison of Constant and Variable Property Solutions for Oil at θ=0°.

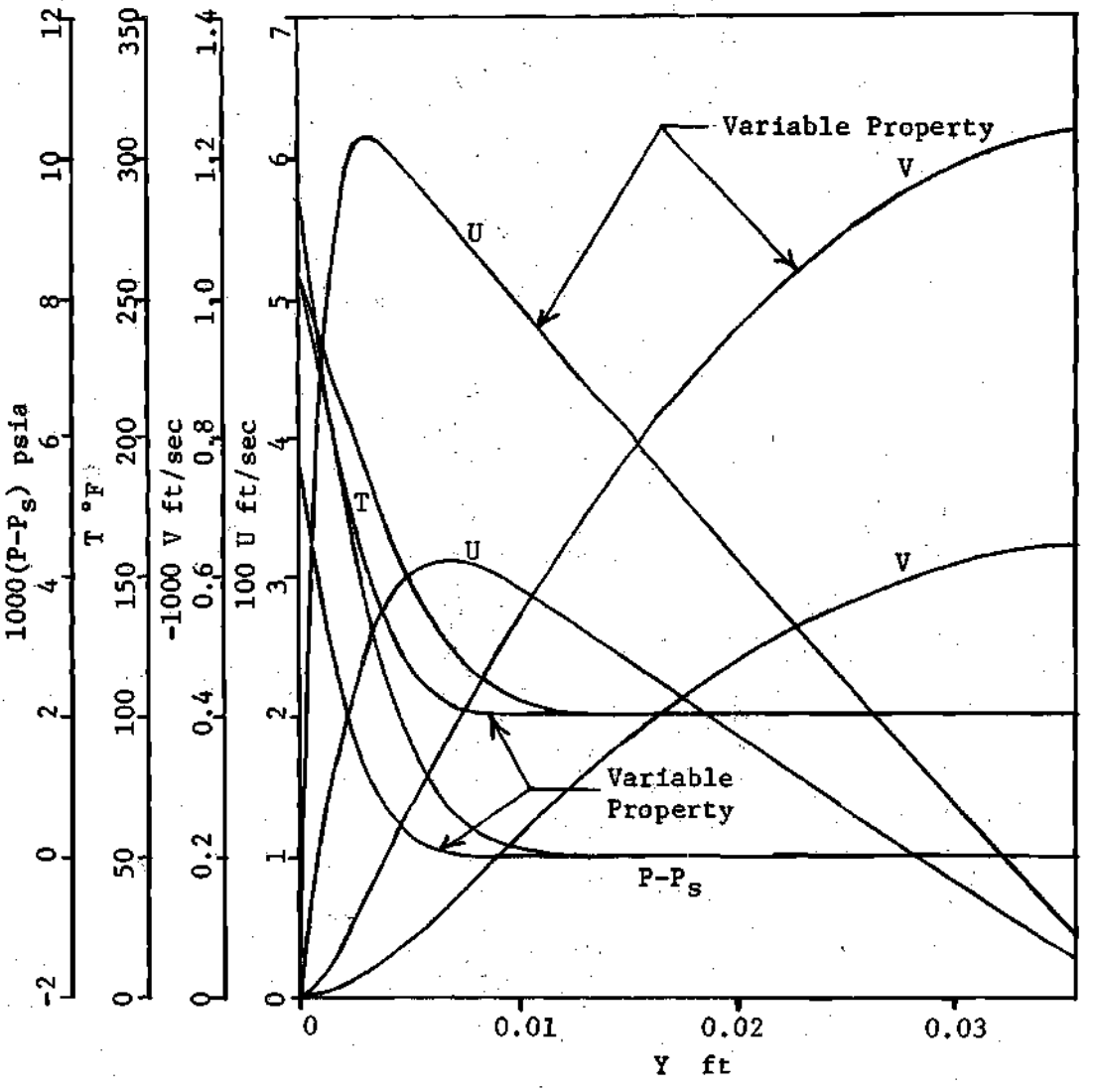

Figure 29. Comparison of Constant and Variable Property Solutions for Oil at θ=45°.

was slightly greater than 100, and a Prandtl number of 0.7 was obtained in all the experiments with air. In the oil experiments the Grashof number varied from 1.5×10^4 to 3.5×10^8 and the range of Grashof numbers in the air experiments was from 1.8×10^8 to 7.2×10^9. The results of these experiments are presented in Figure 32, page 88. A discussion of this figure will be given after the basis for the coordinates is established in the next part of this chapter.

Correlation of Theoretical and Experimental Results

The results of the theoretical and experimental analyses previously discussed belong to a single class of physical phenomena. The classical correlations of heat transfer data have been presented in a form such as

$$Nu_\infty = f(Pr_\infty, Gr_\infty, \theta)$$

Thus, a satisfactory expression of this type was developed. The usual method of least squares did not produce satisfactory results, because all of the data were treated in an unbiased fashion. The data which were produced by the theoretical calculations were much more consistent than the experimental data and were given more weight in the correlation. The form of the equation was taken as

$$Nu_{\infty} = 0.667\left[\frac{Pr_{\infty}^{2}\, Gr_{\infty}\cos\theta}{Pr_{\infty} + 0.952}\right]^{1/4}$$

and certain of the constants were adjusted to provide a better correlation with the present data. This equation was given by Kreith (4).

The form which best explains both the theoretical and the experimental results of this investigation is

$$Nu_{\infty} = 0.65\left[\frac{Pr_{\infty}^{2.25} Gr_{\infty} (\cos\theta)^{0.7}}{Pr_{\infty} + 1.1}\right]^{1/4} \qquad (52)$$

Figure 30, page 86, shows the Nusselt number from the theoretical calculations plotted versus the Nusselt number predicted by equation (52). Considering that the Nusselt number from the equation is the best estimate possible with the present information and that the theoretical calculations contained errors due to the different degrees of convergence, the small amount of scatter is considered reasonable. The experimental data are added to this figure and shown in Figure 31, page 87. In Figure 32, page 88, the data are converted to a form such that

$$Nu_{\infty}\left[\frac{1.1 + Pr_{\infty}}{Pr_{\infty}^{2.25}(\cos\theta)^{0.7}}\right]^{1/4}$$

is plotted versus the Grashof number.

The angle of inclination has been effectively

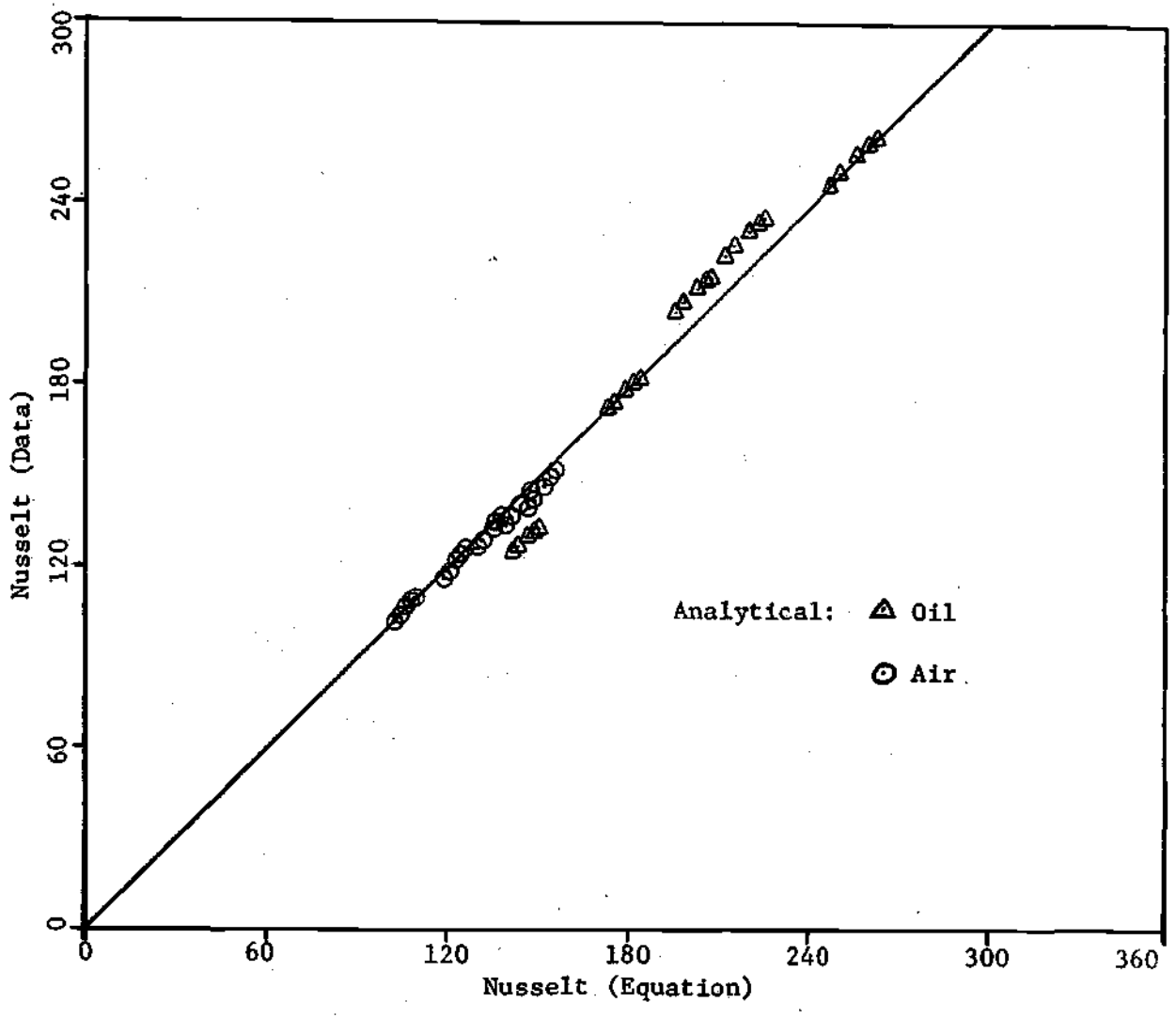

Figure 30. Comparison of Analytical Data.

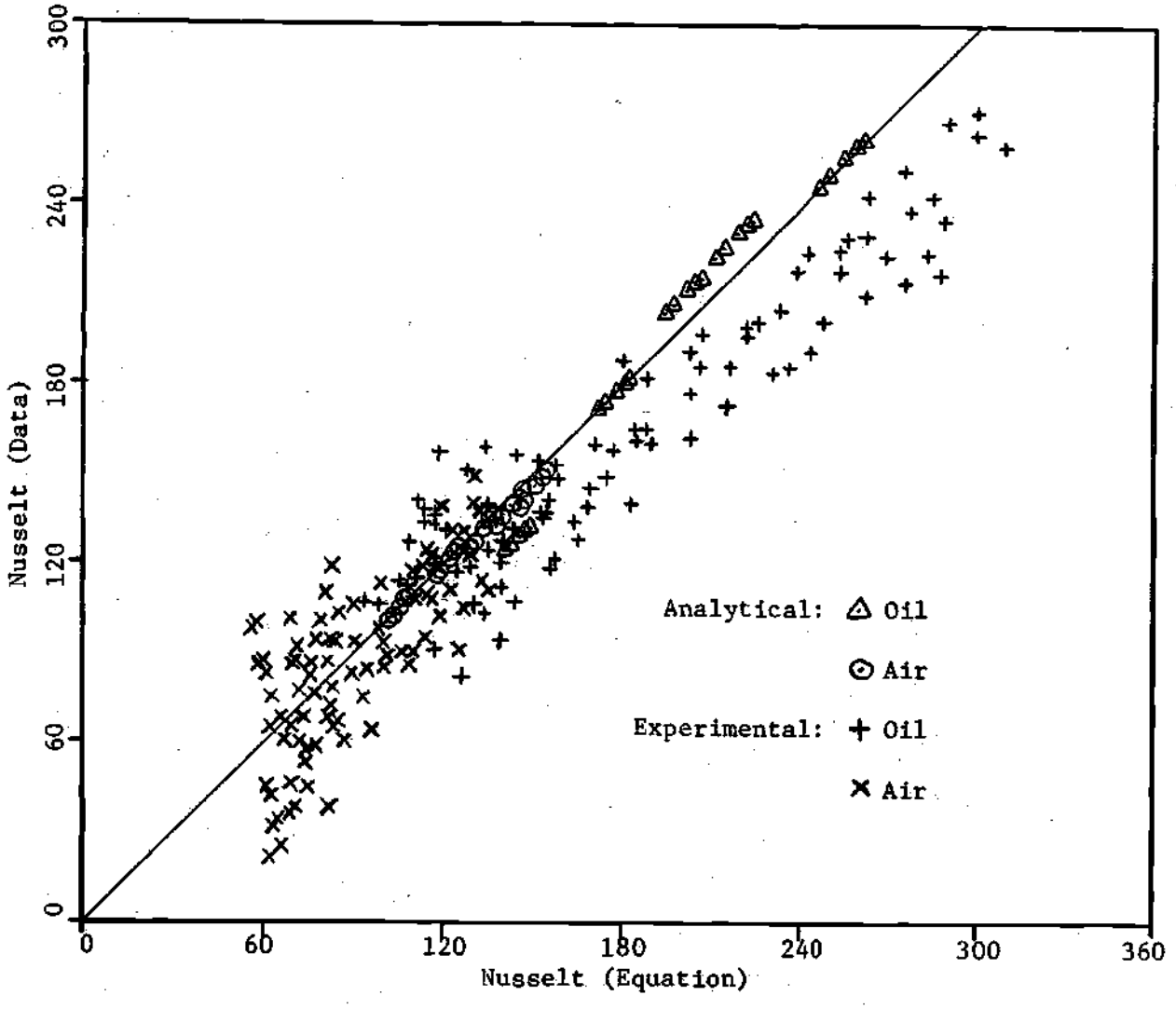

Figure 31. Comparison of Analytical and Experimental Data.

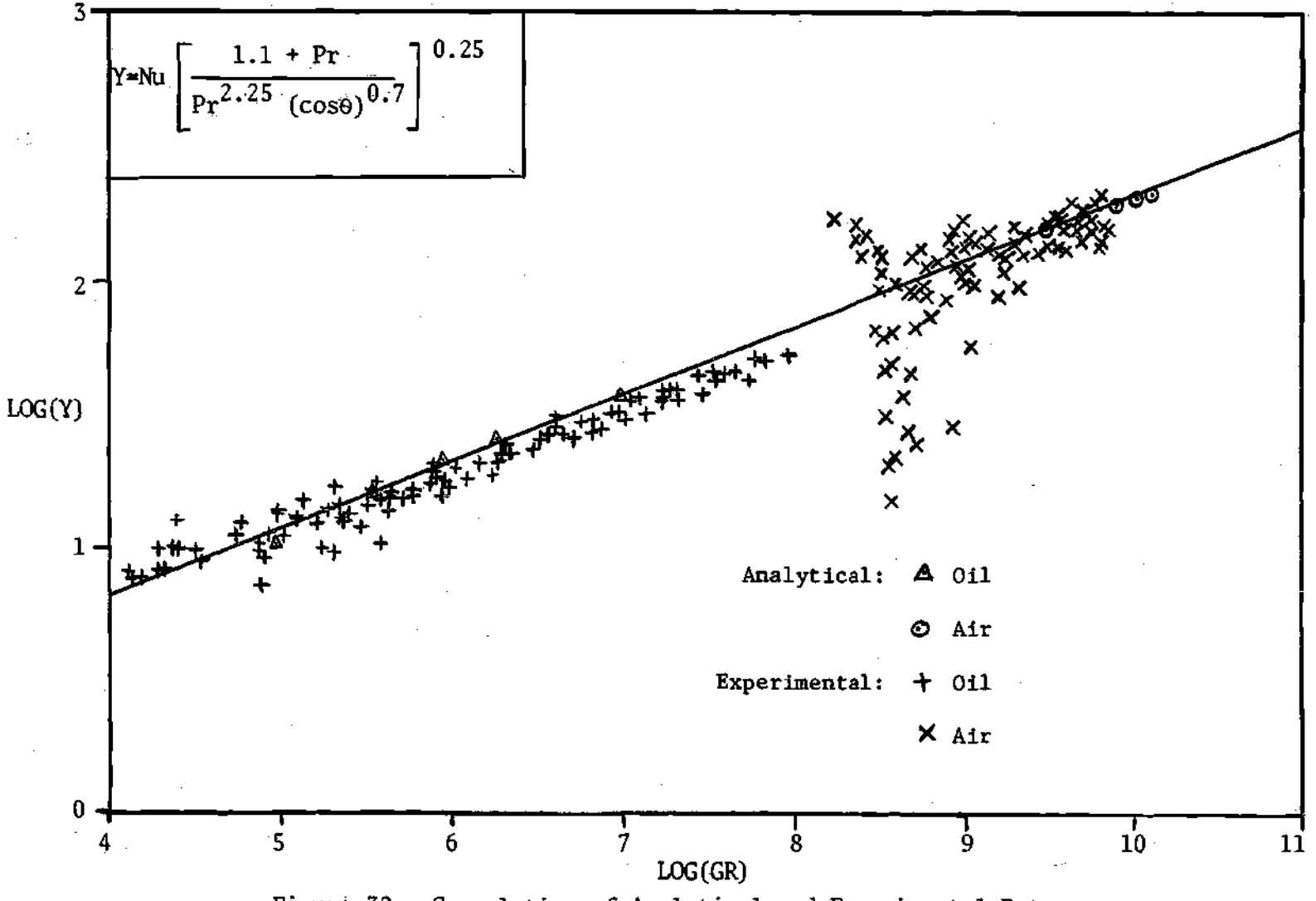

Figure 32. Correlation of Analytical and Experimental Data.

accounted for, because all five points for different angles fall at the same place. (Each triangle and circle is actually five points). The exponent of the Prandtl number was adjusted to account for the variation in property values through the boundary layer. Changing this exponent shifts the air and the oil data relative to each other. The denominator is useful in shifting only the air data because it has little effect on data with a Prandtl number greater than 100. The extreme scatter in the experimental data for air occurs in the lower Grashof range for the air experiments. During experiments in this range, a low wall temperature was required. This meant that the heat rate was reduced. The measurement of electrical power input to the heaters under these conditions was extremely difficult and the magnitude of the errors was increased.

The variation of property values may also be accounted for by calculation of the Nusselt, Grashof, and Prandtl numbers with property values evaluated at the film temperature. The data recorded in Tables 2 and 3 are presented in this manner in Table 4, page 90. This data can be correlated by the equation

$$Nu_f = 0.492\ (\cos\theta)^{0.042} Pr_f^{0.0463} (Pr_f Gr_f)^{0.25} \qquad (53)$$

A correlation of the same form can be derived for the data contained in Tables 2 and 3. The resulting equation is

Table 4. Analytical Results for Property Values Evaluated at Film Temperature.

T_w	T_∞	Pr_f	Gr_f	Angle of Inclination				
				0°	20°	30°	40°	45°
				Nu_f				
120.0	40.0	960.0	1.6×10^6	134.6	133.3	131.4	128.4	126.5
180.0	50.0	399.7	1.6×10^7	187.5	185.6	183.0	178.9	176.3
220.0	60.0	243.4	5.8×10^7	234.0	222.1	219.0	214.1	210.9
240.0	70.0	188.4	1.1×10^8	244.4	242.7	239.6	234.2	230.6
260.0	100.0	130.2	2.2×10^8	271.8	269.1	265.0	258.8	254.4
120.0	70.0	0.7	2.6×10^9	104.9	104.2	101.8	98.7	96.9
160.0	70.0	0.7	4.1×10^9	117.2	115.7	113.3	109.8	107.8
200.0	70.0	0.7	5.3×10^9	123.8	122.1	119.5	115.9	113.7
240.0	70.0	0.7	6.2×10^9	127.7	125.9	123.2	119.5	117.3
280.0	70.0	0.7	6.8×10^9	130.0	128.0	125.4	121.6	119.3

$$Nu_{\infty} = 0.517(\cos\theta)^{0.208} Pr_{\infty}^{0.093} (Pr_{\infty} Gr_{\infty})^{0.25} \qquad (54)$$

These equations were developed by standard least squares techniques and the statistical data obtained in the analysis indicates that equation (53) explains the variation in the data better.

CHAPTER VI

CONCLUSIONS AND RECOMMENDATIONS

Theoretical studies of natural convection heat transfer from a flat plate inclined at various angles from the vertical position were undertaken for both air and a particular oil. The angle of inclination was varied from zero to 45 degrees to reproduce the physical conditions for which experimental data was available.

Conclusions

The primary results of this study are:

1. A numerical solution for the vertical and inclined plate in oil, which treated the physical properties as functions of temperature, produced velocity, temperature, and pressure profiles in the flow field. The average Nusselt number was obtained from the temperature profiles. These data were correlated in terms of the Prandtl and Grashof numbers and the angle of inclination.

2. A similar solution was obtained for air but all properties were constant except density.

3. A computer program was developed that could be used to produce numerical solutions for angles greater than the 45 degrees which was the limit in this study.

4. Other solutions were obtained which permitted a comparison of results when the properties were held constant or considered functions of temperature. The effect of including the momentum equation normal to the plate was obtained by comparing solutions with and without this equation.

Pressure profiles were obtained in the numerical solutions which indicate that the pressure in the flow field is no longer constant along lines normal to the surface as the plate is inclined. The pressure near the wall is slightly higher than the local hydrostatic pressure and the value at the wall increases as the angle of inclination is increased.

Recommendations

It is recommended that the finite difference method developed for the present study be used to investigate other flow phenomena which occur in semi-infinite fluids. A particularly interesting study of this nature would be the natural convection flow below plates inclined at angles greater than 45 degrees. The computer programs in Appendices B and C should produce valid results for angles approaching 70 to 80 degrees.

The transition from laminar to turbulent flow was not observed in the present work and should be the object of future investigations.

APPENDIX A

PROPERTY VALUES AS FUNCTIONS OF TEMPERATURE FOR NECTON-45 OIL

$\rho = C_1 - C_2\ t$ lbm/ft^3

$k = C_3 - C_4\ t$ Btu/hr-ft-°F

$C_p = C_5 + C_6\ t$ Btu/lbm-°F

$\beta = C_2/\rho = C_2/(C_1 - C_2\ t)$ 1/°R

$\ln [\ln(\upsilon \times 10^5)] = C_7 - C_8\ t^{C_9}$ ft^2/sec

$C_1 = 56.903105$

$C_2 = 0.021752109$

$C_3 = 0.0813$

$C_4 = 0.25 \times 10^{-4}$

$C_5 = 0.443$

$C_6 = 0.45 \times 10^{-3}$

$C_7 = 2.0802367$

$C_8 = 0.011883861$

$C_9 = 0.89595891$

The data for viscosity and density were obtained by experiment. The data for the other properties were obtained from Maxwell (32). The equations were developed by standard least squares procedures, and the number of significant figures of some of the constants does not indicate the accuracy of the equations.

APPENDIX B

COMPUTER PROGRAM FOR VARIABLE PROPERTY SOLUTION FOR OIL

The finite difference equations solved by this program are listed below. For subroutine TEMP, the symbols are defined by equation 30, page 29, and the resulting equations are:

$$T_{i,j} = \frac{NUM}{2A_1 + A_2 + 2B_1 + B_2 + C + D}$$

where NUM stands for the weighted average of the four temperatures around the point i,j. The coefficients of these four temperatures are different, depending on the sign of the u and v velocities. The coefficients are given in the following list:

	$T_{i,j+1}$	$T_{i,j-1}$	$T_{i+1,j}$	$T_{i-1,j}$
$u > 0$ and $v > 0$	$B_1 + B_2$	$B_1 + D$	A_1	$A_1 + A_2 + C$
$u > 0$ and $v < 0$	$B_1 + B_2 + D$	B_1	A_1	$A_1 + A_2 + C$
$u < 0$ and $v > 0$	$B_1 + B_2$	$B_1 + D$	$A_1 + C$	$A_1 + A_2$
$u < 0$ and $v < 0$	$B_1 + B_2 + D$	B_1	$A_1 + C$	$A_1 + A_2$

For subroutine UVEL, the symbols are defined by equation 35, page 32, and the resulting equations are:

$$u_{i,j} = [\text{NUM} + B_2 \left(\frac{\Delta y}{2\Delta x}\right)(v_{i+1,j} - v_{i-1,j})$$

$$+ \rho_\infty g \cos\theta \left(1 - \frac{\rho_{i,j}}{\rho_\infty}\right) - \frac{g_c}{2\Delta x}(P_{i+1,j} - P_{i-1,j})]/$$

$$(2A_1 + A_2 + 2B_1 + B_2 + C + D)$$

where NUM stands for the weighted average of the four u velocities around the point i,j. The coefficients are listed below.

	$u_{i,j+1}$	$u_{i,j-1}$	$u_{i+1,j}$	$u_{i=1,j}$
$u > 0$ and $v > 0$	$B_1 + D$	$B_1 + D$	A_1	$A_1 + A_2 + C$
$u > 0$ and $v < 0$	$B_1 + B_2 + D$	B_1	A_1	$A_1 + A_2 + C$
$u < 0$ and $v > 0$	$B_1 + D$	$B_1 + D$	$A_1 + C$	$A_1 + A_2$
$u < 0$ and $v < 0$	$B_1 + B_2 + D$	B_1	$A_1 + C$	$A_1 + A_2$

For subroutine PRES, equation 39, page 36, was solved and for subroutine VVEL, equation 19, page 36, was solved.

```
C       VARIABLE PROPERTY SOLUTION FOR OIL, INCLINED PLATE
        REAL K,KOIL,MU,MUOIL,NU,NU1,NU2
        COMMON U(39,60),V(39,60),T(39,60),P(39,60),H(39,60),
       1       R(39,60),S(39,60),ALPHA,DX,DX2,DY,DY2,ERRP,
       2       ERRT,ERRU,ERRV,G,GS,ITER,M,MAX,ML,MT,M1,GR,
       3       N,NU,NU1,NU2,N1,PR,RHOINF,THETA,TW,TINF,IEXP
        RHOOIL(T)=56.903105-0.021752109*T
        KOIL(T)=(0.0813-0.000025*T)/3600.0
        CPOIL(T)=0.443+0.00045*T
        BETOIL(T)=1.0/(2615.981-T)
        MUOIL(T)=(0.56903105-0.21752109*T/1000.0)*
       1         (EXP(EXP(2.0802367-0.011883861*
       2         (T**0.89595891))))/1000.0
        DO 999 III=1,13
        READ (17) IEXP,U,V,T,P
  998   FORMAT(I20)
  999   WRITE (3,998) IEXP
    1   CALL START
        WRITE (3,9) IEXP
           MAX=1
           M1=M-1
           N1=N-1
           GS=32.16*SIN(3.14159*THETA/180.0)
           G=32.16*COS(3.14159*THETA/180.0)
           DX2=2.0*DX*DX
           DY2=2.0*DY*DY
        DO 2 I=1,M
        DO 2 J=1,N
           H(I,J)=KOIL(T(I,J))
           R(I,J)=RHOOIL(T(I,J))
    2      S(I,J)=MUOIL(T(I,J))
           ITER=0
    3      ITER=ITER+1
        IF (KEYSW(2)) 11,11,10
   10   CALL PRES
   11   IF (KEYSW(16)) 13,13,12
   12   CALL TEMP
   13   IF (KEYSW(32)) 15,15,14
   14   CALL UVEL
   15   IF (KEYSW(64)) 17,17,16
   16   CALL VVEL
   17   IF (KEYSW(1)) 6,6,4
    4   CALL NUSELT
    6   IF (KEYSW(4)) 3,3,7
    7   CALL NUSELT
        WRITE (17) IEXP,U,V,T,P
        IF (KEYSW(8)) 1,1,8
    8   STOP
    9   FORMAT('1',9X,'BEGIN EXPERIMENT NO.',I4,////)
        END
```

```
      SUBROUTINE TEMP
      REAL K,KOIL,MU,MUOIL,NU,NU1,NU2
      COMMON U(39,60),V(39,60),T(39,60),P(39,60),H(39,60),
     1       R(39,60),S(39,60),ALPHA,DX,DX2,DY,DY2,ERRP,
     2       ERRT,ERRU,ERRV,G,GS,ITER,M,MAX,ML,MT,M1,GR,
     3       N,NU,NU1,NU2,PR,RHOINF,THETA,TW,TINF
      RHOOIL(T)=56.903105-0.021752109*T
      KOIL(T)=(0.0813-0.000025*T)/3600.0
      CPOIL(T)=0.443+0.00045*T
      BETOIL(T)=1.0/(2615.981-T)
      MUOIL(T)=(0.56903105-0.21752109*T/1000.0)*
     1         (EXP(EXP(2.0802367-0.011883861*
     2         (T**0.89595891))))/1000.0
      DO 7 L1=1,MAX
         ERRT=0.0
      DO 7 J=2,N1
      DO 7 I=2,M1
         A1=1.0/(DX*DX)
         B1=1.0/(DY*DY)
         A2=A1+ABS(H(I+1,J)-H(I-1,J))/DX2
         B2=B1+ABS(H(I,J+1)-H(I,J-1))/DY2
         D=R(I,J)*CPOIL(T(I,J))/H(I,J)
         C=D*ABS(U(I,J))/DX
         D=D*ABS(V(I,J))/DY
      IF (U(I,J)) 2,2,1
    1    A2=A2+C
      GO TO 3
    2    A1=A1+C
    3 IF (V(I,J)) 5,5,4
    4    B1=B1+D
      GO TO 6
    5    B2=B2+D
    6    Z=(A1*T(I+1,J)+A2*T(I-1,J)+B2*T(I,J+1)+B1*
     1     T(I,J-1))/(A1+A2+B1+B2)
         ERRT=ERRT+ABS(Z-T(I,J))
         T(I,J)=Z
         H(I,J)=KOIL(Z)
         R(I,J)=RHOOIL(Z)
    7    S(I,J)=MUOIL(Z)
      IF (KEYSW(1)) 9,9,8
    8 WRITE (3,10) ITER,ERRT
    9 RETURN
   10 FORMAT(10X,'ITERATION NO.',I4,5X,'ERRT=',F12.4)
      END
```

```
      SUBROUTINE UVEL
      REAL K,KOIL,MU,MUOIL,NU,NU1,NU2
      COMMON U(39,60),V(39,60),T(39,60),P(39,60),H(39,60),
     1       R(39,60),S(39,60),ALPHA,DX,DX2,DY,DY2,ERRP,
     2       ERRT,ERRU,ERRV,G,GS,ITER,M,MAX,ML,MT,M1,GR,
     3       N,NU,NU1,NU2,N1,PR,THOINF,THETA,TW,TINF
      DO 7 L1=1,MAX
         ERRU=0.0
      DO 7 J=2,N1
      DO 7 I=2,M1
         A1=S(I,J)/(DX*DX)
         B1=S(I,J)/(DY*DY)
         A2=A1+ABS(S(I+1,J)-S(I-1,J))/(DX*DX)
         B2=ABS(S(I,J+1)-S(I,J-1))/DY2
         C=R(I,J)*ABS(U(I,J))/DX
         D=R(I,J)*ABS(V(I,J))/DY
         E=B2*DY*(V(I+1,J)-V(I-1,J))/(2.0*DX)
         B2=B2+B1
      IF (U(I,J)) 2,2,1
    1    A2=A1+C
      GO TO 3
    2    A1=A1+C
    3 IF (V(I,J)) 5,5,4
    4    B1=B1+D
      GO TO 6
    5    B2=B2+D
    6    Z=(A1*U(I+1,J)+A2*U(I-1,J)+B2*U(I,J+1)+B1*U(I,J-1)-
     1      16.08*(P(I+1,J)-P(I-1,J))+RHOINF*G*(1.0-R(I,J)/
     2      RHOINF)+E)/(A1+A2+B1+B2)
         ERRU=ERRU+ABS(Z-U(I,J))
    7    U(I,J)=Z
      IF (KEYSW(1)) 9,9,8
    8 WRITE (3,10) ITER,ERRU
    9 RETURN
   10 FORMAT(10X,'ITERATION NO.',I4,5X,'ERRU=',F12.4)
      END
```

```
      SUBROUTINE PRES
      REAL K,KOIL,MU,MUOIL,NU,NU1,NU2
      COMMON U(39,60),V(39,60),T(39,60),P(39,60),H(39,60),
     1       R(39,60),S(39,60),ALPHA,DX,DX2,DY,DY2,ERRP,
     2       ERRT,ERRU,ERRV,G,GS,ITER,M,MAX,ML,MT,M1,GR,
     3       N,NU,NU1,NU2,N1,PR,RHOINF,THETA,TW,TINF
         ERRP=0.0
      DO 7 I=2,M1
      DO 7 J1=1,N1
         J=60-J1
         Z=P(I,J+1)+DY*(R(I,J)*(U(I,J)*(V(I+1,J)-V(I-1,J))/
     1     (2.0*DX)+V(I,J)*(V(I,J+1)-V(I,J-1))/(2.0*DY))+
     2     RHOINF*GS*(1.0-R(I,J)/RHOINF)-S(I,J)*((V(I+1,J)-
     3     2.0*V(I,J)+V(I-1,J))/(DX*DX)+(V(I,J+1)-
     4     2.0*V(I,J)+V(I,J-1))/(DY*DY))-2.0*((S(I,J+1)-
     5     S(I,J-1))/(2.0*DY))*((V(I,J+1)-V(I,J-1))/
     6     (2.0*DY))-((S(I+1,J)-S(I-1,J))/(2.0*DX))*
     7     (((U(I,J+1)-U(I,J-1))/(2.0*DY))+((V(I+1,J)-
     8     V(I-1,J))/(2.0*DX))))/32.16
         ERRP=ERRP+ABS(Z-P(I,J))
     7   P(I,J)=Z
      IF (KEYSW(1)) 9,9,8
     8 WRITE (3,10) ITER,ERRP
     9 RETURN
    10 FORMAT(10X,'ITERATION NO.',I4,5X,'ERRP=',F12.4)
      END


      SUBROUTINE VVEL
      REAL K,KOIL,MU,MUOIL,NU,NU1,NU2
      COMMON U(39,60),V(39,60),T(39,60),P(39,60),H(39,60),
     1       R(39,60),S(39,60),ALPHA,DX,DX2,DY,DY2,ERRP,
     2       ERRT,ERRU,ERRV,G,GS,ITER,M,MAX,ML,MT,M1,GR,
     3       N,NU,NU1,NU2,N1,PR,RHOINF,THETA,TW,TINF
         ERRV=0.0
      DO 1 J=2,N1
      DO 1 I=2,M1
         Z=V(I,J-1)-DY*(U(I+1,J)-U(I-1,J))/(2.0*DX)
         ERRV=ERRV+ABS(Z-V(I,J))
     1   V(I,J)=Z
      IF (KEYSW(1)) 3,3,2
     2 WRITE (3,4) ITER,ERRV
     3 RETURN
     4 FORMAT(10X,'ITERATION NO.',I4,5X,'ERRV=',F12.4)
      END
```

```
      SUBROUTINE NUSELT
      REAL K,KOIL,MU,MUOIL,NU,NU1,NU2
      COMMON U(39,60),V(39,60),T(39,60),P(39,60),H(39,60),
     1       R(39,60),S(39,60),ALPHA,DX,DX2,DY,DY2,ERRP,
     2       ERRT,ERRU,ERRV,G,GS,ITER,M,MAX,ML,MT,M1,GR,
     3       N,NU,NU1,NU2,N1,PR,RHOINF,THETA,TW,TINF
          L1=ML+1
          L2=MT-3
          SUM=0.0
      DO 1 I=L1,L2,2
    1     SUM=SUM+4.0*(H(I,1)+H(I,2))*(TW-T(I,2))
     1           +2.0*(H(I+1,1)+H(I+1,2))*(TW-T(I+1,2))
          NU1=DX*((H(ML,1)+H(ML,2))*(TW-T(ML,2))+4.0*
     1       (H(MT-1,1)+H(MT-1,2))*(TW-T(MT-1,2))+(H(MT,1)+
     2       H(MT,2))*(TW-T(MT,2))+SUM)/(6.0*DY*H(1,1)*
     3       (TW-TINF))
          NU2=NU1+DX*(7.0*(H(ML+2,1)+H(ML+2,2))*
     1       (TW-T(ML+2,2))-(H(ML,1)+H(ML,2))*(TW-T(ML,2))-
     2       4.0*(H(ML+1,1)+H(ML+1,2))*(TW-T(ML+1,2)))/
     3       (6.0*DY*H(1,1)*(TW-TINF))
      IF (KEYSW(1)) 3,3,2
    2 WRITE (3,4) ITER,NU1,NU2
    3 RETURN
    4 FORMAT(10X,'ITERATION NO.',I4,5X,'NUSSELT NOS.=',
     1       2F12.3)
      END
```

APPENDIX C

COMPUTER PROGRAM FOR CONSTANT PROPERTY SOLUTION FOR AIR

The finite difference equations solved by this program are listed below. For subroutine TEMP, the symbols are defined by equation 12, page 38, and the resulting equations are:

$$T_{i,j} = \frac{NUM}{2A_x + 2A_y + B + C}$$

where NUM stands for the weighted average of the four temperatures around the point i,j. The coefficients of these four temperatures are different, depending on the sign of the u and v velocities. The coefficients are given in the list below.

	$T_{i,j+1}$	$T_{i,j-1}$	$T_{i+1,j}$	$T_{i-1,j}$
$u > 0$ and $v > 0$	A_y	$A_y + C$	A_x	$A_x + B$
$u > 0$ and $v < 0$	$A_y + C$	A_y	A_x	$A_x + B$
$u < 0$ and $v > 0$	A_y	$A_y + C$	$A_x + B$	A_x
$u < 0$ and $v < 0$	$A_y + C$	A_y	$A_x + B$	A_x

For subroutine UVEL, the symbols are defined by equation 47, page 39, and the resulting equations are:

$$u_{i,j} = [\text{NUM} + g \cos\theta \left(1 - \frac{\rho_{i,i}}{\rho_\infty}\right) - \frac{g_c}{2\, x\rho_\infty}(P_{i+1,j} - P_{i-1,j})] \,/$$

$$(2A_x + 2A_y + B + C)$$

where NUM stands for the weighted average of the four u velocities around the point i,j. The coefficients are listed below:

	$u_{i,j+1}$	$u_{i,j-1}$	$u_{i+1,j}$	$u_{i-1,j}$
$u > 0$ and $v > 0$	A_y	$A_y + C$	A_x	$A_x + B$
$u > 0$ and $v < 0$	$A_y + C$	A_y	A_x	$A_x + B$
$u < 0$ and $v > 0$	A_y	$A_y + C$	$A_x + B$	A_x
$u < 0$ and $v < 0$	$A_y + C$	A_y	$A_x + B$	A_x

For subroutine PRES, equation 49, page 40, was solved and for subroutine VVEL, equation 19, page 41, was solved.

```
      REAL K,KOIL,L,MU,MUOIL,NU,NU1,NU2
      COMMON U(39,60),V(39,60),T(39,60),P(39,60),ALPHA,AXT,
     1       AXU,AYT,AYU,DT,DU,DX,DY,ERRT,ERRU,FNU,G,GR,ITER,
     2       K1,K2,K3,K4,L,M,MAX,ML,MT,M1,M2,N,NU,NU1,NU2,N1,
     3       N2,PERCNT,PR,RHOINF,THETA,TOP,TW,TINF,W,GS,ERRP
      DIMENSION A(2,25)
         MAX=2
    1 READ (6) TW,TINF,THETA,RHOINF,NU,ALPHA,PR,GR,NU1,NU2,
     1         FNU,DX,DY,M,N,ML,MT,XL,XT,IEXP
    3 DO 4 I=1,M
      DO 4 J=1,N
    4    P(I,J)=0.0
      READ (4) IEXP,U,V,T
    5    M1=M-1
         N1=N-1
      WRITE (3,13) IEXP
         GS=32.16*SIN(3.14159*THETA/180.0)
         G=32.16*COS(3.14159*THETA/180.0)
         AXT=ALPHA/(DX*DX)
         AXU=NU/(DX*DX)
         AYT=ALPHA/(DY*DY)
         AYU=NU/(DY*DY)
         DU=2.0*(AXU+AYU)
         DT=2.0*(AXT+AYT)
         ITER=0
    6    ITER=ITER+1
      CALL VVEL
      CALL PRES
      CALL UVEL(1)
      CALL TEMP
      IF (KEYSW(1)) 9,9,7
    7 CALL NUSELT
      IF (KEYSW(2)) 9,9,8
    8 CALL OUT(1)
    9 IF (KEYSW(4)) 6,6,10
   10 CALL NUSELT
         A(1,IEXP)=NU1
         A(2,IEXP)=NU2
      WRITE (12) IEXP,U,V,T,P
      IF (KEYSW(8)) 1,1,11
   11 DO 12 I=1,IEXP
   12 WRITE (3,14) I,A(1,I),A(2,I)
      STOP
   13 FORMAT('1',9X,'BEGIN EXPERIMENT NO.',I4,////)
   14 FORMAT(10X,I4,2F20.6)
      END
```

```
      SUBROUTINE PRES
      REAL K,KOIL,L,MU,MUOIL,NU,NU1,NU2
      COMMON U(39,60),V(39,60),T(39,60),P(39,60),ALPHA,AXT,
     1       AXU,AYT,AYU,DT,DU,DX,DY,ERRT,ERRU,FNU,G,GR,ITER,
     2       K1,K2,K3,K4,L,M,MAX,ML,MT,M1,M2,N,NU,NU1,NU2,N1,
     3       N2,PERCNT,PR,RHOINF,THETA,TOP,TW,TINF,W,GS,ERRP
      RHO(T)=39.667215/(T+460.0)
      DO 10 J=2,N1
      DO 10 I=2,M1
         B1=AXU
         B2=AXU
         C1=AYU
         C2=AYU
         B=ABS(U(I,J))/DX
         C=ABS(V(I,J))/DY
         ERRP=0.0
      IF (U(I,J)) 4,4,5
    4    B1=B1+B
      GO TO 6
    5    B2=B2+B
    6 IF (V(I,J)) 7,7,8
    7    C1=C1+C
      GO TO 9
    8    C2=C2+C
    9    C3=P(I,J-1)+RHOINF*DY*(B1*V(I+1,J)+B2*V(I-1,J)
     1      +C1*V(I,J+1)+C2*V(I,J-1)-(DU+B+C)*V(I,J)-GS*(1.0
     2      -RHO(T(I,J))/RHOINF))/32.16
         ERRP=ERRP+ABS(C3-P(I,J))
   10    P(I,J)=C3
      IF (KEYSW(1)) 12,12,11
   11 WRITE (3,13) ITER,ERRP
   12 RETURN
   13 FORMAT(10X,'ITERATION NO.',I4,5X,'ERRP=',F12.4)
      END
```

```
      SUBROUTINE UVEL(L2)
      REAL K,KOIL,L,MU,MUOIL,NU,NU1,NU2
      COMMON U(39,60),V(39,60),T(39,60),P(39,60),ALPHA,AXT,
     1       AXU,AYT,AYU,DT,DU,DX,DY,ERRT,ERRU,FNU,G,GR,ITER,
     2       K1,K2,K3,K4,L,M,MAX,ML,MT,M1,M2,N,NU,NU1,NU2,N1,
     3       N2,PERCNT,PR,RHOINF,THETA,TOP,TW,TINF,W,GS,ERRP
      RHO(T)=39.667215/(T+460.0)
      RHOOIL(T)=56.903105-0.021752109*T
      DO 10 L1=1,MAX
    3    ERRU=0.0
      DO 10 J=2,N1
      DO 10 I=2,M1
         B1=AXU
         B2=AXU
         C1=AYU
         C2=AYU
         B=ABS(U(I,J))/DX
         C=ABS(V(I,J))/DY
      GO TO (53,54),L2
   53    D=G*(1.0-RHO(T(I,J))/RHOINF)-32.16*(P(I+1,J)-
     1     P(I-1,J))/(2.0*RHOINF*DX)
      GO TO 55
   54    D=G*(1.0-RHOOIL(T(I,J))/RHOINF)-32.16*(P(I+1,J)-
     1     P(I-1,J))/(2.0*RHOINF*DX)
   55 IF (U(I,J)) 4,4,5
    4    B1=B1+B
      GO TO 6
    5    B2=B2+B
    6 IF (V(I,J)) 7,7,8
    7    C1=C1+C
      GO TO 9
    8    C2=C2+C
    9    C3=(B1*U(I+1,J)+B2*U(I-1,J)+C1*U(I,J+1)+C2*U(I,J-1)+
     1       D)/(DU+B+C)
         ERRU=ERRU+ABS(C3-U(I,J))
   10    U(I,J)=C3
   13 IF (KEYSW(1)) 15,15,14
   14 WRITE (3,16) ITER,ERRU
   15 RETURN
   16 FORMAT(10X,'ITERATION NO.',I4,5X,'ERRU=',F12.4)
      END
```

```
      SUBROUTINE TEMP
      REAL K,KOIL,L,MU,MUOIL,NU,NU1,NU2
      COMMON U(39,60),V(39,60),T(39,60),P(39,60),ALPHA,AXT,
     1       AXU,AYT,AYU,DT,DU,DX,DY,ERRT,ERRU,FNU,G,GR,ITER,
     2       K1,K2,K3,K4,L,M,MAX,ML,MT,M1,M2,N,NU,NU1,NU2,N1,
     3       N2,PERCNT,PR,RHOINF,THETA,TOP,TW,TINF,W,GS,ERRP
      DO 10 L1=1,MAX
    3 ERRT=0.0
      DO 10 J=2,N1
      DO 10 I=2,M1
      B1=AXT
      B2=AXT
      C1=AYT
      C2=AYT
      B=ABS(U(I,J))/DX
      C=ABS(V(I,J))/DY
      IF (U(I,J)) 4,4,5
    4 B1=B1+B
      GO TO 6
    5 B2=B2+B
    6 IF (V(I,J)) 7,7,8
    7 C1=C1+C
      GO TO 9
    8 C2=C2+C
    9 C3=(B1*T(I+1,J)+B2*T(I-1,J)+C1*T(I,J+1)+C2*T(I,J-1))
     1   /(DT+B+C)
      ERRT=ERRT+ABS(C3-T(I,J))
   10 T(I,J)=C3
   13 IF (KEYSW(1)) 15,15,14
   14 WRITE (3,16) ITER,ERRT
   15 RETURN
   16 FORMAT(10X,'ITERATION NO.',I4,5X,'ERRT=',F12.4)
      END
```

```
      SUBROUTINE VVEL
      REAL K,KOIL,L,MU,MUOIL,NU,NU1,NU2
      COMMON U(39,60),V(39,60),T(39,60),P(39,60),ALPHA,AXT,
     1       AXU,AYT,AYU,DT,DU,DX,DY,ERRT,ERRU,FNU,G,GR,ITER,
     2       K1,K2,K3,K4,L,M,MAX,ML,MT,M1,M2,N,NU,NU1,NU2,N1,
     3       N2,PERCNT,PR,RHOINF,THETA,TOP,TW,TINF,W,GS,ERRP
    3 ERRV=0.0
      DO 4 J=2,N1
      DO 4 I=2,M1
      C3=V(I,J-1)-DY*(U(I+1,J)-U(I-1,J))/(2.0*DX)
      ERRV=ERRV+ABS(C3-V(I,J))
    4 V(I,J)=C3
    7 IF (KEYSW(1)) 9,9,8
    8 WRITE (3,10) ITER,ERRV
    9 RETURN
   10 FORMAT(10X,'ITERATION NO.',I4,5X,'ERRV=',F12.4)
      END


      SUBROUTINE NUSELT
      REAL K,KOIL,L,MU,MUOIL,NU,NU1,NU2
      COMMON U(39,60),V(39,60),T(39,60),P(39,60),ALPHA,AXT,
     1       AXU,AYT,AYU,DT,DU,DX,DY,ERRT,ERRU,FNU,G,GR,ITER,
     2       K1,K2,K3,K4,L,M,MAX,ML,MT,M1,M2,N,NU,NU1,NU2,N1,
     3       N2,PERCNT,PR,RHOINF,THETA,TOP,TW,TINF,W,GS,ERRP
      L1=ML+1
      L2=MT-3
      SUM=0.0
      DO 1 I=L1,L2,2
    1 SUM=SUM+4.0*(TW-T(I,2))+2.0*(TW-T(I+1,2))
      NU1=DX*(6.0*TW-T(ML,2)-4.0*T(MT-1,2)-T(MT,2)+SUM)/
     1       (3.0*DY*(TW-TINF))
      NU2=NU1+DX*(2.0*TW+T(ML,2)+4.0*T(L1,2)-
     1       7.0*T(ML+2,2))/(3.0*DY*(TW-TINF))
      IF (KEYSW(1)) 3,3,2
    2 WRITE (3,4) ITER,NU1,NU2,FNU
    3 RETURN
    4 FORMAT(10X,'ITERATION NO.',I4,5X,'NUSSELT NOS.=',
     12F12.3,5X,'OSTRACH PREDICTED',F12.3)
      END
```

APPENDIX D

DERIVATION OF DIFFERENTIAL EQUATIONS

The Navier-Stokes equations for two dimensional steady flow of a Newtonian fluid are (see for example references 7 and 9):

$$\rho\left(u\frac{\partial u}{\partial x} + v\frac{\partial u}{\partial y}\right) = \frac{\partial}{\partial x}\left[\mu\left(2\frac{\partial u}{\partial x} - \frac{2}{3}\left\{\frac{\partial u}{\partial x} + \frac{\partial v}{\partial y}\right\}\right)\right]$$

$$+ \frac{\partial}{\partial y}\left[\mu\left(\frac{\partial u}{\partial y} + \frac{\partial v}{\partial x}\right)\right] + X - g_c\frac{\partial P}{\partial x} \qquad \text{D-1}$$

$$\rho\left(u\frac{\partial v}{\partial x} + v\frac{\partial v}{\partial y}\right) = \frac{\partial}{\partial x}\left[\mu\left(\frac{\partial u}{\partial y} + \frac{\partial v}{\partial x}\right)\right]$$

$$+ \frac{\partial}{\partial y}\left[\mu\left(2\frac{\partial v}{\partial y} - \frac{2}{3}\left\{\frac{\partial u}{\partial x} + \frac{\partial v}{\partial y}\right\}\right)\right]$$

$$+ Y - g_c\frac{\partial P}{\partial y} \qquad \text{D-2}$$

The continuity equation is

$$\frac{\partial \rho u}{\partial x} + \frac{\partial \rho v}{\partial y} = 0 \qquad \text{D-3}$$

If the effect of variable density is assumed to have negligible effect on the continuity equation, it becomes

$$\frac{\partial u}{\partial x} + \frac{\partial v}{\partial y} = 0 \qquad \text{D-4}$$

For the inclined coordinate system shown below, the components of the body force are

$$X = \rho g_x = -\rho\ g \cos\theta \qquad \text{D-5}$$

$$Y = \rho g_y = \rho\ g \sin\theta \qquad \text{D-6}$$

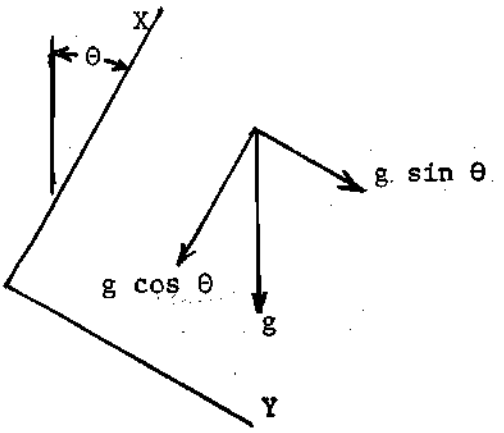

The hydrostatic pressure distribution is given by the equation

$$P_s = \rho_\infty \frac{g}{g_c}(y \sin\theta - x \cos\theta) \qquad \text{D-7}$$

Let $$\bar{P} = P - P_s \qquad \text{D-8}$$

so that $$P = \bar{P} + P_s \qquad \text{D-9}$$

and $$\frac{\partial P}{\partial x} = \frac{\partial \bar{P}}{\partial x} + \frac{\partial P_s}{\partial x} = \frac{\partial \bar{P}}{\partial x} - \rho_\infty \frac{g}{\partial x} \cos\theta \qquad \text{D-10}$$

$$\frac{\partial P}{\partial y} = \frac{\partial \bar{P}}{\partial y} + \frac{\partial P_s}{\partial y} = \frac{\partial \bar{P}}{\partial y} + \rho_\infty \frac{g}{g_c} \sin\theta \qquad \text{D-11}$$

These terms can be substituted into the Navier-Stokes equations, D-1 and D-2, to give

For equation D-1:

$$\rho\left(u\frac{\partial u}{\partial x} + v\frac{\partial u}{\partial y}\right) = \frac{\partial}{\partial x}\left(2\mu\frac{\partial u}{\partial x}\right) + \frac{\partial}{\partial y}\left[\mu\left(\frac{\partial u}{\partial y} + \frac{\partial v}{\partial x}\right)\right]$$

$$- \rho\ g\ \cos\theta - g_c\frac{\partial \bar{P}}{\partial x} + \rho_\infty\ g\ \cos\theta$$

$$\rho\left(u\frac{\partial u}{\partial x} + v\frac{\partial u}{\partial y}\right) = \frac{\partial}{\partial x}\left(2\mu\frac{\partial u}{\partial y}\right) + \frac{\partial}{\partial y}\left[\mu\left(\frac{\partial u}{\partial y} + \frac{\partial v}{\partial x}\right)\right]$$

$$- g_c\frac{\partial \bar{P}}{\partial x} + \rho_\infty\ g\ \cos\theta\ \left(1 - \frac{\rho}{\rho_\infty}\right)$$

For equation D-2:

$$\rho\left(u\frac{\partial v}{\partial x} + v\frac{\partial v}{\partial y}\right) = \frac{\partial}{\partial x}\left[\mu\left(\frac{\partial u}{\partial y} + \frac{\partial v}{\partial x}\right)\right] + \frac{\partial}{\partial y}\left(2\mu\frac{\partial v}{\partial y}\right)$$

$$+ \rho g \sin\theta - g_c\frac{\partial \bar{P}}{\partial y} - \rho_\infty\ g\ \sin\theta$$

$$\rho\left(u\frac{\partial v}{\partial x} + v\frac{\partial v}{\partial y}\right) = \frac{\partial}{\partial x}\left[\mu\left(\frac{\partial u}{\partial y} + \frac{\partial v}{\partial x}\right)\right] + \frac{\partial}{\partial y}\left(2\mu\frac{\partial v}{\partial y}\right)$$

$$- g_c\frac{\partial \bar{P}}{\partial y} - \rho_\infty\, g\ \sin\theta\ \left(1 - \frac{\rho}{\rho_\infty}\right)$$

BIBLIOGRAPHY

1. Garrison, D. C., "Natural Convection Heat Transfer From Cones," Master's Thesis, Georgia Institute of Technology, August, 1960.

2. Merk, H. J. and Prins, J. A., "Thermal Convection in Laminary Boundary Layers, I," Appl. Sci. Res., Section A, Vol. 4, pp. 11-24.

3. Hering, R. G. and Grosh, R. J., "Laminar Free Convection from a Non-Isothermal Cone," Int. J. Heat Mass Transfer, Vol. 5, 1962, pp. 1059-1068.

4. Kreith, F., Principles of Heat Transfer, International Textbook Company, 1962, pp. 309.

5. Holman, J. P., Heat Transfer, McGraw-Hill Book Company, Inc., 1963, pp. 158.

6. Rich, B. R., "An Investigation of Heat Transfer from an Inclined Flat Plate in Free Convection," Transactions of the ASME, Vol. 75, No. 4, May, 1953, pp. 489-499.

7. Bird, R. B., Stewart, W. E., and Lightfoot, E. N., Transport Phenomena, John Wiley and Sons, Inc., pp. 333.

8. Ostrach, S., "An Analysis of Laminar Free Convection Flow and Heat Transfer About a Flat Plate Parallel to the Direction of the Generating Body Force," NACA Report 1111, 1953.

9. McAdams, W. H., Heat Transmission, McGraw-Hill Book Company, Inc., 1954, pp. 172-173.

10. Lorenz, H. H., "Die Warmeubertragung von Einer Ebenen, senkrechten Platte on Ol bei Naturlicher Konvektion," Z. Techn. Physik, 1934, pp. 362-366.

11. Touloukian, Y. S., Hawkins, G. A., and Jacob, M., "Heat Transfer by Free Convection from Heated Vertical Surfaces to Liquids," Transactions of the ASME, Vol. 70, 1948, pp. 13-18.

12. Brown, A. I., and Marco, S. M., Introduction to Heat Transfer, McGraw-Hill Book Company, Inc., 1958, pp. 162.

13. Yang, K. T., "Possible Similarity Solutions for Laminar Free Convection on Vertical Plates and Cylinders," Transactions of the ASME, Series E., J. of Applied Mechanics, Vol. 27, 1960, pp. 230-236.

14. Morgan, G. W. and Warner, W. H., "On Heat Transfer in Laminar Boundary Layers at High Prandtl Number," Journal of the Aeronautical Sciences, Vol. 23, No. 10, October, 1956, pp. 937-948.

15. Stewartson, K., "On the Free Convection from a Horizontal Plate," Kurze Mitteilungen, Vol. 9a, 1958, pp. 276-282.

16. Tritton, D. J., "Turbulent Free Convection Above a Heated Plate Inclined at a Small Angle to the Horizontal," Journal of Fluid Mechanics, Vol. 16, 1963, pp. 417-435.

17. Tritton, D. J., "Transition to Turbulence in Free Convection Boundary Layers on an Inclined Heated Plate," Journal of Fluid Mechanics, Vol. 16, 1963, pp. 417-435.

18. Prandtl, L., Essentials of Fluid Dynamics, Hafner Publishing Company, 1952, pp. 382.

19. Michiyoshi, I., "Heat Transfer from an Inclined Thin Flat Plate by Natural Convection," Transactions Japanese Society of Mechanical Engineers, Vol. 30, 1964 (translated by Hideo Yamada).

20. Sparrow, E. M., and Gregg, J. L., "The Variable Fluid Property Problem in Free Convection," Transactions of the ASME, Vol. 80, May, 1958, pp. 8790886.

21. Fritsch, C. A., and Grosh, R. J., "Free Convection Heat Transfer to a Supercritical Fruit," International Developments in Heat Transfer, Proceedings of the 1961-1962 Heat Transfer Conference, Boulder, Colorado, pp. 1010-1016.

22. Hellums, J. D., "Finite Difference Computation of Natural Convection Heat Transfer," Ph.D. Thesis, Chemical Engineering Department, University of Michigan, 1961.

23. Richtmyer, R. D., Difference Methods for Initial-Value Problems, Interscience Publishers, Inc., New York, 1964.

24. Douglas, S. S., "Natural Convection From an Inclined Isothermal Surface, Experimental Study 1 - Flat Plate, Heated Side Down," Master's Thesis, Mississippi State University, May, 1963.

25. Patel, N. K., "Natural Convection From an Inclined Isothermal Surface, Experimental Study 4 - Flat Plate, Heated Side Down and Heated Side Up," Master's Thesis, Mississippi State University, January, 1964.

26. Farmer, W. P., "Natural Convection From a Vertical Isothermal Surface in Oil," Master's Thesis, Mississippi State University, June, 1964.

27. Morris, D. H., "Natural Convection From an Inclined Isothermal Surface in Oil, Flat Plate, Heated Side Down," Master's Thesis, Mississippi State University, August, 1964.

28. Barnes, W. S., "Natural Convection From an Inclined Isothermal Flat Plate in Oil, Heated Side Down," Master's Thesis, Mississippi State University, June, 1965.

29. Moorehead, E. S., "Natural Convection From an Inclined Isothermal Flat Plate in Oil, Heated Side Down," Master's Thesis, Mississippi State University, August, 1965.

30. Young, G. M., "Natural Convection From an Inclined Isothermal Flat Plate in Oil, Heated Side Down," Master's Thesis, Mississippi State University, August, 1965.

31. Farmer, W. P. and McKie, W. T., "Natural Convection From a Vertical Isothermal Surface in Oil," ASME paper number 64-WA/HT-12, 1964.

32. Maxwell, J. B., Data Book on Hydrocarbons, D. Van Nostrand Company, Inc., 1962.

VITA

Will T. McKie, Jr. was born in Clarksdale, Mississippi, on August 10, 1931. His parents are Bess Tittle McKie and the late Will T. McKie, Sr. He attended the Clarksdale, Mississippi, City Schools, graduating in 1950. He entered Mississippi State University in 1950 and received his B. S. in Mechanical Engineering there in 1954. After working fifteen months in the Construction Division of the Tennessee Valley Authority he was employed by Mississippi State University as an instructor in the Mechanical Engineering Department. He received an M.S. in Mechanical Engineering in 1958 and was promoted to Assistant Professor in 1959.

In 1960, Mr. McKie received a leave of absence from Mississippi State University to attend the Georgia Institute of Technology as an N. S. F. Science Faculty Fellow. In 1961 he was awarded the Schlumberger Fellowship and received a Ford Foundation loan. In 1962 he returned to his present position as Associate Professor of Mechanical Engineering at Mississippi State University.

Mr. McKie was married in 1953 to the former Ruby Linwood Nichols. They have a son, James William, and a daughter, Edith Linwood.